การแปรเปลี่ยนหินผนังและการเกิดแร่ของพรอสเปกต์ เอ และ พรอสเปกต์เอชเวสต์
ของแหล่งแร่ทองคำชาตรี จังหวัดพิจิตรและเพชรบูรณ์ ประเทศไทย

นาย ภูริวิทย์ สังข์ศิริ

Wallrock Alteration and Mineralization of the A and the H West Prospects,

Chatree Gold Deposit, Changwat Phichit and Phetchabun, Thailand

Mr. Phuriwit Sangsiri

A Thesis Submitted in Partial Fulfillment of the Requirements

for the Degree of Master of Science Program in Geology

Department of Geology

Faculty of Science

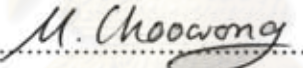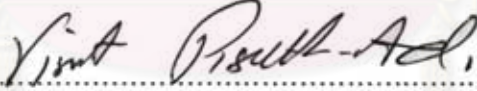Chulalongkorn University

Academic Year 2010

Thesis Title	Wallrock Alteration and Mineralization of the A and the H West Prospects, Chatree Gold Deposit, Changwat Phichit and Phetchabun, Thailand
By	Phuriwit Sangsiri
Field of Study	Geology
Thesis Advisor	Associate Professor Visut Pisutha-Arnond, Ph.D.

Accepted by the Faculty of Science, Chulalongkorn University in Partial Fulfillment of the Requirements for the Master's Degree
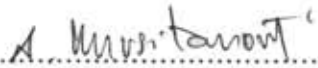
.... Dean of the Faculty of Science

(Professor Supot Hannongbua, Dr. rer. nat.)

THESIS COMMITTEE

.... Chairman

(Associate Professor Montri Choowong, Ph.D.)

.... Thesis Advisor

(Associate Professor Visut Pisutha-Arnond, Ph.D.)

.... Examiner

(Assistant professor Chakkaphan Sutthirat, Ph.D.)

.... External Examiner

(Somboon Kositanont, Ph.D.)

ภูริวิทย์ สังข์ศิริ: การแปรเปลี่ยนหินผนังและการเกิดแร่ของพรอสเปกต์ เอ และ พรอส-เปกต์เอชเวสต์ ของแหล่งแร่ทองคำชาตรี จังหวัดพิจิตรและเพชรบูรณ์ ประเทศไทย (Wall rock Alteration and Mineralization of the A and the H West Prospects, Chatree Gold Deposit, Changwat Phichit and Phetchabun, Thailand) อ. ที่ปรึกษาวิทยานิพนธ์หลัก: รศ. ดร. วิสุทธิ์ พิสุทธอานนท์, 116 หน้า.

เหมืองแร่ทองคำชาตรีเป็นแหล่งแร่ทองคำที่ใหญ่ที่สุดในประเทศไทยในปัจจุบันที่ตั้งอยู่ห่างจากกรุงเทพฯไปทางทิศเหนือประมาณ 280 กิโลเมตร ตรงเขตรอยต่อของจังหวัดพิจิตร และเพชรบูรณ์ งานวิจัยนี้เน้นการศึกษาในรายละเอียดการแปรเปลี่ยนหินผนังที่สัมพันธ์กับการเกิดแร่ในพื้นที่พรอสเปกต์ เอ และพรอสเปกต์เอชเวสต์ ถึงแม้ว่าได้มีผู้ทำการศึกษาเรื่องการเกิดแร่และการแปรเปลี่ยนหินผนังมาก่อนหน้านี้แล้ว แต่การศึกษาดังกล่าวนั้นไม่ได้ศึกษาในรายละเอียดอย่างเป็นระบบ หรือ ศึกษาเฉพาะจุดเท่านั้น โดยเฉพาะอย่างยิ่งในเรื่อง การแปรเปลี่ยนหินผนัง ดังนั้นในการศึกษาครั้งนี้จะเน้นศึกษาในรายละเอียดของการแปรเปลี่ยนหินผนังที่สัมพันธ์กับการเกิดแร่โดยใช้วิธีการย้อมสี การศึกษาแผ่นหินบาง แผ่นหินขัดมัน และแผ่นหินบางขัดมัน ภายใต้กล้องจุลทรรศน์ รวมทั้งการศึกษาเคมีของแร่แปรสภาพและสินแร่

หินผนังของแหล่งแร่ทองคำชาตรีประกอบไปด้วย 4 หน่วยหิน ได้แก่ หน่วยหินตะกอนภูเขาไฟเนื้อแสดงริ้ว (หน่วยหิน 1) หน่วยหินตะกอนและหินตะกอนภูเขาไฟสีอ่อน (หน่วยหิน 2) หน่วยหินภูเขาไฟสีเข้มกลุ่มแอนดีไซต์ (หน่วยหิน 3) และหน่วยหินแอนดีไซต์เนื้อดอก (หน่วยหิน 4) ซึ่งพรอสเปกต์ เอ ประกอบไปด้วยหน่วยหินที่ 1 ถึง 3 เท่านั้นเนื่องจากข้อมูลจากหลุมเจาะที่ยังลึกไม่เพียงพอ ส่วนพรอสเปกต์เอชเวสต์ มีหน่วยหิน1 หน่วยหิน 3 และ หน่วยหิน 4 ส่วนหน่วยหิน 2 ไม่ปรากฏในบริเวณนี้

จากข้อมูลการศึกษาในอดีตรวมกับการศึกษาในครั้งนี้ พบว่าสายแร่ที่ปรากฏในพื้นที่ศึกษาทั้งสองพื้นที่มีลักษณะที่คล้ายคลึงกันมาก ซึ่งประกอบไปด้วย สายแร่ลำดับที่ 1 คือแร่ควอตซ์เนื้อคาลซีโดนิคสีเทา สายแร่ลำดับที่ 2 คือแร่ควอตซ์และไพไรต์แสดงผลึกหน้าสมบูรณ์ สายแร่ลำดับที่ 3 คือสายแร่ทองคำหลัก สายแร่ลำดับที่ 4 คือแร่ควอตซ์ คาร์บอนเนต และ/หรือ พรีไนท์ สายแร่ลำดับที่ 5 คือสายแร่แคลไซต์ชนิดไม่มีเหล็กเกิดร่วม และสายแร่ลำดับที่ 6 คือลูมอนไทต์

การแปรเปลี่ยนของหินผนังในพื้นที่ศึกษาพบว่า มีการเปลี่ยนแปลงใกล้สายแร่เป็นแบบซิลิซิฟิเคชั่น แบบโพแทสสิค และแบบฟิลลิค ส่วนแบบโพพิลิติกเกิดไกลจากสายแร่ออกไป แบบซิลิซิฟิเคชั่นเกิดร่วมกับสายแร่ลำดับที่ 1 สายแร่ลำดับที่ 3 เกิดร่วมกับแบบโพแทสสิคในส่วนใกล้สายแร่ที่สุด ถัดออกไปเป็นแบบฟิลลิค ซึ่งสัมพันธ์กับสายแร่ลำดับที่ 4 คลอไรต์เป็นแร่หลักในการแปรเปลี่ยนชนิดโพพิลิติก ซึ่งสัมพันธ์กับสายแร่ลำดับที่ 3 ถึง 5 ในขณะที่แร่กลุ่มคาร์บอนเนตที่เกิดจากการแปรเปลี่ยนส่วนมากสัมพันธ์กับสายแร่ลำดับที่ 5 ขนาดของการแปรเปลี่ยนในพรอสเปกต์เอชเวสต์ มีขนาดเล็กในระดับ 1-2 มิลลิเมตรถึง 20 เซนติเมตรข้างสายแร่ ส่วนพรอสเปกต์ เอ มีขนาดใหญ่กว่า ที่กว้าง 5 ถึง 30 เมตร

ภาควิชา..............ธรณีวิทยา...................ลายมือชื่อนิสิต.........................

สาขาวิชา............ธรณีวิทยา...................ลายมือชื่อ อ.ที่ปรึกษาวิทยานิพนธ์หลัก.........................

ปีการศึกษา..............2553...................

5072418023 : MAJOR GEOLOGY

KEYWORDS : Chatree / Gold / Mineralization / Alteration

Phuriwit Sangsiri : Wall rock Alteration and Mineralization of the A and the H West Prospects, Chatree Gold Deposit, Changwat Phichit and Phetchabun, Thailand. ADVISOR: Assoc. Prof. Visut Pisutha-Arnond, Ph. D., 116 pp.

The Chatree Gold mine is presently the major gold deposit in Thailand located about 280 km north of Bangkok, on the border of Phetchabun and Pichit Provinces. This study was focussed mainly on wall rock alteration in relation to mineralization of the A and the H West Prospects. Even though many workers have previously studied on mineralization and wall rock alteration on these Prospects, those studies are still considered sporadic or focused on small areas, particularly on the wall rock alteration, of those Prospects. This study is therefore aimed at systematically characterizing in more details on the host rock alteration in relation to the mineralization by using staining technique, standard petrographic studies of thin sections, polish sections and polish thin sections in combination with electron probe microanalysis of altered and ore minerals.

The rock units in the Chatree gold deposit comprise 4 units as Unit 1: fiamme breccias, Unit 2: epiclastic and fine volcaniclastic sedimentary facies and rhyolite breccia facies, Unit 3: polymictic and Monomict ic andesite breccia, and Unit 4: andesite porphyry. The A Prospect is reported only Units 1 to 3 while the lowest unit (Unit 4) is omitted due to the insufficient depth of drilled holes. The H West Prospect consists of three units as Unit 1, Unit 3, and Unit 4, while the volcaniclastics of Unit 2 is absent in this area.

Based on previous and this studies, the A and H West Prospects possess similar nature of mineralization and six vein stages have been identified in these two Prospects, namely. Stage I: gray chalcedony, Stage II: quartz–euhedral pyrite, Stage III: major gold mineralization, Stage IV: quartz–carbonate±prehnite veinlets, Stage V: non-ferroan calcite veinlets, and Stage VI: laumontite.

The A and H West Prospects comprise several mineral alteration halo, including silicification, potassic, and phyllic alterations that are proximal to the veins, whereas propyritic alteration is distal from the veins. The alteration minerals selectively replaced in the vein host rocks. The silicification was related to the Stage I mineralization. The gold-bearing Stage III mineralization was related to the potassic alteration proximal to the ore zone, while sericite±quartz or phyllic alteration was found next away from the ore zone in the Stage IV mineralization. Chlorite or porpylitic alteration was found distal to the ore zone in the Stages III-V. The late carbonate is assumed to occur in the stage V. The alteration halos in the H West Prospect are rather narrow (normally about 1-2 mm scale or may be up to 20 cm wide around veins system) as compared with those found in the A Prospect (normally 5 – 30 m scale).

Department : Geology...   Student's Signature ....

Field of Study : Geology...   Advisor's Signature ....

Academic Year : 2010...

ACKNOWLEDGMENTS

CONTENTS

LIST OF FIGURES

Page

Figure 2.8 Summarize vein styles of Pre-gold mineralization and Post-gold mineralization (modified from Salam, 2010). Detail: stage I show grey silica breccia/veining with strong silicified angular clasts of porphyritic andesite, stage II show quartz – chlorite – sercite – sulphide matrix of pyroxene pyric andesite breccias clasts, stage IV show quartz-carbonate-chlorite cut through polymictic andesitic polymictic andesitic lithic breccias, stage V show jig saw fit breccia, matrix of carbonate± quartz assemblage, and stage VI show zeolite-quartz-carbonate- veins

Page

Page

LIST OF TABLES

CHAPTER I
INTRODUCTION

1.1 Introduction

Gold is a precious element which is useable in many ways. In various countries, gold is used as a standard for monetary exchange, in coinage and in jewelry. In addition, gold can be made into thread and used in embroidery. Gold is ductile and malleable, meaning it can be drawn into very thin wire and can be beaten into very thin sheets known as gold leaf. The concentration of free electrons in gold metal is 5.90×10^{22} cm^{-3} which means that gold is highly conductive to electricity, and has been used for electrical wiring in some high energy applications (silver is even more conductive per volume, but gold has the advantage of corrosion resistance). (http://en.wikipedia.org/wiki/Gold)

Chatree Gold deposit is presently the major gold deposit in Thailand. Construction of the Chatree took place between December 2000 and October 2001 with commissioning throughout November 2001. It was completed within time and under budget and commercial production commenced on 27 November 2001. Total company ore reserve was 1.47 million ounces of gold as of 30 June 2009. Mineral Resources amount to 3.10 million ounces of gold, and 24.14 million ounces of silver. (www.kingsgate.com.au)

Chatree is located on the eastern edge of the Tertiary Chao Phraya Basin about 280 km north of Bangkok, on the boundary of Phetchabun and Pichit Provinces (Figure 1.1). The mine situates within a north-south trending Upper Permian and Triassic volcanic arc sequences formed as subduction associated with the collision of the Indochina and Shan-Thai crustal blocks, the volcanic belt along Loei fold belt that extends from Lao PDR. (Diemar, 1990)

Figure1.1 Location of Chatree gold deposit (www.kingsgate.com.au).

1.2 Location and Accessibility

The Chatree gold deposit is located on the boundary between Thap Klo District, Phetchabun Province and Wang Pong District, Phichit Province, central Thailand. It is approximately 280 kilometres north of Bangkok and about 35 km southeast of Phichit. Coordinates of the mine are approximately $100^o\ 36^/$ E and $16^o\ 19^/$ N. Khao Mo rises steeply 100 meters above the level of the plain, whereas Khao Pong rises gently for 30 metres above the lower land.

The journey to the Chatree gold deposit can be conveniently made by car via the route from Thap Khlo District, Phichit Province (Highway Number 11: In-Buri - Phitsanulok), about 20 km distance, and then turning right to Highway Number 1301 (Khao Chet Luk – Wang Pong) to the Chatree mine, about 10 km distance.

The Chatree gold deposit covers an area of 7.5 km by 2.5 km and consists of at least 5 gold–rich vein systems (A, C, D, H and Q) (Figure 1.2) (http://www.kingsgate.com.au).

1.3 Exploration History

In 1987, Thai Goldfield Limited has defined gold exploration target along Loei – Petchabun volcanic belt. One of the potential areas is the Khao Mo (now the A Prospect of the Chatree gold mine). They used panning and soil sampling above break of slope as the primary tool. The potential was recognized by M.G. Diemar in September 1988. After that in 1991, the Department of Mineral Resources completed soil geochemical exploration of the B Prospect (South of the Chatree) and trenching of the A Prospect with ground electromagnetic conductivity survey. The semi-detailed drilling program used grid auger laterite geochemical exploration on area between the A and B Prospects. These techniques had found pathfinder element and led to the discovery of the C, D, E, F and H Prospects. Following auger geochemical exploration the Rotary Air Blast (RAB) was used for depicting mineralization zone and later resource evaluation was accomplished by diamond drilling and reverse circulation drilling (Diemar et al., 1992). Since 1995 Akara Mining Co., Ltd. has established from joint venture between Prae Lignite Co. Ltd. (a subsidiary of Ban Pu Public Company Ltd., Thailand) and Issara Mining Ltd. (a subsidiary of Kingsgate Consolidated NL of Australia). Akara Mining Co. Ltd, is the sponsor of this research.

1.4 Hypothesis

The epithermal gold deposit is a target of precious mineral deposit. The wall rock alteration correlation with mineralization is one of popular method for finding gold. Gemmell (2004) demonstrated that the alteration mineralogy zonation related consequentially to ore zone. The alteration mineralogy and zonation were determined using a combination of surface mapping, drill core logging, petrology, Short Wavelength Infrared (SWIR) Spectral Analysis, XRD and potassium feldspar staining (HF and sodium colbatinitrite). In all cases the development of quartz-adularia-illite is proximal to mineralization. Next away from the mineralization the alteration became illite-smectite rich before passing into a distal propylitic assemblage containing varying proportions of albite, chlorite, epidote and chlorite.
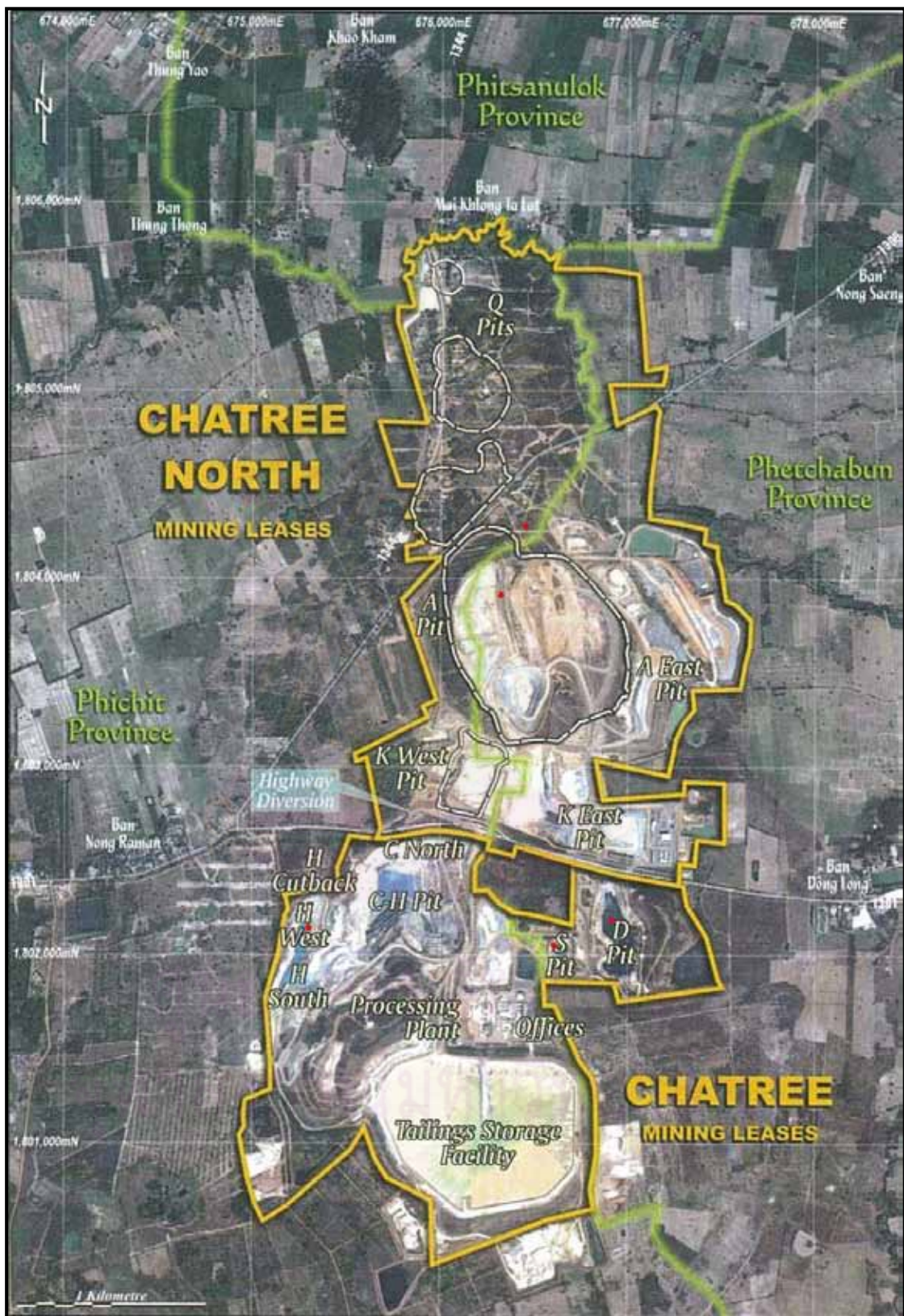
Figure1.2 Location and the propose pits (white dash line) with mining leases (yellow line) of Chatree gold deposit (www.kingsgate.com.au).

1.5 Aim of This Study

The many previous workers studied about mineralization and wall rock alteration (i.e. Tomkinson (2004), Salam (2010), James and Cumming (2007), Cumming et al. (2008), Dedenczuk (1998), Greener (1999), etc.). However, these works were spotted studies or study in small areas. This study is aimed at systematically characterizing in more details on the host rock alteration in relation to the mineralization in the study areas by using staining technique, standard petrographic studies of thin sections, polish sections and polish thin sections in combination with electron probe microanalysis of altered and ore minerals.

The main aims of this study are:
1. to describe and interpret the alteration characteristics of the A Prospect and the H West Prospect at the Chatree deposit, such as mineral assemblages, mineral zonation, overprint relationships and alteration timing, correlation with vein styles and mineralization.
2. to document alteration style of the A and H West Prospects by contrasting of the 2 prospects.

1.6 Methodology

The methodology was summarized in Figure 1.3. Literature review was firstly carried out to check information and problem from previous researches. Field investigations were undertaken for pit mapping in the study area. Sampling of every rock units were stained for K-feldspar and also used for standard petrographic studies.

Drilled core study and sampling were carried out in 2 steps. The first step was a preliminary survey of all rock units, including interesting points, in the whole study areas. The second step was the detailed investigation of the sections 20000mN in the A Prospect and the 5480mN and 6230mN in the H West Prospect. Totally 741 samples were logged and sampling for the total distance of 7824 m.

Standard petrographic studies were employed on thin-section, polished-section and polished-thin section for the total of 75 samples to observe and identify characteristics of alteration minerals. Carbonates in thin-sections were identified by staining. Ore minerals were observed using polished section and polished-thin section in a standard reflected light microscopy. Electron microprobe microanalysis (EPMA) was undertaken to determine chemical compositions of alteration and ore minerals. X-ray diffraction (XRD) analysis of alteration minerals was also employed as an auxillary equipment

Staining of K-feldspar

Potassic alteration was identified by the presence of K-feldspar which can be stained yellow. The method was described by Bailey and Stevens (1960). Firstly, the samples were cut and polished before staining. Next, dipped the polished face into the concentrate hydrofluoric acid for approximately half minute. Then, rinsed the wet slab face in the distilled water bath. After that, dipped the same face of the slab in the same manner as above, into the 20 percent solution of sodium cobaltnitrite for approximately half minute. Later, rinsed the slab in the distilled water again and dry off.
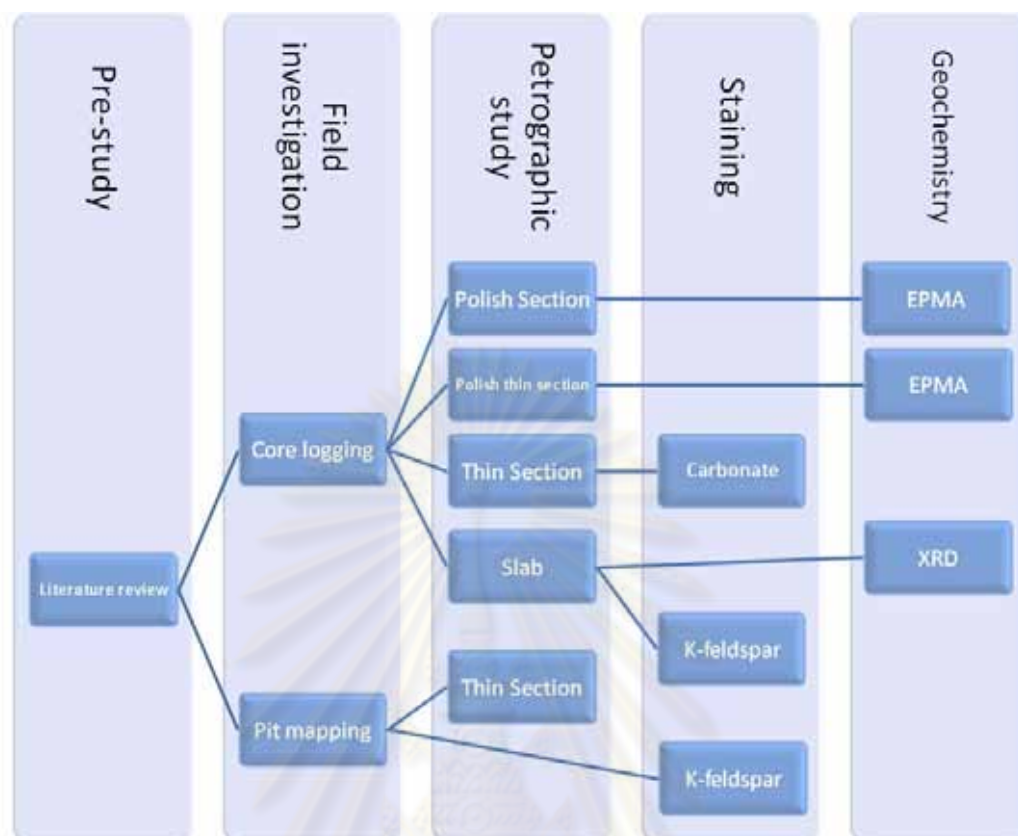
Figure 1.3 Flow chart showing the methodology.

Staining of Carbonate

Carbonate mineral group is one of major constituents of gangue and alteration minerals. The identification and discrimination of carbonate minerals in hand specimens or thin sections, were made easier by the use of simple chemical staining methods. The Alizarin red and potassium ferricyanide composite test was used for discriminating between four different types of carbonates (calcite, ferroan calcite, dolomite and ferroan dolomite) in a single series of operation. The test and results were described by Evamy (1963). The solution was obtained by mixing 0.2 % HC1, 0.2 % alizarin red, and 0.5-1.0 % potassium ferricyanide. Specimen was soaked in cold dilute acid solution for half minutes. The results of the test are as follows: calcite is red, ferroan calcite is blue, dolomite is no coloring, ferroan dolomite is pale blue and ankerite is dark blue.

Electron probe micro-analyzer (EPMA)

An electron probe micro-analyzer is a microbeam instrument used primarily for the in situ non-destructive chemical analysis of minute solid samples. The probe determine the composition of an unknown phase quantitatively, XRF-WDS analysis is much more involved, requiring instrument standardization based on standards of known composition, followed by evaluation of quantitative results and assessment of errors. The standards were summarized in table 1.1. This analysis was performed at Department of Geology, Faculty of Science, Chulalongkorn University. The electron microprobe machine is model JXA 8100, work as XRF-WDS, excitation voltage 15 kV and current 2.40×10^{-8} A. The samples were the polished sections and polished-thin sections.

Table 1. 1 Summary standard of EPMA analysis

Type of standard	Name of Standard	Element	Concentration	Type of standard	Name of Standard	Element	Concentration
Mineral Standard	Potassium	K2O	23.80	Oxide Standard	Magnosite	MnO	99.9
	Titanium	TiO2	46.33		Nickel oxide	NiO	99.9
	Phosonate	P2O5	35.87		Periclase	MgO	99.99
	Barite	BaO	65.12		Corundum	Al2O3	99.99
		SrO	0.68		Cobalt oxide	CoO	99.9
		SO3	34.10		Eskolalite	Cr2O3	99.99
	Zinc oxide	ZnO	99.80		Lead Vanadium Germanium oxide	PbO	79.29
		SiO2	0.13			GeO2	7.42
		Al2O3	0.20			V2O	12.88
	Fayalite	FeO	70.15			SiO2	0.38
		SiO2	29.49	Pure metal standard	Gold	Au	99.99
	Wallastonite	MgO	0.15		Silver	Ag	99.99
		SiO2	50.94		Cadmium	Cd	99.9
		CaO	48.00		Copper	Cu	99.99
		MnO	0.09		Zirconia	Zr	99.9
		FeO	0.11	Sulphide standard	Stibnite	Sb	71.48
	Jadite	Na2O	15.10			S	28.44
		MgO	0.10	Internal standard	Arsenic	As	-
		Al2O3	25.10		Molybdenum	Mo	-
		SiO2	59.40				
		FeO	0.13				

X-ray powder diffraction (XRD)

X-ray powder diffraction is most widely used for the identification of unknown minerals. The samples were prepared to powdered solid samples. This analysis was performed at Department of Geology, Faculty of Science, Chulalongkorn University. The X-ray diffractometer is model D8 Advance, Bruker AXS from Germany, work as 40 kV and 30 mA. The conditions are 2theta 5–70 degree with increment 0.10 degree and scan speed 2 degree per minute. Programs used Diffrac plus#1 software of the Bruker Analytical X-Ray System (D8 Immediate Measurement) and interpreted by Eva Program with PDF-2 Database.

1.7 Thesis Design

This thesis is presented in 5 chapters:

Chapter 1 introduces the thesis topic briefly, discussing the general background. The objective and overview of the field and laboratory analytical methods are presented.

Chapter 2 demonstrates and overviews the regional geological setting, district geology, and geology of study areas including mineralization and alterations. It is mainly based on previous studies and on the published literatures, however part of this chapter includes the work carried out by this study.

Chapter 3 presents the general geology of the A Prospect, including its structural feature. This chapter is detailed the nature of vein types and their characteristic, with related alteration product. The main propose is to evaluate mineral assemblages, texture and paragenesis of alteration and mineralization.

Chapter 4 is documented the details of the H West Prospect similar to those of the Chapter 3.

Chapter 5 concludes synthesis and synopsis of this thesis, presents and compares importance alteration characteristics of each prospect. This chapter also discussion what was found in the individual chapters. Some suggestions for future work are shown in last section.

CHAPTER II
GEOLOGY

2.1 Tectonic Evolution

Thailand comprises a complex assembly of two alloctonous microcontinents, namely Shan-Thai Terrane in the west and Indochina Terrane in the east, with the N-S trending linear Nan-Sra Kaeo suture as their entity (Bunopas, 1992). Additionally, Charusiri et al. (2002) proposed the other two tectonic blocks, viz. Lampang-Chiang Rai and Nakhon Thai, immediately western and eastern sides of the Nan-Sra Kaeo suture, respectively. Paleogeographical reconstruction shows that both Shan-Thai and Indochina microcontinents were thought to be cratonic fragments of the Southern Hemisphere supercontinent, "Gondwana". Shan-Thai Terrane was connected to northwestern Australian Gondwanaland margin. Metcalfe (1996) referred by De Little (2005) suggested that during the Lower Palaeozoic, Shan-Thai Terrane rifted off the Indain-Australian margin. This separation from Gondwanaland coincided with marine transgression synchronous with the formation of Palaeotethys. The Shan-Thai Terrane migrated northwards toward the paleoequator and eventually collided with the Indochina Terrane block during the Permain-Triassic (Charusiri et al. 2002).

The Indochina Terrane block was derived from north and north eastern margin of Gondwanaland. It began to drift away from Gondwanaland during the Devonain to Early Carboniferous (Metcalfe (1996) referred by De Little (2005)). During Early Triassic the Indochina Terrane collided with the Shan-Thai, which resulted in the closer of Paleotethys. Closure and stitching of these terranes occurred along the Nan Suture (Charusiri et al., 2002)

Suture zones in Thailand occurred as branch sutures or tectonic lines and were inferred to correlate with Langcangjiang and Changning-Menglian sutures in Tibet and Yunnan. Three suture zones of Thailand are called Chiang Mai-Chiang Rai, Nan-Uttaradit and Loei-Phetchabun sutures (Figure 2.1).
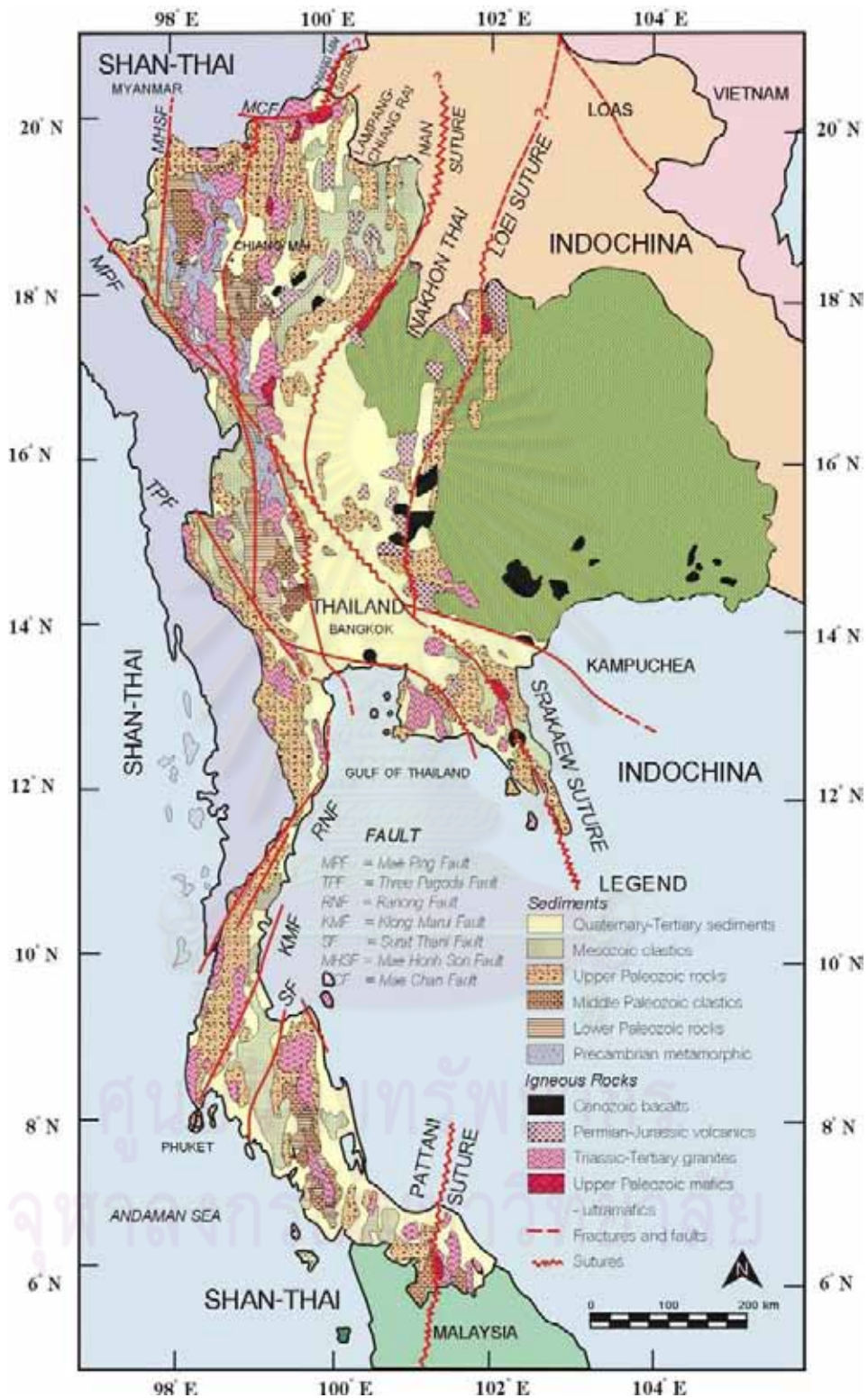
Figure 2.1 Geological map of Thailand showing plates and sutures of Thailand (Charusiri et al., 2002).

2.2 Regional Geology

The Loei–Phetchabun area is sometime called Loei-Phetchabun volcanic belt, which extended from Loei southward along the western margin of the Khorat Plateau (Figure 2.2). The Chatree gold deposit or Chatree mine is located in this belt. The Leoi-Phetchabun volcanic belt is mainly calc-alkali rocks. Volcanic rocks in this belt are basaltic andesite and andesite crosscut and flowed over middle Permian limestone and locally overlain by Triassic sedimentary rocks. Panjasawatwong and Phaejuy (2008) reported that oceanic Island-Arc mafic volcanic lavas in association with mid-ocean ridge volcanic rocks also occurred in this belt. Some volcanic rocks in this belt were dated to have an age of 235 ± 4 Ma (Jungyusuk and Khositanont, 1992). Charusiri (1989) referred by Kromkhun (2005), Intasopa (1993) and Khin Zaw et al. (1999) suggested that rocks from this belt are Triassic to Miocene, by using Ar/Ar and Rb/Sr geochronological data. Moreover, three magmatic episodes were suggested along the belt including 373 – 361 Ma, 225 – 275 Ma and 9 – 57 Ma.
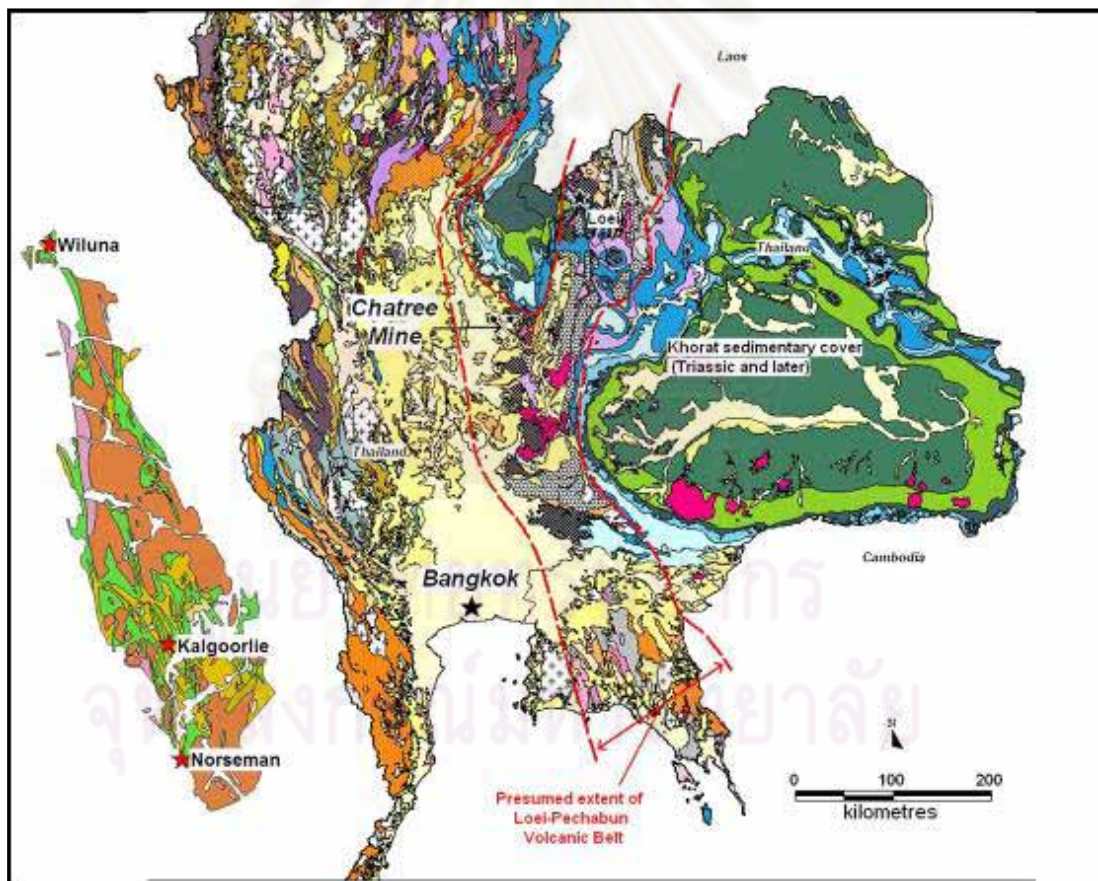
Figure 2.2 Geology of Loei-Petchabun volcanic belt and location of the Chatree mine (after Salam, 2007a).

2.3 District Geology

This part documents the district scale geology of Wang Pong, Chon Dean and around the Chatree gold deposit.

At Chon Dean district in Petchabun province, about 15 km to south-east direction of the Chatree mine, the oldest rocks are siltstone, sandstone, conglomerate and thin limestone beds of Carboniferous age (Crossing, 2004; Salam, 2006, 2007a and 2007b). These rocks were capped by Permian limestone. These volcanic rocks were overlaid by Huai Hin Lat Formation, which was deposited in Upper Triassic. In addition, volcanics to sub-volcanics and deeper level plutonic igneous rocks in the area were reported by Jungyusuk and Khositanont (1992). Those volcanic rocks range from mafic to felsic and occur as lava flows, pyroclastic deposits, dykes and sills. Among those rocks the dominant pleases are andesite, andesitic tuff, basaltic andesite, andesite breccia, rhyolite and rhyolitic tuffaceous rocks. Their ages range from Middle-Upper Permian to Lower Jurassic. Most plutonic rocks are overlaid by unconsolidated sediments. Nevertheless, stocks and dykes of granite and granodiorite were discovered by airbone magnetic.

Wang Pong area, 10 km east of Chatree, consists of three volcanic rock units and two plutonic rock units. Volcanic rocks are andesite porphyry, agglomerate and crystal tuff. Plutonic rocks namely biotite granite and granodiorite. The petrogenesis suggested that igneous rocks in Wang Pong were partial melting of a lithospheric mantle protolith metasomatically enriched before the collision of Shan-Thai and Indochina lithospheric plates in late Triassic (Kamvong et al., 2006). After the collision, mountains uplift along suture and at the same time granites were intruded into sediments and rhyolites were extruded on the land surface (Bunopas and Vella, 1983). Those intrusions were believed to associate with Cu-Fe-Pb-Zn and Au mineralization (Charusiri et al., 2002).

Crossing (2004) reported that around the Chatree gold deposit was dominated by a volcano-sedimentary sequence (yellow color in the map; Figure 2.3) which digitated laterally with terrigenous sediments. The volcano-sedimentary sequence is gently folded, producing open horizontal folds with north to NNW trending sub-horizontal axes. Faulting consists of early N-S structures which are displaced by later NE and NW trending structures, and occasionally by E-W trending structures. Limestone reef (marine blue in the map; Figure 2.3) development commenced in shallow marine environments away from volcanic centers or alternatively in between periods of volcanic activity. On the landward side the volcanic sediments and limestones interdigitate with continentally derived terrigenous sediments.

Moreover, the Chatree gold deposit contains 2 types of volcanic centers; several andesititic volcanic centers and a couple of rhyolitic centers (Crossing, 2006). Intrusions of "early" (pre gold mineralization) diorite to dolerite and "late" diorites occur in the region. There are also stocks and swarms of dykes that are thought to be exploiting pre–existing fractures and faults that postdate mineralization in the area and granitic intrusions are associated with regional structural trends. (Corbett, 2006; 2005; Crossing, 2006). Petrochemical results revealed that they were A-type granite and diorite (?). A porphyritic granodiorite stock was reported to intrude into andesite at the N zone of Chatree property   (Mahotorn et al., 2008). The age from feldspar phyric andesite in one of flow units yielded a LA-ICP-MS U-Pb zircon age of 250±6 Ma (Early Triassic). Adularia from gold bearing veins used laser ablation Ar-Ar

method yielded an age of 250±0.8 Ma (Early Triassic). The age of post mineral dykes analyzed by LA-ICP-MS U-Pb zircon of 238±6 Ma (Middle Triassic) and 244±7 Ma (Early Triassic) (Khin Zaw et al., 2007).
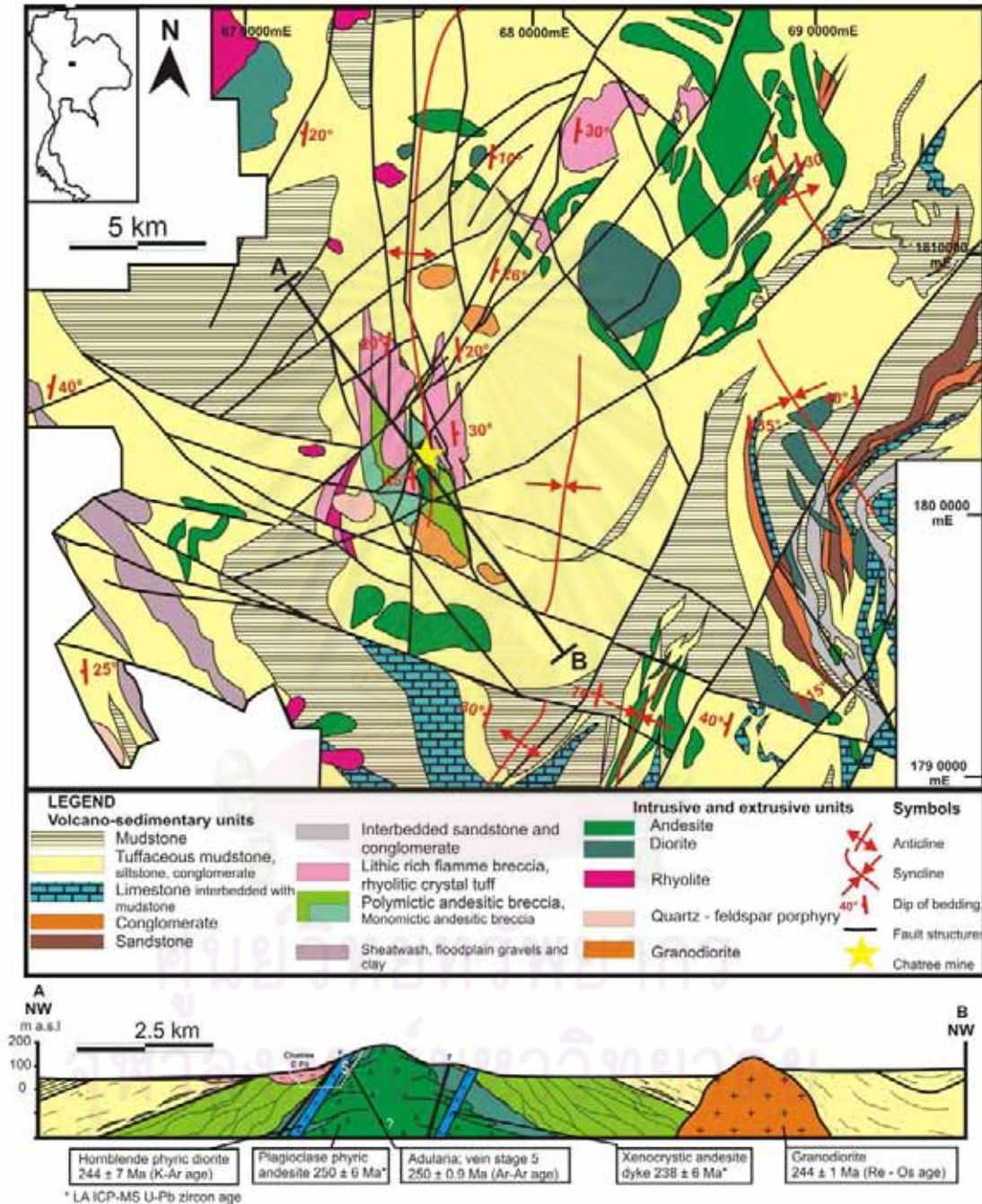
Figure 2.3 Picture demonstrated district geology around the Chatree Gold Deposits with cross section (Crossing, 2006).

2.4 An Overview of Geology of Chatree Gold Deposit

A summary stratigraphic column and a generalised stratigraphic correlation of rock units in the Chatree mine area, based on the works of by Cumming (2004), Cumming et al. (2006), Salam (2006) and Salam (2008a and 2008b), are shown in Figure 2.4 (east-west cross section), Figure 2.5 (north-south cross section) and Figure 2.6 (geologic map). The stratigraphic units from higher to lower in the stratigraphy are as follows:

Unit 1: Fiamme breccia (and andesitic volcaniclastic facies); Lithic rich fiamme breccia, quartz rich fiamme breccia, polymictic hematitic breccia and polymictic mud matrix breccia

Unit 2: Epiclastic and fine volcaniclastic sedimentary facies and rhyolite breccia facies; includes inter-bedded volcaniclastic sandstones, laminated carbonaceous mudstones and minor limestone and calcareous siltstone and rhyolitic breccia facies.

Unit 3: Polymict and monomict andesite breccia facies; this group includes massive polymictic andesitic breccia, andesitic basaltic breccia which is inter - bedded and overlain by volcaniclastic sandstones, laminated carbonaceous mudstones and minor limestone. This group also includes some isolated zones of the monomictic andesitic breccia, plagioclase phyric andesite and hornblende phyric andesite.

Unit 4: Polymict and monomictic andesitic breccia facies and coherent andesite; This group includes the monomictic andesitic breccia, plagioclase phyric andesite and hornblende phyric andesite and some polymictic andesitic breccia. There is isolated small scale bodies of dacite – rhyolite in this stratigraphic unit.

The uppermost unit (Unit 1) was thought to non-conformably overly the lower units (Units 2 – 4). Beside these four rock units, there are also andesite, dacite and basalt dykes cross-cut the whole succession.

In addition, Salam (2006) and Salam (2008) suggested that between unit 2 and unit 3, and unit 3 and unit 4 there were punctuated by thin fiamme breccia.
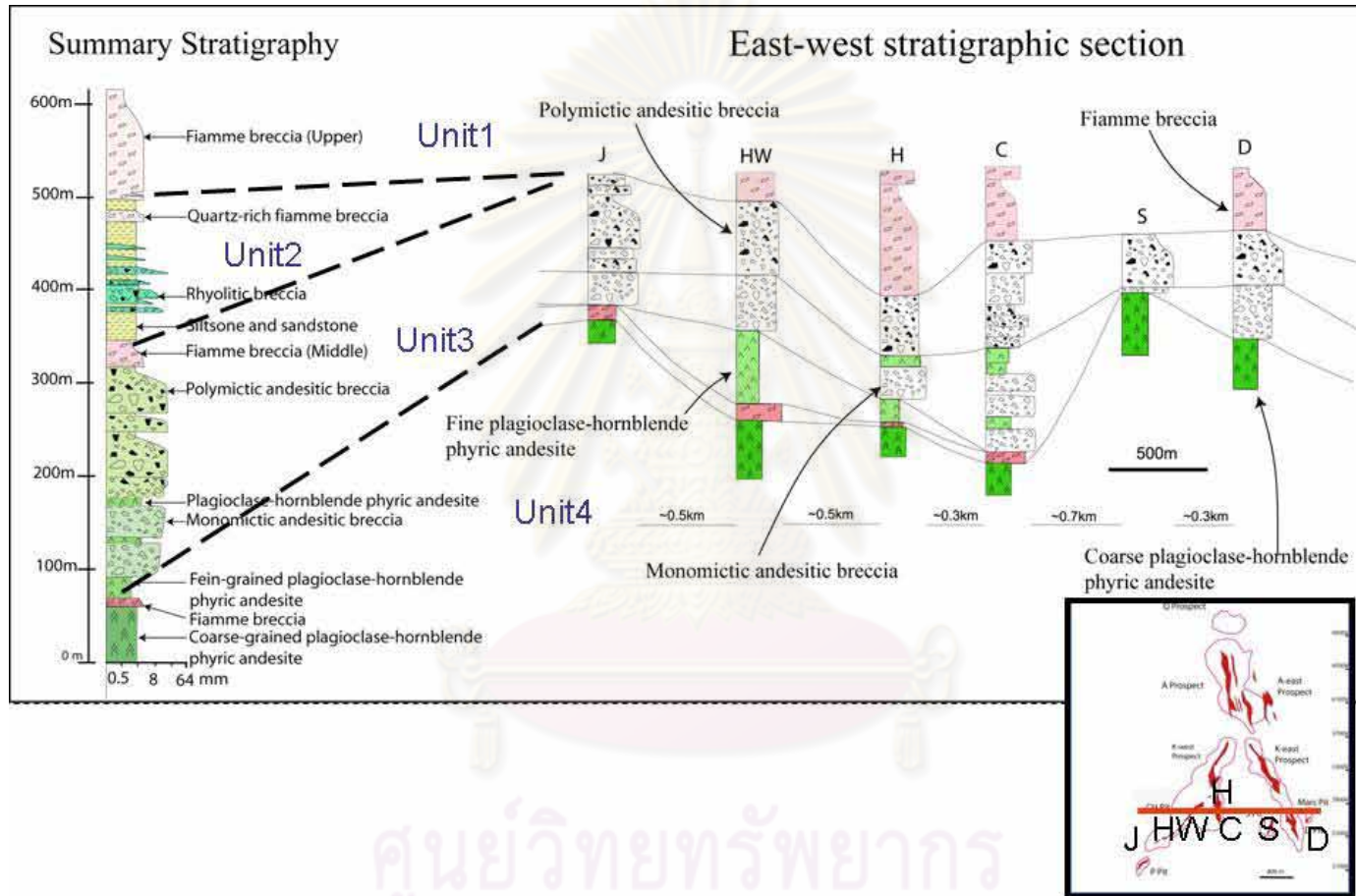
Figure 2.4 Stratigraphic correlation of rock units in the Chatree mine area from west to east prospects and a summary of general stratigraphy (modified from Salam, 2008a).
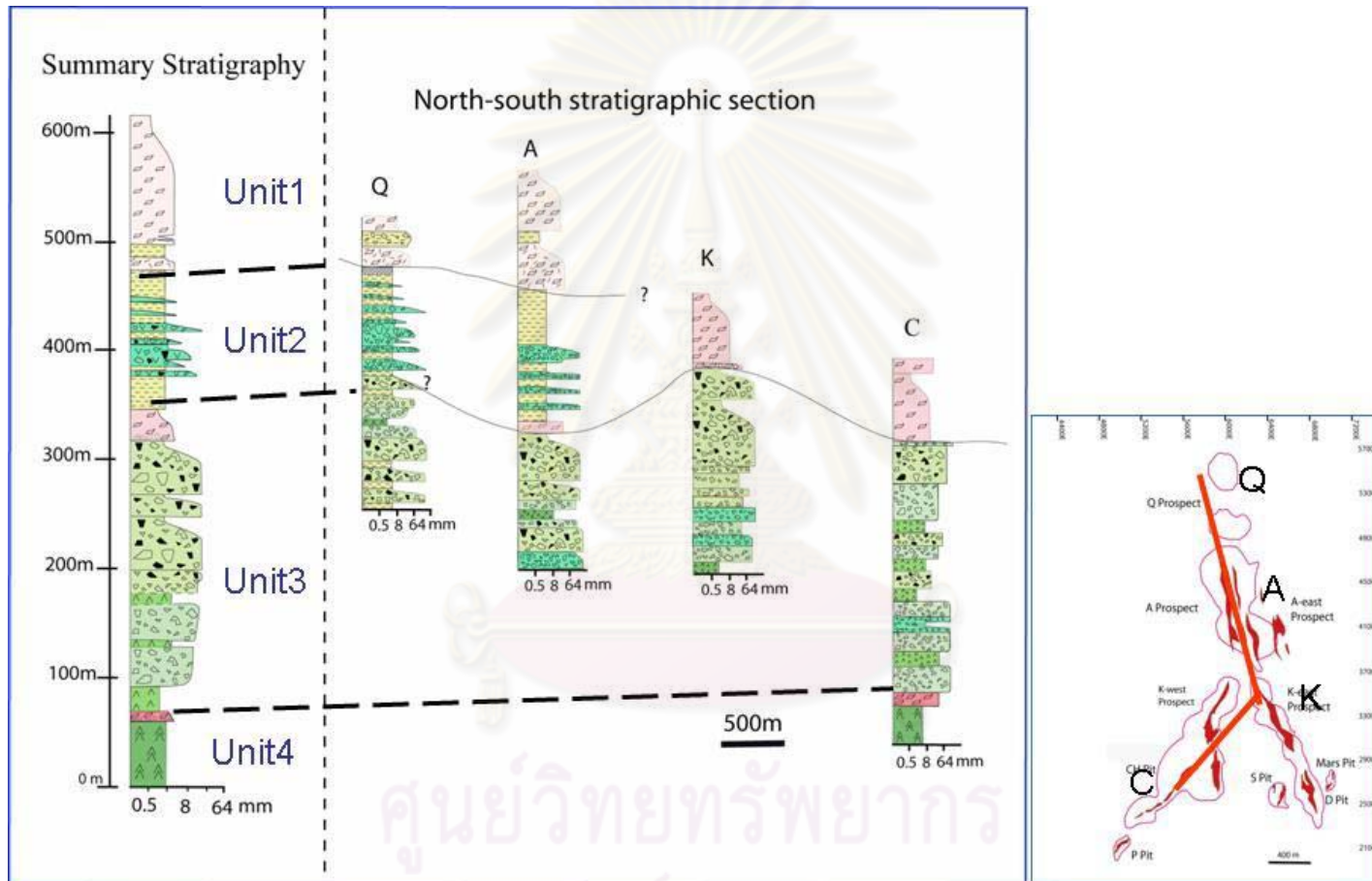
Figure 2.5 Stratigraphic correlation of rock units in the Chatree from north to south prospects and a summary of general stratigraphy. In addition, the stratigraphic unit2 present north of Chatree deposit only (modified from Salam, 2008a).
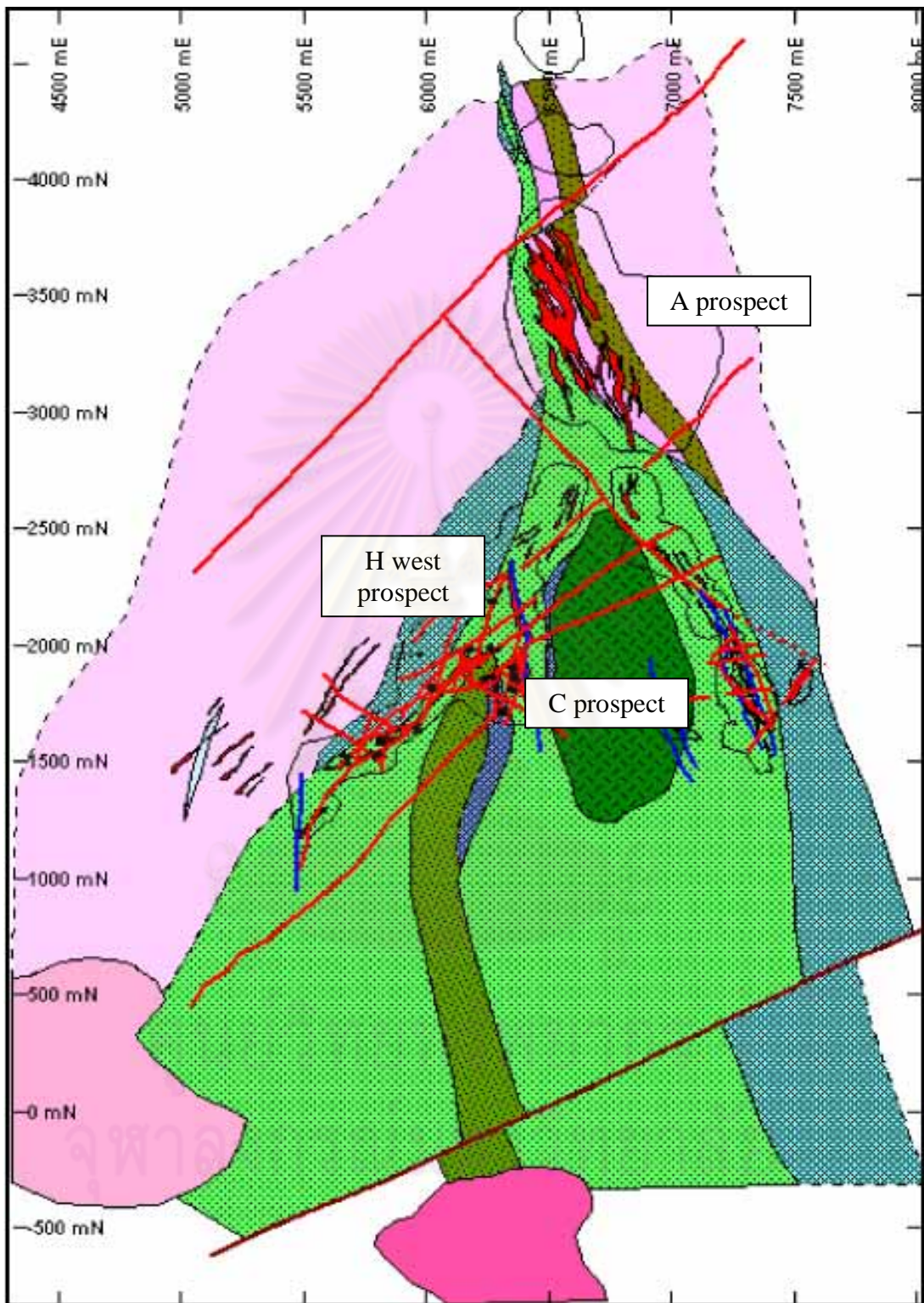
Figure 2.6 Geologic map of the Chatree area and mineralization zone. Note legend on the next page (modified from Salam, 2006).

Legent

Polymictic andesitic lithic breccia and volcanic sedimentary rocks

Volcanic siltstone, sandstone: Partly laminated and interbeded with pebbly sandstone with greenish grey

Fiamme breccia and volcanic siltstone and sandstone : Light grey

Polymictic andesitic lithic breccia and matrix rich polymictic andesitic lithic breccia

Microporphyritic andesite: Dark green, microporphyritic, commonly with zeolite veinning

Lithic rich fiamme breccia : Light grey to brownish grey with volcanic siltstone and sandstone at bottom

Andesite and basaltic andesite porphyry : Dark green porphyriytic, typically with orange K-feldspar phenocrysts.

Plutonic rock: Quartz porphyry

Plutonic rock: Granodiorite (?)

Figure 2.6 (cont.) Legend of geologic map on the last page.

Cumming et al. (2006) described the history of volcanism over time for the Chatree Deposit. The major events, from older to younger include:

1. Effusive and explosive eruption processes: producing the plagioclase phyric and hornblende phyric andesite and the monomictic andesite breccia and rhyodacite breccia facies. The monomictic andesitic breccia is interpreted to represent in situ autoclastic (autobreccia) facies associated with the plagioclase and hornblende phyric andesite, and re-sedimented autoclastic breccia facies (polymict and monomict andesite breccia and polymictic – monomictic rhyolite breccia) records the break up and redeposition of this autobreccia. The coherent with autobrecciated margins occur prior to and after sector collapse events (as shown from exposures in the CH pit).

2. Collapse and mass flow processes have been recorded through the polymictic andesitic and basaltic breccia facies, polymictic andesitic breccia facies, hematitic breccia facies and the polymictic mud matrix breccia lower and higher up in the stratigraphy.

3. Explosive eruption processes have emplaced the lithic and quartz rich fiamme breccia facies and record syn eruptive pyroclastic deposits (fiamme breccia facies). Accretionary lapilli layers suggest phreatoplinean explosive events from a vent(s) that were very near or above water.

4. Normal sedimentation processes are recorded in the fine grained volcaniclastic sedimentary packages. The lithologies for which reasonable lateral transport can be inferred are the fine volcaniclastic and epiclastic sediments and they mark sea floor position in the volcanic succession through time and represent a hiatus of volcanic activity.

2.5 Mineralization, Vein Stages and Paragenesis

The major facture/fault structure of Chatree gold deposit is orientated along NW-SE, NE-SW and N-S strike, moderate to steeply dipping. Interpretation from geophysic information shows the structure extending for a few km (Hill, 2004a and 2004b).

Previous works from Chatree mines' geologists suggested that one is aligned in NNW-SSE trending 340° striking 50°-60° SW dipping and structure extending a total distance of 2 km. This trend composes K-east, A, A-east and Q trend. The other is NE-SW trending 35° striking 45°-50° NW dipping extending for 1 km. This trend comprises K west-A east Trend. NNW structures are better run away and terminated NE structures. Based on the orebody continuity and resistivity interpretation suggest the orebody at intersection between 2 major structures such as A-east usually broader size and gentler dipping than or body that run away on single structure (Figure 2.7). Gold occurs as veins and breccias. A chronology of vein types established on the basis of cross-cutting relationship.

Many researchers suggested vein stage and paragenesis. Tomkinson (2004) has reported 4 stages of mineralization.

James and Cumming (2007) and Salam (2006) were presented six stages of mineralization: stage 1 silica replacement veins, stage 2 grey silica breccia and veins/veinlets, stage 3 quartz ± carbonate ± chlorite - pyrite ± sphalerite ± chalcopyrite ± galena-electrum breccia and veins/veinlets, stage 4 quartz-carbonate-

adularia (K-feldspar?)-chlorite-epidote, stage 5 quartz ± carbonate veins, and stage 6 quartz-carbonate-zeolite veins. Moreover, two hypothesizes of mineralization interpreted as first, mineralization was synchronous with volcanism, or second, mineralization postdated the volcanic succession (Cumming et al., 2006).

Specification in the H Prospect, five stages of vein were reported by Kromkhun (2005); stage 1 hydrothermal breccia and grey quartz veins; stage 2 quartz, calcite, chlorite, illite, smectite, ankerite, dolomite, epidote, adularia, pyrite, hematite, rhodochrosite, chalcedony, sphalerite, galena, chalcopyrite and electrum in decrease order; stage 3 recrystallised quartz with minor pyrite, K-feldspar, calcite and altered epidote; stage 4 calcite veins; and stage 5 pink fibrous laumontite.
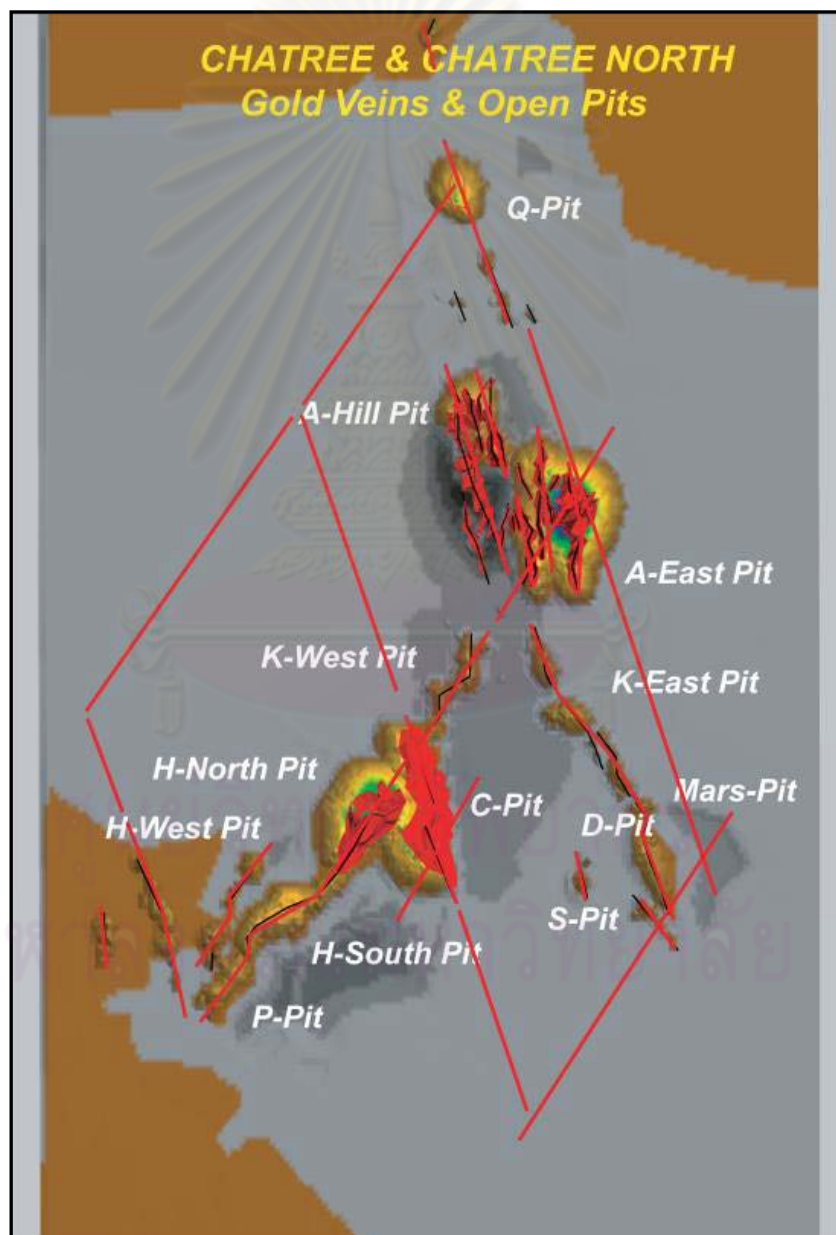
Figure 2.7 Trends of mineralized vein zones at the Chatree gold deposit (Cumming et al., 2006).

This study mainly follows the last updated paragenesis of Salam (2010), including partly from James and Cumming (2007) that presented as 6 stages.

Stage I, quartz breccias and veins. This stage consist pale gray silica occurs as matrix of braccias in the lower plagioclase phyric andesite and polymictic andesitic breccia facies with wider zones above the orebody in the epiclastic and volcaniclastic sedimentary facies.

Stage II, quartz–chlorite–sericite–sulphide.

Stage III, mineralization stage. This stage consists of quartz±carbonate± chlorite-adularia-sulphide-electrum veins. The sulphides comprise pyrite, sphalerite, chalcopyrite and galena. Electrum occurs as free grains and inclusions mainly in pyrite, minor in sphalerite and chalcopyrite.

Stage IV, quartz-carbonate±(K-feldspar)-chlorite-pyrite veins. Non mineralized coarse grained calcite, comb quartz, dark green quartz-chlorite and quartz – sericite-pyrite veins occur in open spaces.

Stage V, quartz±carbonate veins/veinlets crosscut the gold-silver bearing stage.

Stage VI, zeolite-quartz-carbonate veins/veinlets usually infill late fractures.

From 6 stages that was separated into 3 sub-group as 1) Pre-gold mineralization; stage I and stage II, 2) Gold mineralization; stage III and 3) Post-gold mineralization; stage IV, state V and stage VI. Those were summarized in Figures 2.8 and 2.9.
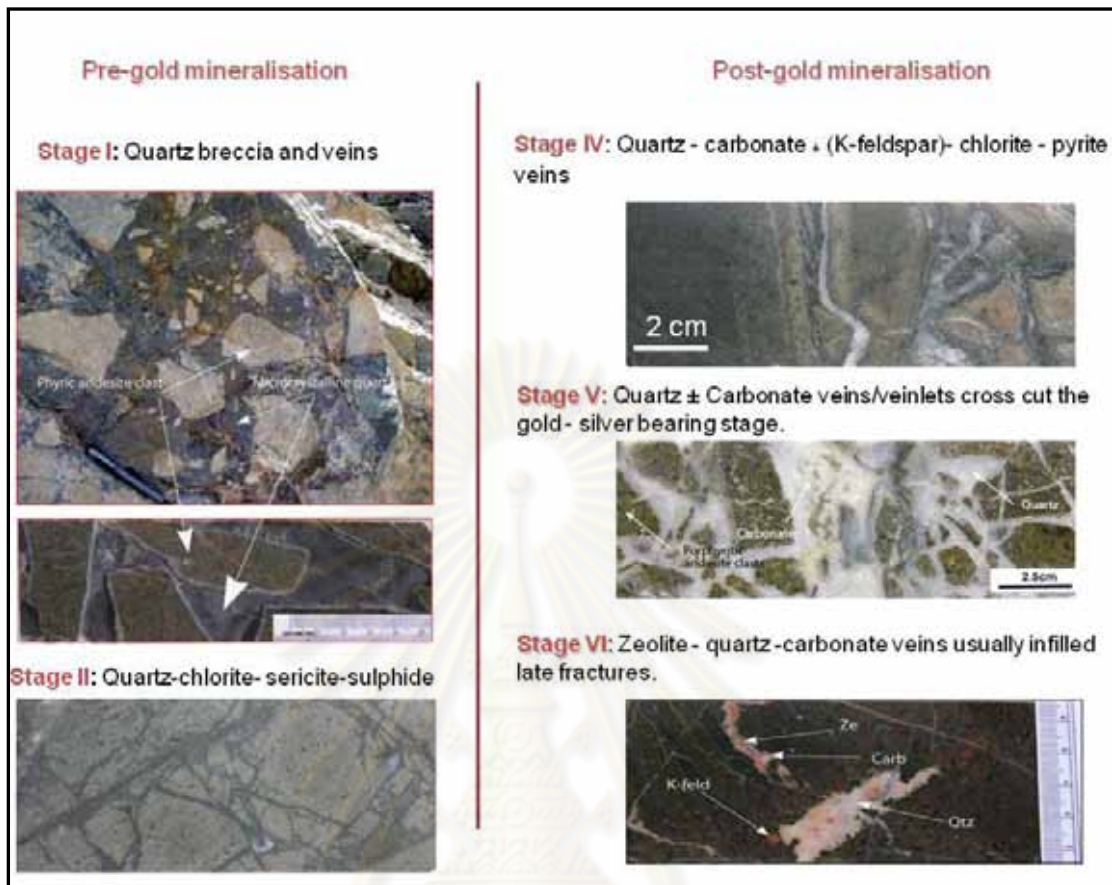
Figure 2.8 Summary of vein styles of pre-gold mineralization and post-gold mineralization (modified from Salam, 2010). Details: **Stage I** shows grey silica breccia/veining with strong silicified angular clasts of porphyritic andesite; **Stage II** shows quartz–chlorite–sericite–sulphide matrix of pyroxene pyric andesite breccias clasts; **Stage IV** shows quartz-carbonate-chlorite cut through polymictic andesitic polymictic andesitic lithic breccias; **Stage V** shows jig saw fit breccia, matrix of carbonate±quartz assemblage; and **Stage VI** shows zeolite-quartz-carbonate- veins cut through porphyritic andesite.
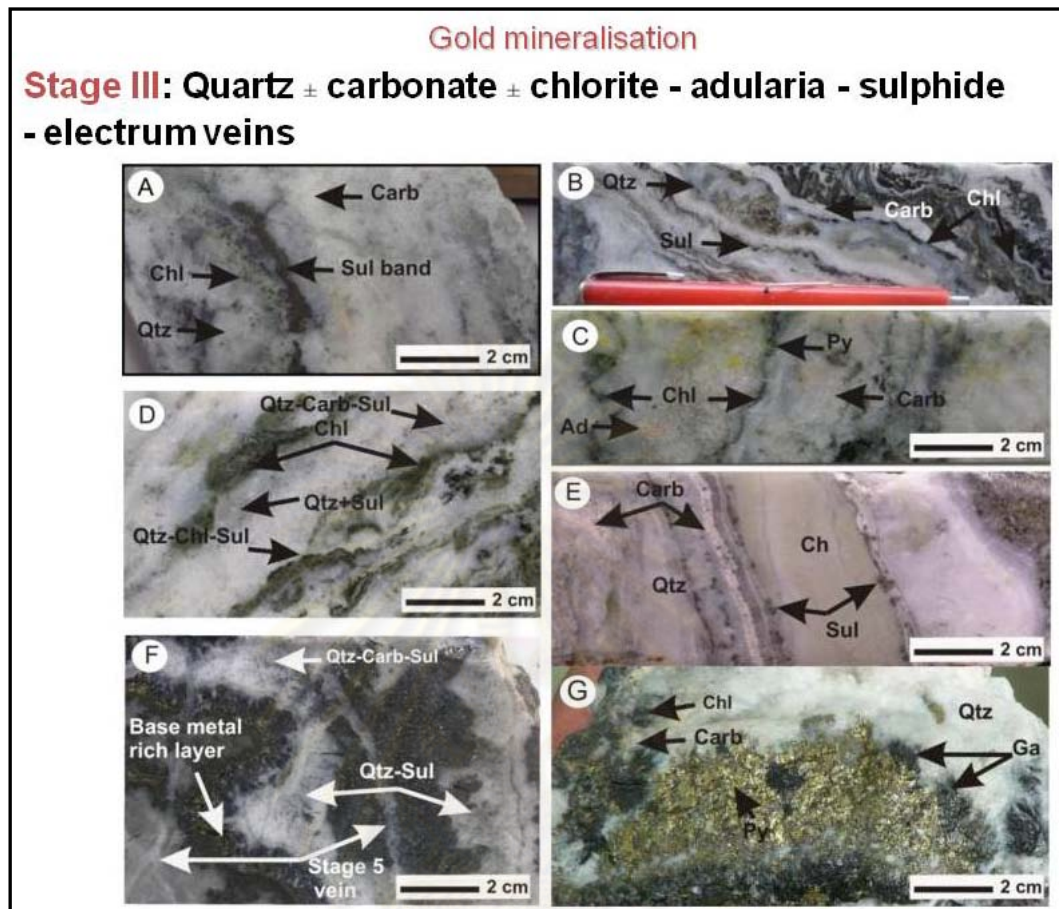
Figure 2.9 Summary of vein styles and gold mineralization (modified from Salam, 2010). Details: A; Sulphide-rich layer and patches in quartz±carbonate±chlorite vein, B; Well banded quartz, carbonate, chlorite and chalcedony with sulphide layer (dark), C; Quartz±carbonate±chlorite±sulphide vein, quartz-carbonate banded. Adularia (pink) and stained in yellow (top), chlorite layers (dark), D; Quartz±carbonate± chlorite±sulphide vein, moderately banded with chlorite bands, E; Well banded quartz, chalcedony with thin sulphide layers, F; Base metal rich quartz-carbonate vein, coarse-grained sphalerite-galena-chalcopyrite band (left) and fine disseminated (white), and G; Coarse-grained sulphide mainly pyrite and marcasite (?).

2.6 Alteration

Dedenczuk (1998), Greener (1999), Krompkhun (2005) showed that zones of silicification, argillic and phyllic alteration assemblages were common. Silica and chalcedony occurs as isolated zones in the lower parts of the succession (in the plagioclase and hornblende phyric andesite in the C and H Zones) and as pervasive silica alteration in the fine volcaniclastic and epiclastic sedimentary facies in and around the position of the ore body in the A and Q Prospects. Argillic and phyllic alteration assemblages include illite, smectite (and montmorillite), pyrite, and kaolinite. Phyllic alteration assemblages include illite, illite-smectite and sericite has been observed at the H zone. Argillic alteration occurs as replacement above the ore zone in the H Pit and illite, smectite-illite decreases with distance away from the ore body

James and Cumming (2007) suggested the alteration assemblages at Chatree are 1) Silica, 2) Sericite-illite-quartz-pyrite, chlorite-(epidote)-calcite-pyrite, montmorillonite-interlayered illite-smectite, and 3) K-feldspar-quartz-sericite-pyrite.

Pervasive silica is the earliest alteration phase and occurs in stratigraphic Unit 2 specifically in the fine-grained volcano-sedimentary facies, rhyolite and dacite breccia and quartz-rich fiamme breccia. The most highly silicified zones have replaced both clasts and matrix in the rhyolitic and dacitic breccias. Higher gold grades correlate well with these silicified zones.

Sericite-illite (illite-smectite)-quartz-pyrite alteration has been related to gold-bearing mineralisation (Stage 3) and occurs in the lower stratigraphic units particularly in volcaniclastic and coherent rocks. This alteration is directly related to quartz± carbonate±chlorite±adularia-electrum veins/veinlets and occurs as haloes (with variable thickness) on the margins of these veins.

More intense (propylitic) chlorite-epidote-calcite-pyrite (± epidote) alteration occurs lower down in the succession (in Units 4 and 3) and is related to the post-mineralized quartz-carbonate-adularia ± chlorite veins.

The alteration from James and Cumming (2007) was summarized in Table 2.1.

Table 2.1 Summarized alteration assemblages of Chatree gold deposit (James and Cumming, 2007).

Alteration assemblages	Mineral assemblage and texture	Location
Silicic	Silica Quartz and chalcedony	As isolated zones in lower stratigraphic units 1 and 2 and pervasive through stratigraphic unit 3 and associated with ore zone
Argillic	Kaolinite, montmorillite and illite - smectite	Blanket like zone of hanging wall in H zone; occurs at shallow depths
Phyllic	Illite, illite – smectite and sericite	
Propylitic	Illite – Chlorite-quartz-epidote-carbonate –chlorite-sericite- hematite and epidote-chlorite-illite	Occurs in lower parts of the stratigraphy in C-H zone in the Plagioclase phyric andesite and lower Polymictic breccia facies
zeolite	laumonite	Upper zone of H Zone

CHAPTER III

GEOLOGY, MINERALIZATION AND ALTERATION AT
THE A PROSPECT

3.1 Lithology and Stratigraphy

In the generalized stratigraphy of the Chatree gold deposit, the host rocks of the area generally comprise four units. However, in the A Prospect only Units 1 to 3 are described in details in ascending order hereafter while the lowest unit (andesite porphyry of Unit 4) is omitted due to the insufficient depth of drilled holes (Figure 3.1). The stratigraphic units of the A Prospect from higher to lower sequences are the following; Unit 1: Fiamme breccias unit, Unit 2: Epiclastic and fine volcaniclastic sedimentary interbedded with rhyolite breccia unit, and Unit 3: Polymictic and monomictic andesitic breccia unit.

The Unit 1 of the A Prospect is fiamme breccia consisting of 2 facies, namely, quartz-rich and lithic-rich facies. Single bed is more than 40 m thick and may be up to 100 m thick. Cumming et al. (2006) classified this rock unit based on the presence of fiamme and the amount of quartz versus other lithic fragments. Lithic-rich fiamme breccia has only 5% quartz (Figure 3.2) whereas quartz-rich rhyolitic fiamme breccia contains upto 30% quartz (Figure 3.3). In general, this unit is grey to green in color due to the high percentage of dark-green-chlorite-altered fragments (Salam, 2006). The lithic clasts consist of aphyric to plagioclase phyric and chlorite fragments which are finely vesicular and occasionally silicified lithic clasts. As compared with other units, the rocks of this unit are rather dense, least silicified and poorly mineralized, which suggests that they were not strongly affected by hydrothermal fluid.

The Unit 2 of the A Prospect is the interbedded/intercalated epiclastic or volcaniclastic sediments and polymictic rhyolitic breccia, breccias (Figure 3.4). This unit has the continuous contact with the upper fiamme unit in such a way that the transition zone comprises quartz-rich rhyolitic fiamme breccia interbedded with brown volcanic siltstone and sandstone. Salam (2006) found the evidence of mineralization in quartz-rich rhyolitic faimme breccia in the transition zone, which implies that the quartz-rich rhyolitic fiamme braccia of the uppermost unit was pre-mineralization.

The volcaniclastic sandstones and siltstones and pebbly sandstones contain less than 2mm rounded to angular plagioclase crystals, andesite fragments and Fe-Ti oxide grains. Most of this unit depicts thinly bedded, well sorted and gradational from mud or silt size to sand size. This pattern has suggested that their origin in localized reworking and weathering of the andesitic centre nearby and deposited by turbidity currents or local mass flow of the regional andesitic source. In part, the rocks are finely-laminated to thinly-bedded with dark grey to black carbonaceous mudstone. In addition, crystal-rich rhyolitic sandstone is also found interbedded, as gradational to thinly-bedded, with siltstone and mudstone in the area in directly associated with the rhyolite breccia facies (briefly described). This sandstone is composed of dominant rounded-clear-quartz grains, plagioclase crystals and occasionally andesite and rhyolite lithic grains, which have the sizes less than 2mm. Such evidence indicates that not only the local rhyolitic breccia facies, but also other source areas in the region were also reworked as well. All evidences demonstrated that they were deposited in subaqueous conditions below the wave base in a shallow marine environment (Cumming et al., 2006).
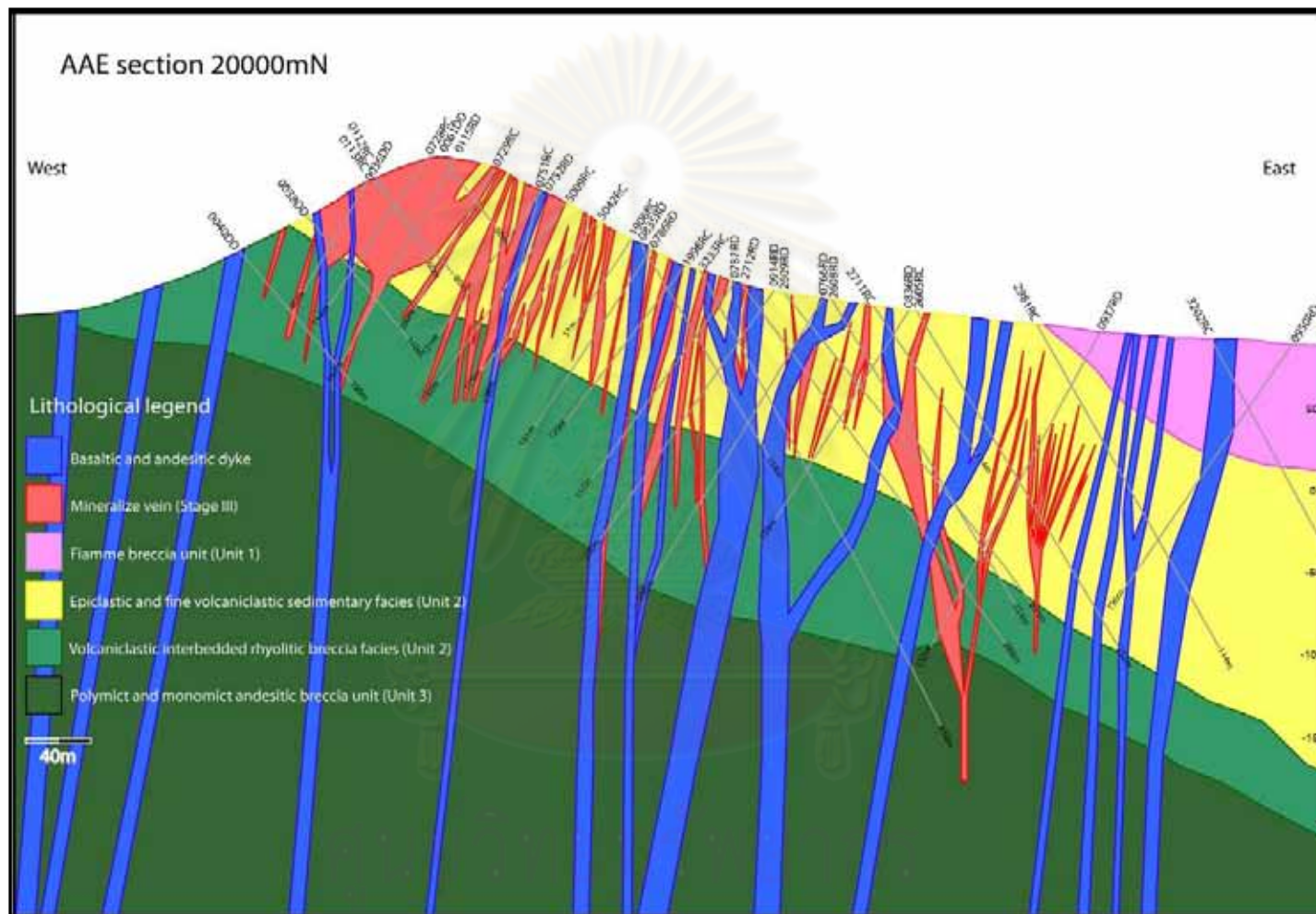
Figure 3.1 East–West cross section 20000mN of the A Prospect showing generally east dipping (Looking north) of three host rock units (Unit 1 is pink, Unit 2 is yellow and light green, Unit 3 is dark green), with mineralized vein (stage III; red) and all cut by dyke (blue).
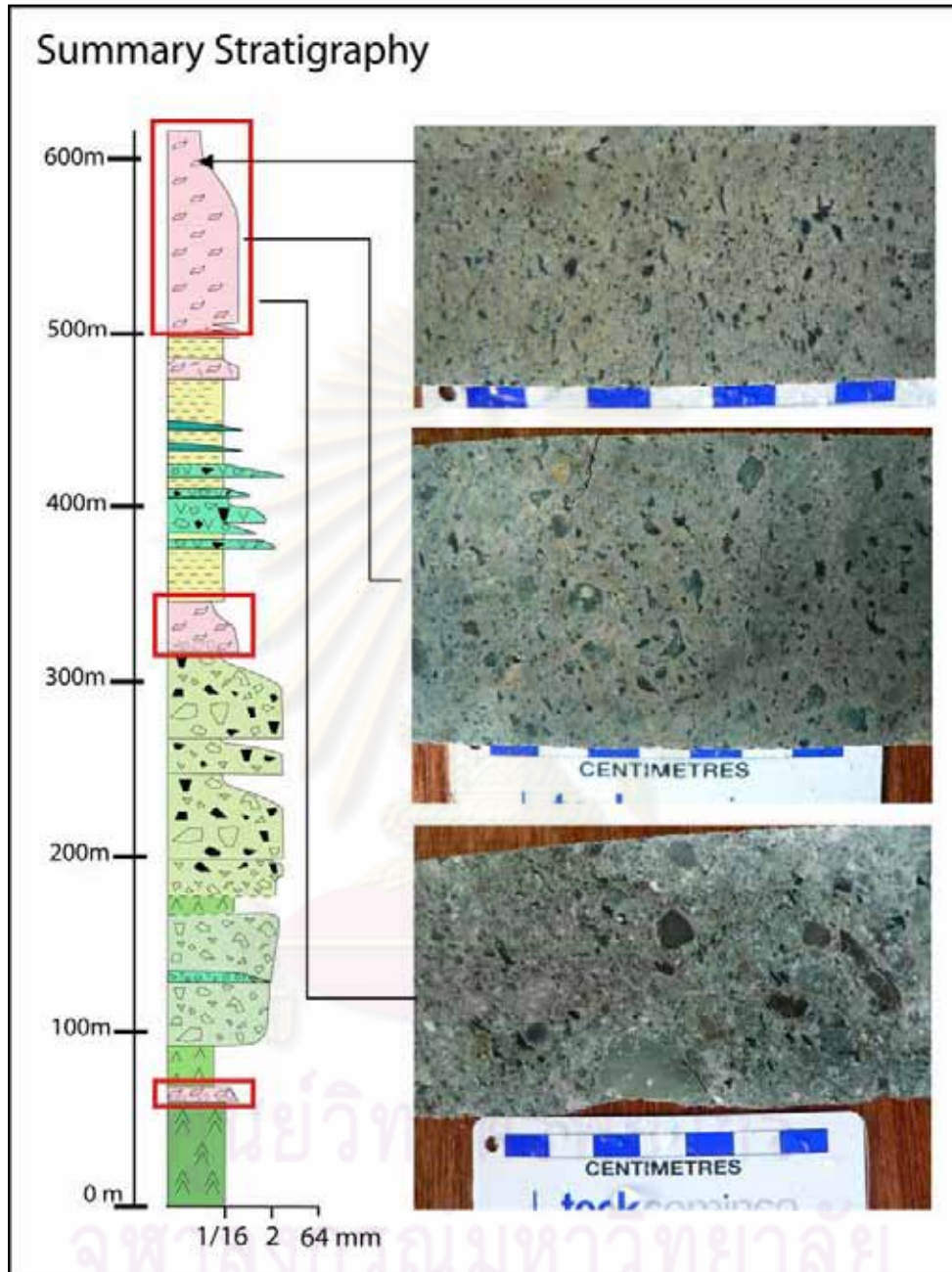
Figure 3.2 Stratigraphic column showing the upper Unit 1 of lithic-rich fiamme breccia with slab samples (Salam, 2008).
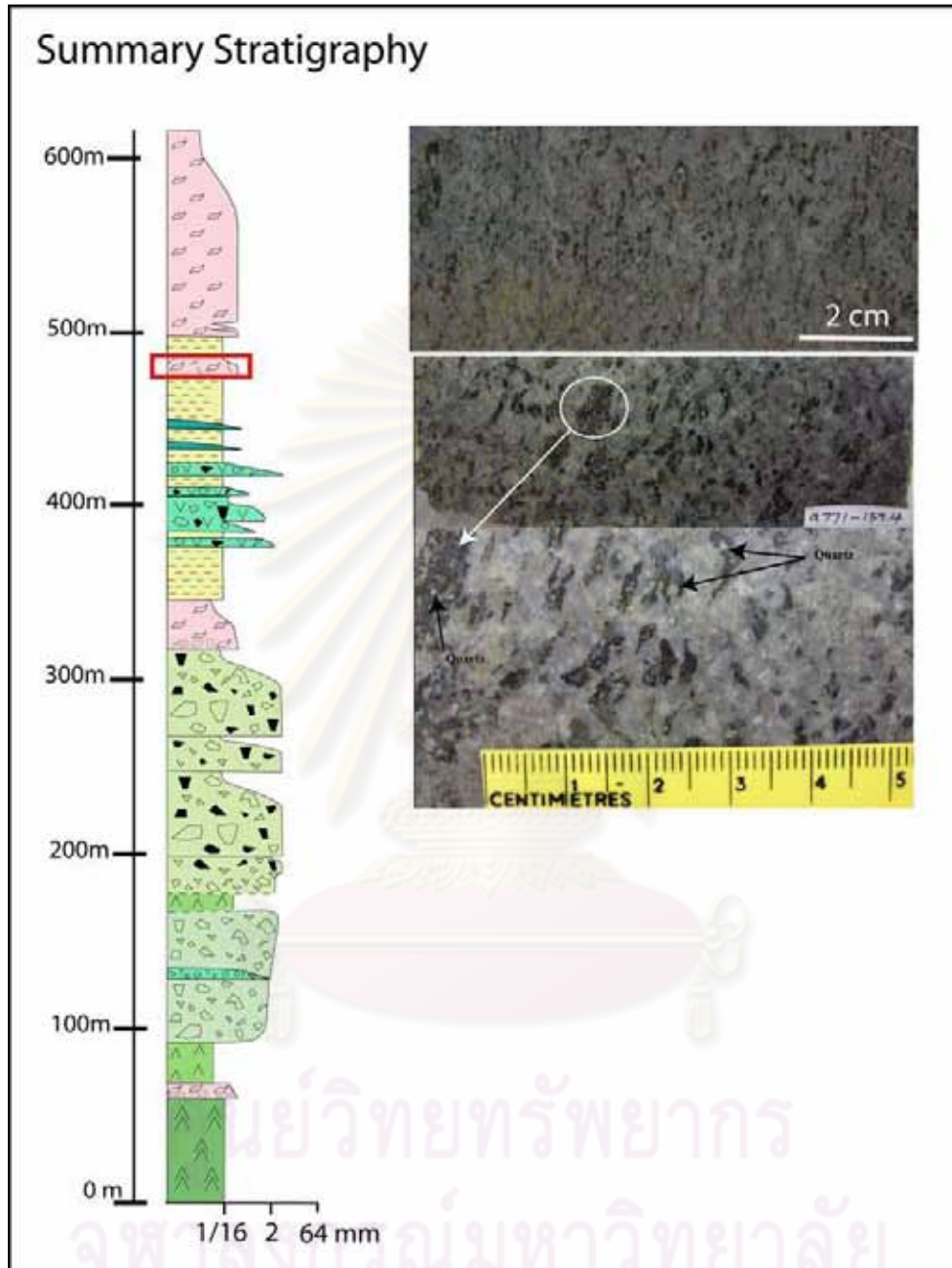
Figure 3.3 Stratigraphic column showing the upper Unit 1 of quartz-rich fiamme breccia with slap samples (Salam, 2008).

.
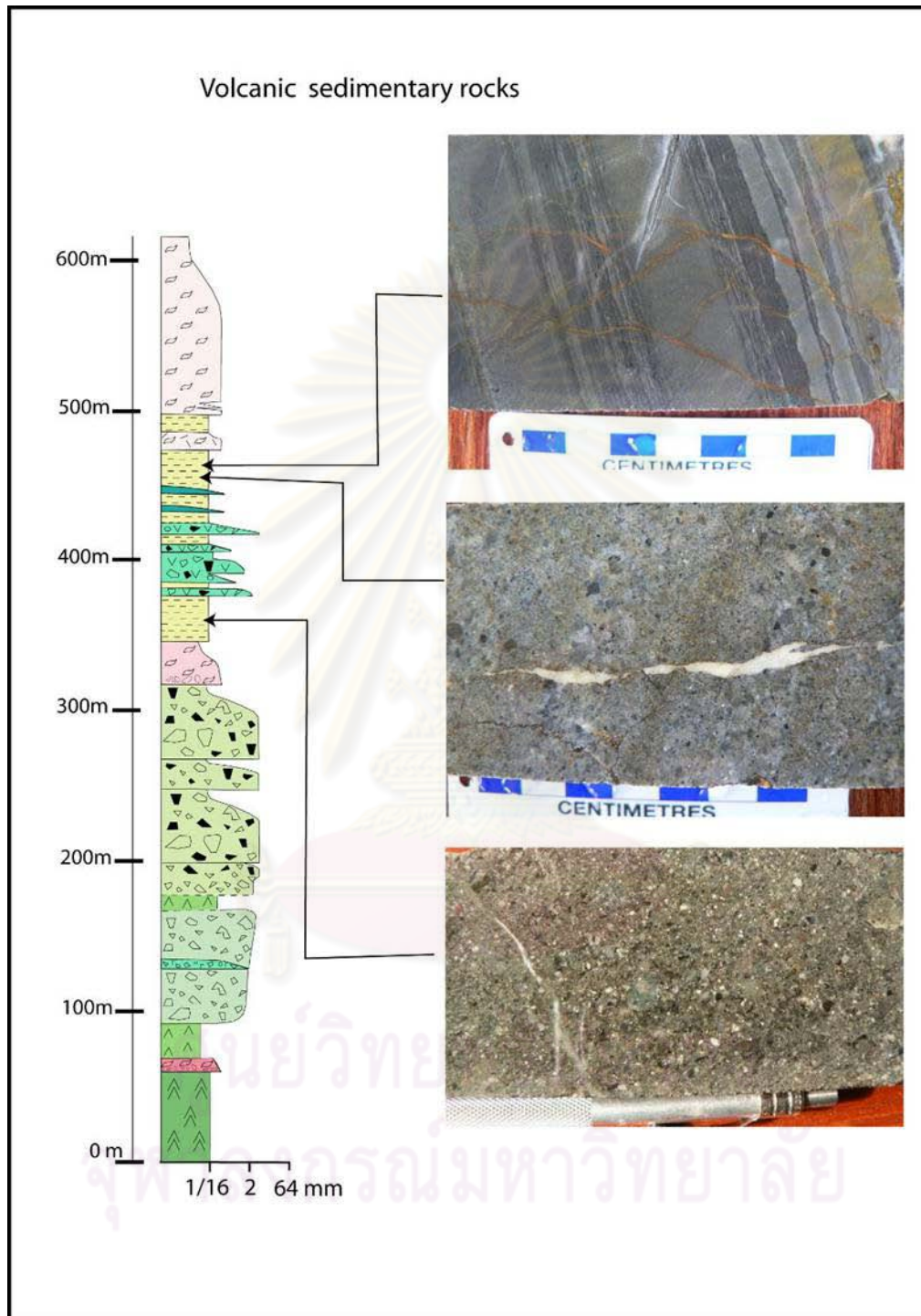
Figure 3.4 Stratigraphic column showing middle Unit 2 of volcanic sedimentary and epiclastic rocks with slab samples (Salam, 2008).

Moreover, rhyolitic breccia facies are also mapped as a part of the middle unit in the A Prospect (Figure 3.1). Polymictic rhyolitic breccia is composed of angular to rounded quartz-phyric-rhyolite clasts and plagioclase-to-hornblende-phyric-andesite clasts in sandstone and siltstone matrix. The rock shows clast-supported and rounded rhyolite fragments which indicate that rhyolite was re-worked and re-deposited in sedimentary hosts.

Fiamme rock is partly found in the A Prospect, It is believed that the same sequence of middle fiamme facies is also occurs at the H Prospect hanging wall. This facies is light gray to light brown and comprises angular to subangular clasts of fiamme for the most part and minor andesite clasts. It forms at the base of polymictic andesitic lithic breccia and volcanic sedimentary rocks. Locally dark gray limestone underlies this fiamme facies.

The lower part of Unit 2 shows the intercalation between dominant volcanic sedimentary rock and polymictic andesitic breccia. These subunits are composed mostly of volcanic mudstone and sandstone at the top and carbonaceous mudstone at the bottom. Matrix rich polymictic andesitic breccia and lithic rich polymictic andesitic breccia are also formed as thin lenses in the lower part of Unit 2 (Salam, 2006).

The Unit 3 is polymictic and monomictic andesitic breccia. The polymictic andesitic breccia is very thick bed (up to 40m thick), poorly sorted, and comprises mainly subangular-to-angular andesite fragments. Five types of clast have been observed in this unit as dominantly subangular-plagioclase-phyric andesite and plagioclase-hornblende-phyric andesite clasts, minor chlorite-replaced clasts, and rarely mudstone and aphyric-amydaloidal-basalt clasts (Figure 3.5). Cumming et al. (2006) suggested that this subunit was deposited in debris avalanche and mass flow processes, which were evident from angular clasts, poorly sorting, fewer abrasion clasts, and reworked and granulated aggregates consistent with fracturing, quench fragmentation and auto-brecciation of various lavas. The monomictic andesitic breccias occur as lense-like, poorly sorted and clast supported. All clasts are phyric andesite and irregular jigsaw clasts sitting in the same composition groundmass (Figure 3.6). Cumming et al. (2006) interpreted as auto-bracciated part of andesitic lava or shallow sill. This subunit is possible peperite or hyaloclastite.
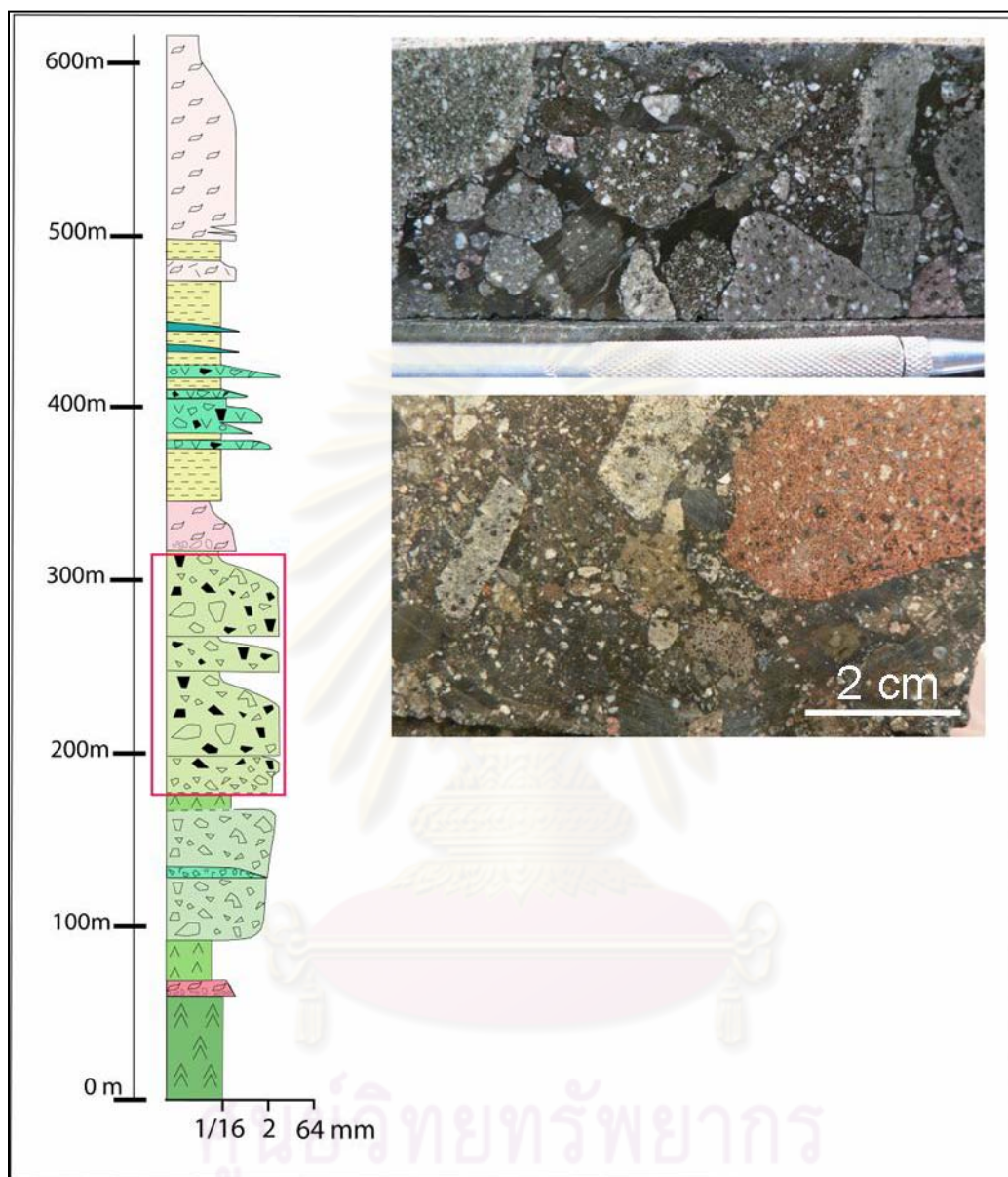
Figure 3.5 Stratigraphic column showing lower Unit 3 of polymictic andesitic breccia with slab samples (Salam, 2008).
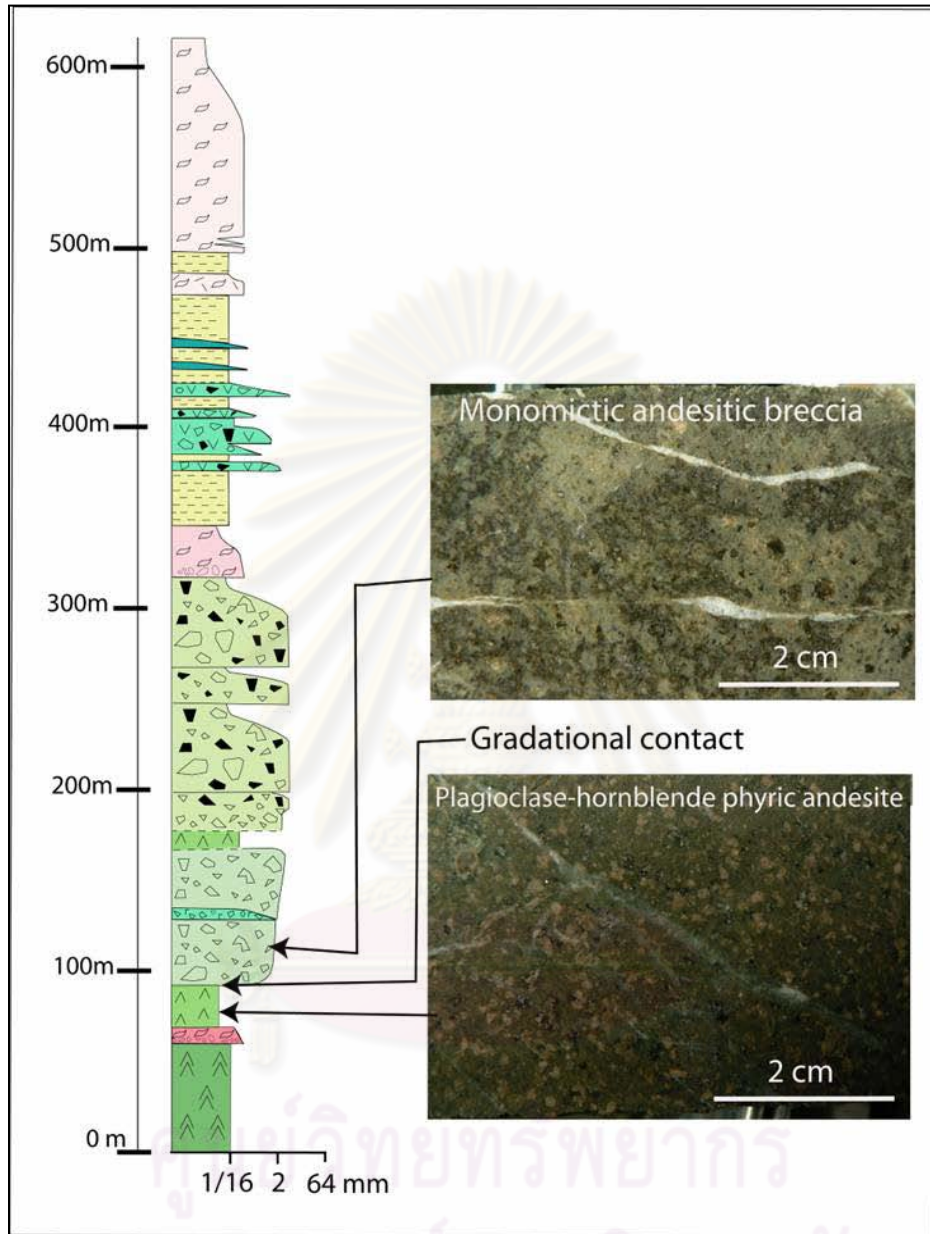
Figure 3.6 Stratigraphic column showing lower Unit 3 of monomictic andesitic breccia and plagioclase hornblende phyric andesite with slab samples (Salam, 2008).

3.2 Mineralization

This part presents the nature of mineralization including descriptions of vein morphology, texture, mineralogy and paragenesis. Moreover, this part also reports on the occurrence of ore minerals such as pyrite, chalcopyrite and sphalerite. The vein characteristics were carried out from detailed logging of drill cores. The petrographic study of mineral assemblage and texture was done by using thin sections, polished sections and polished thin-sections. Polished sections and polished thin-sections were also used for electron microprobe micro-analysis to find out the composition of some minerals.

The A Prospect of the Chatree deposit has many features such as age, tectonic setting and host rocks which are consistent with a low-sulphidation ephithermal deposit (Dedenczuk, 1998; Deimars, 1999; and Krompkhun, 2005). At least six vein stages have been identified in the A Prospect based on those of Tomkinson (2004), Cumming et al. (2006), Salam (2007), Salam (2010) and this study. Major vein structures of the A Prospect mineralization zone are oriented in NNW and NW directions with 50-60° SW dipping and structure extending to a total distance of 2 km.

The followings are vein morphology, texture, mineralogy and paragenesis documented from early Stage I to late Stage VI.

Stage I: Grey Chalcedony

The Stage I mineralization commonly occurs as grey silica breccia clasts in other stage veins or as rim of multi-stage veins. Consequently, Stage I lacks continuity and is not able to locate on the pit map and cross section.

Figure 3. 7 Photograph showing gray silica breccia clasts (Stage I) surrounded by quartz and non-ferroan calcite veins (Stage IV).

Stage II: Quartz–Euhedral Pyrite Vein

This stage is characterized mainly by milky quartz veins with minor non-ferroan calcite, chlorite patches, euhedral fine-grained pyrite (Figure 3.8) and sericite (Salam, 2010). Stage II vein mineralization looks very similar to the Stage III veining but the Stage II lacks of continuity and contain few amount of gold grade (less than 0.1 g/t Au). This stage is separated from massive quartz-carbonate of Stage III by the shape of pyrite, which is mostly anhedral. The EPMA analysis shows the chemical composition of sphalerite $(Zn_{0.91}$ $Fe_{0.09})$ $(S_{0.89})$ with $Au_{0.05}$ (Table 3.1) that suggest sphalerite (Stage III) replace euhedral pyrite (Stage II) (Figure 3.9).
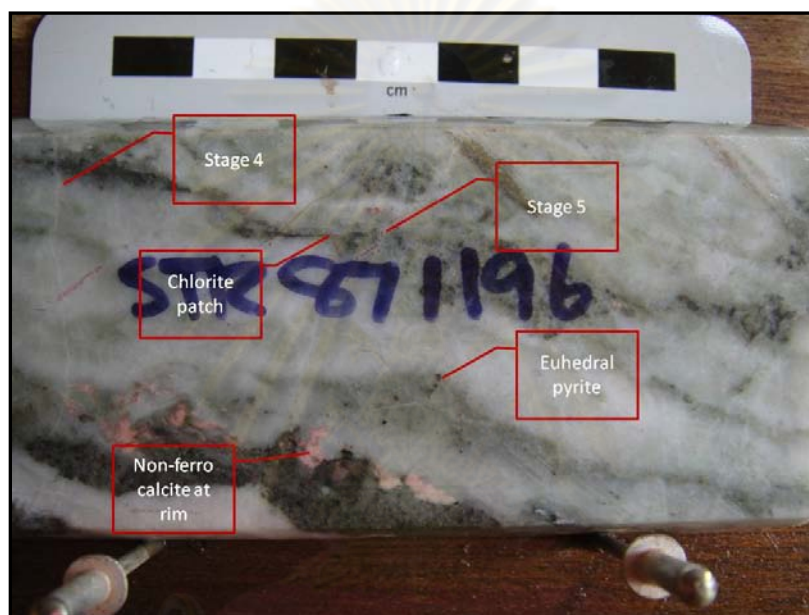
Figure 3. 8 Photograph showing Stage II vein comprising mostly milky quartz with minor non-ferroan (pink-stained) calcite, chlorite patch and euhedral pyrite. The Stage II vein is crosscut by Stage IV and Stage V veinlets (stained slab).

Table 3.1 The result of EPMA analyses of sphalerite (stage III) replaces euhedral pyrite (stage II) calculated in terms of atomic proportions.

No.	Sb	As	Ti	Mn	Au	Cd	S	Zn	Fe	Ag	Pb	V	Cu	Ni	Mo
2	0.00	0.00	0.00	0.01	0.05	0.00	0.84	0.88	0.08	0.00	0.00	0.00	0.00	0.00	0.00
3	0.00	0.00	0.00	0.01	0.05	0.00	0.85	0.84	0.11	0.00	0.00	0.00	0.01	0.00	0.00
4	0.00	0.00	0.00	0.01	0.05	0.00	0.84	0.87	0.09	0.00	0.00	0.00	0.00	0.00	0.00
5	0.00	0.00	0.00	0.01	0.05	0.00	0.84	0.84	0.11	0.00	0.00	0.00	0.00	0.00	0.00
6	0.00	0.00	0.00	0.01	0.05	0.00	0.84	0.85	0.09	0.00	0.00	0.00	0.00	0.00	0.00
7	0.00	0.00	0.00	0.01	0.05	0.00	0.84	0.85	0.11	0.00	0.00	0.00	0.00	0.00	0.00
11	0.00	0.00	0.00	0.01	0.05	0.00	0.85	0.84	0.10	0.00	0.00	0.00	0.02	0.00	0.00
12	0.00	0.00	0.00	0.01	0.05	0.00	0.86	0.87	0.08	0.00	0.00	0.00	0.00	0.00	0.00
13	0.00	0.00	0.00	0.01	0.05	0.00	0.86	0.86	0.09	0.00	0.00	0.00	0.00	0.00	0.00
14	0.00	0.00	0.00	0.01	0.05	0.00	0.84	0.86	0.10	0.00	0.00	0.00	0.00	0.00	0.00
15	0.00	0.00	0.00	0.01	0.05	0.00	0.85	0.88	0.07	0.00	0.00	0.00	0.00	0.00	0.00
16	0.00	0.00	0.00	0.01	0.05	0.00	0.84	0.90	0.05	0.00	0.00	0.00	0.00	0.00	0.00
19	0.00	0.00	0.00	0.01	0.05	0.00	0.87	0.86	0.09	0.00	0.00	0.00	0.00	0.00	0.00
20	0.00	0.00	0.00	0.02	0.05	0.00	0.89	0.88	0.07	0.00	0.00	0.00	0.00	0.00	0.00
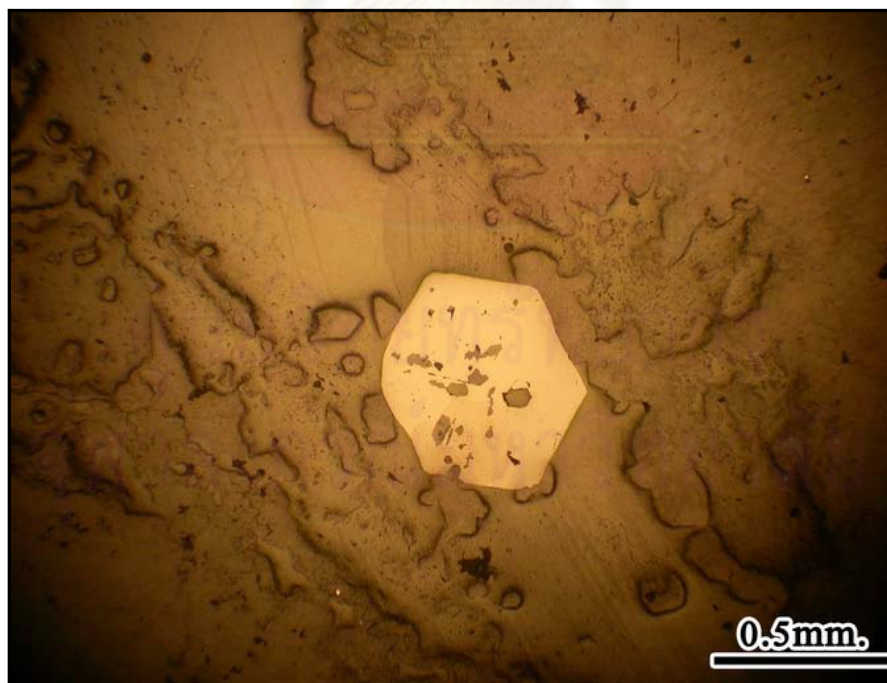
Figure 3. 9 Photomicrograph showing sphalerite (Stage III) replaces euhedral pyrite (Stage II) in quartz vein (reflected light).

Stage III: Major Gold Mineralization

This is the main gold mineralization stage of the A Prospect. The veins generally dip steep west (70° – 80°) and strike NNW, and vary from 1 cm to 20 cm in width.

There are three vein mineralization styles that are recognized in this stage, namely, crustiform–colloform banding, breccia filling and massive veining. Details of each style are described as follows:

a) Crustiform–colloform banding style: mineralised veins typically show crustiform and colloform banded texture and are normally associated with ore grade Au-Ag mineralization of the so-called "ginguro" (Corbett, 2002). Veins comprise mainly milky white quartz and chalcedony, minor chlorite and dolomite, trace hematite, ferroan calcite (Figure 3.10) and sulphide minerals. The sulphide minerals, which occur as band or layer, are composed of pyrite, sphalerite, chalcopyrite and electrum. The ore microscopy shows an intimately intergrown polymineralic sulphide aggregate in the Stage III veins (Figure 3.11). Electrum often forms at the rim of pyrite and as inclusions in pyrite grains. Small amounts of electrum inclusions were also observed in sphalerite and chalcopyrite grains.

This textural style also occurs as breccia filling that comprises angular silicified fine-grained sedimentary rocks cemented by crustiform-colloform banding of milky white quartz and chalcedony (Figure 3.12). The banding veins contain 8.22 g/t Au on the average (up to 71.30 g/t Au).

b) Breccia filling style: generally, this style comprises polymictic brecciated clasts of host rocks and early vein, gray silica, quartz, and andesite (Figure 3.13). The clasts are angular to subangular (size various from 1mm to 3 cm), poorly sorted and cemented by grey quartz, minor carbonate and trace disseminated pyrite in the forms of matrix support texture. Pyrite grains often contain inclusions of electrum and sphalerite (Figure 3.14). The breccia style contains 13.63 g/t Au on the average typically varies from 2.89 to 37.75 g/t Au.

c) Massive veining style: The mineral assemblages in veins are comprised major quartz (various varities such as milky, rock crystal and amethyst) and carbonate (mainly dolomite, subordinate ferroan calcite, and trace rhodochrocite) (Figure 3.15) with minor adularia and disseminated sulphides. The sulphide minerals comprise mainly pyrite with sphalerite and electrum inclusions (Figure 3.14). The massive veins can contain up to 137.05 g/t Au with 10.08 g/t Au on the average. Moreover, massive vein style can also form as cement of hydrothermal breccias and stockwork veining (Figure 3.16).
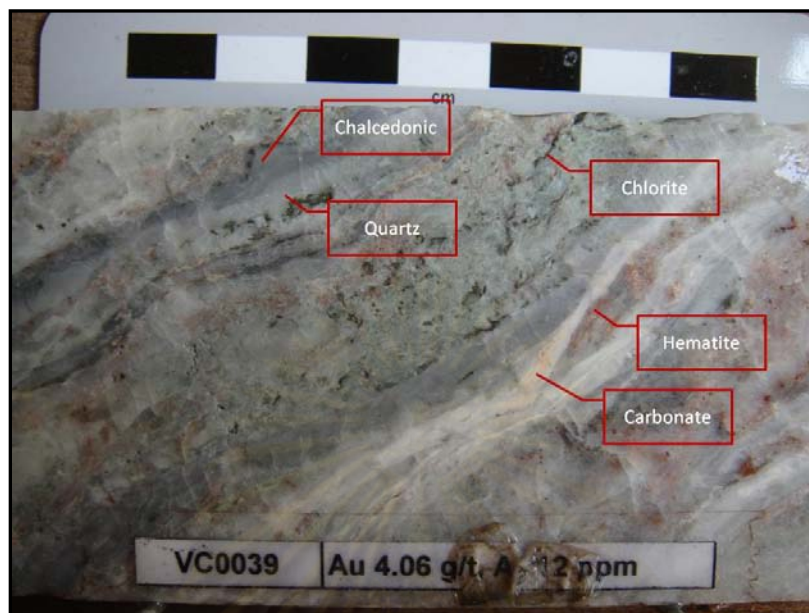
Figure 3. 10 Photograph displaying crustiform-colloform Stage III vein, which consists of quartz, carbonates (major dolomite and trace ferroan calcite), chalcedonic band with patches of chlorite and hematite.
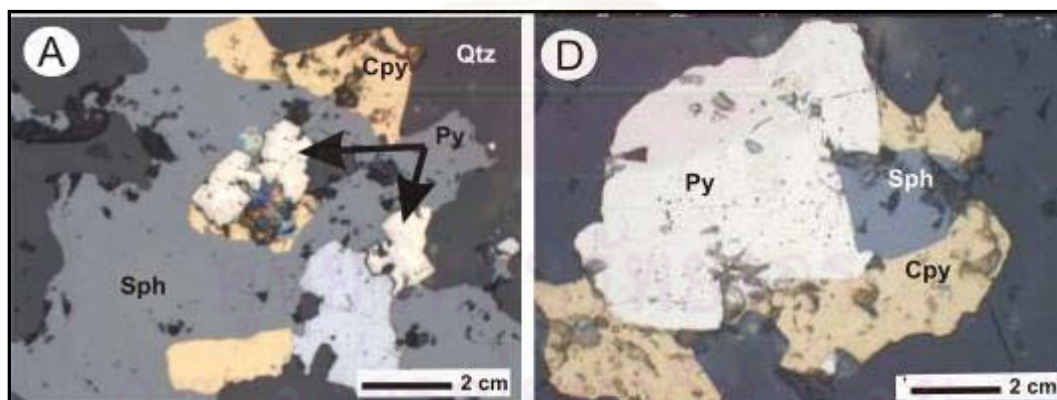
Figure 3. 11 Photomicrograph of sulphide banding (Stage III) mineralization showing A. Close association of pyrite, sphalerite, and chalcopyrite surrounded by quartz. D. pyrite associated with sphalerite and chalcopyrite (Figures from Salam, 2006).
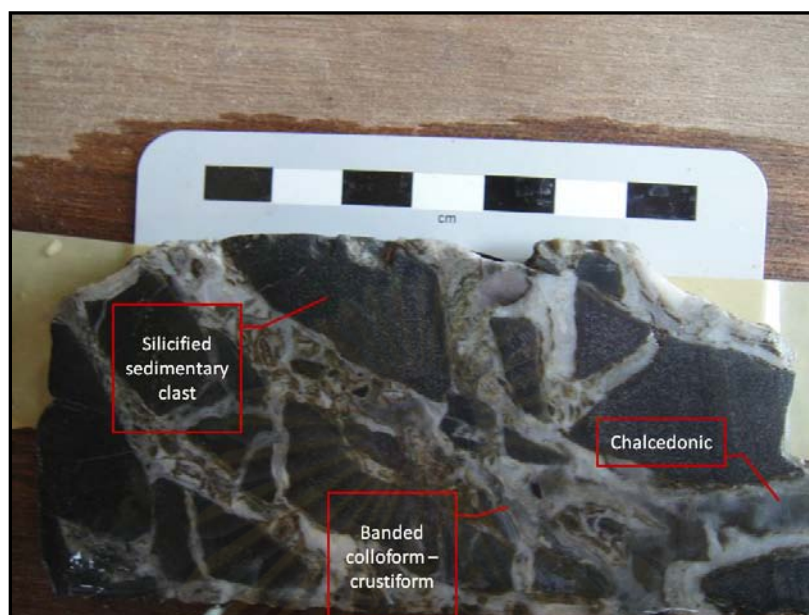
Figure 3. 12 Photograph showing angular silicified fine-grained sedimentary rock fragments cemented by crustiform–colloform banding of milky white quartz and chalcedony.
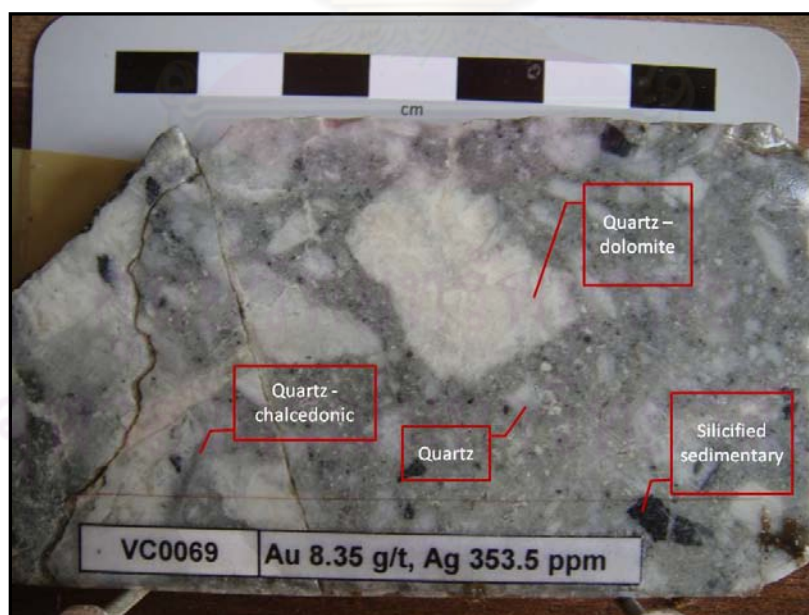
Figure 3. 13 Photograph displaying breccias of quartz, quartz–chacedony, quartz–dolomite and silicified lithic clasts that are cemented by grey quartz and minor carbonate
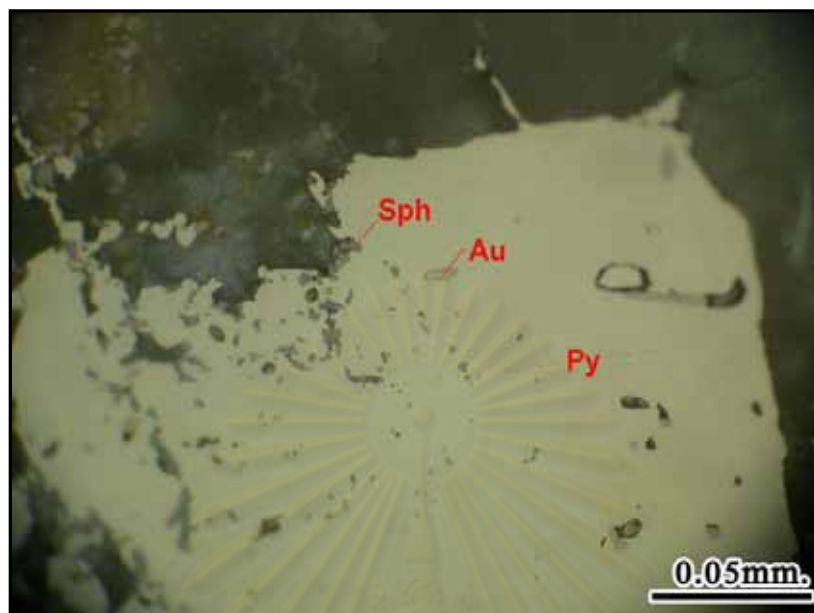
Figure 3. 14 Photomicrograph showing disseminated pyrite (Py) with sphalerite (Sph) and electrum (Au) inclusions (Reflected light).

Figure 3. 15 Photograph showing massive quartz-dolomite vein with disseminated patches of sulphides.
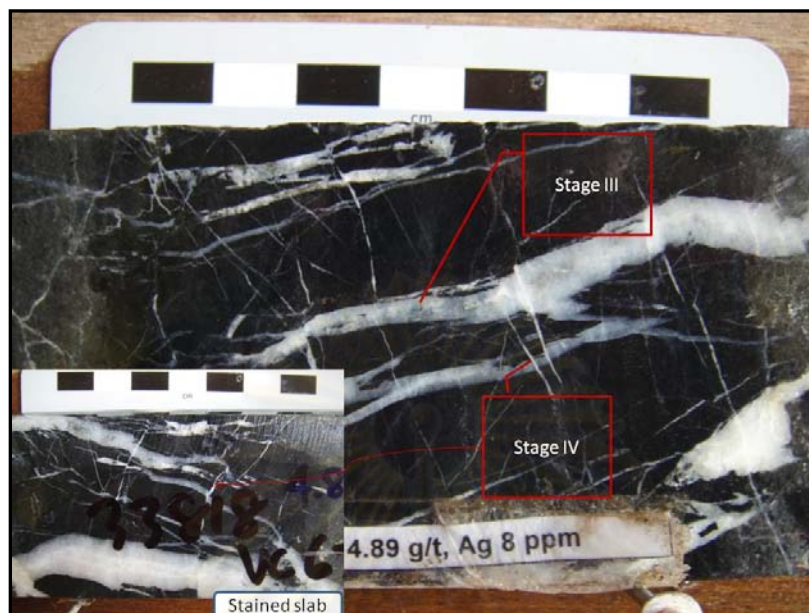
Figure 3. 16 Photograph displaying stockwork of quartz–dolomite veins (Stage III), crosscut by quartz-dolomite veinlets (Stage IV).

Stage IV: Quartz-Carbonate Veinlets

The stage IV mineralization is characterized by quartz-carbonate veins that clearly crosscut the stage III vein system. It typically is 1-2mm wide. The mineralization of the Stage IV veins is composed mainly of transparent quartz (Figure 3.16) with minor non-ferroan calcite, dolomite, rhodochrosite and pyrite. Pyrite is the major sulphide mineral in this stage that normally forms as sulphide-rich layers infilling the innermost veins.

Stage V: Non-ferroan Calcite Veinlets

The non-ferroan calcite veinlets form the fifth vein stage that crosscut all other vein stages and all rock units. The stage V veinlets are usually 1mm wide and also exist as small patches (Figure 3.17), discontinuous trails and stockworks in wall rocks. The stage V mineralization comprises essentially of non-ferroan calcite.

Stage VI: Zeolite Occurrence

The occurrence of zeolite marks the latest stage in the A Prospect. Zeolite fills fractures in late andesitic dykes (Figure 3.18).

Figure 3. 17 Photograph displaying non-ferroan calcite veinlets (Stage V) crosscut massive quartz-dolomite (Stage III) and gray chacedony (Stage I).

Figure 3. 18 Outcrop showing zeolite (pink) filling fractures in andesitic dyke (green).

3.3 Wall rock Alterations

In epithermal system, alterations vary laterally and vertically, often showing zonation in response to composition and temperature of fluid and the fluid interactive with wall rock. The hydrothermal mineral assemblages can be used as indicators of temperature range and fluid conditions. This section describes mineral alteration petrography and paragenesis based on diamond drill core logging (especially selected section; 20000mN), thin sections, carbonate staining and K-feldspar staining technique. These alterations are described following each rock unit:

Alteration in Unit 1: Fiamme breccia unit occurs at the top of the A Prospect sequence (Figure 3.1). This unit is poorly hosted the mineralization. Hand specimens show green fiamme clasts, 1mm to 3mm, sit in very fine grain groundmass (Figure 3.19). This unit does not react with cold diluted hydrochloric acid and is non-magnetic. As observed under microscopic, this unit is made up of fiamme clasts and volcanic clasts (Figure 3.20) in finer-grained groundmass consisting of major quartz and glass fragments with carbonates (Figure 3.20). Fiamme clasts commomly show bend layers affected by compression (Figure 3.20). The fiamme and volcanic clasts are completely altered to carbonates and chlorite (Figure 3.20). The alteration has destroyed much of the internal structure. The fractures are also sealed by carbonates (Figure 3.20). A rare amount of pyrite is present as disseminated grains.

Figure 3. 19 Photograph of core sample displaying completely chlorite-replaced-fiamme clasts of the fiamme unit.
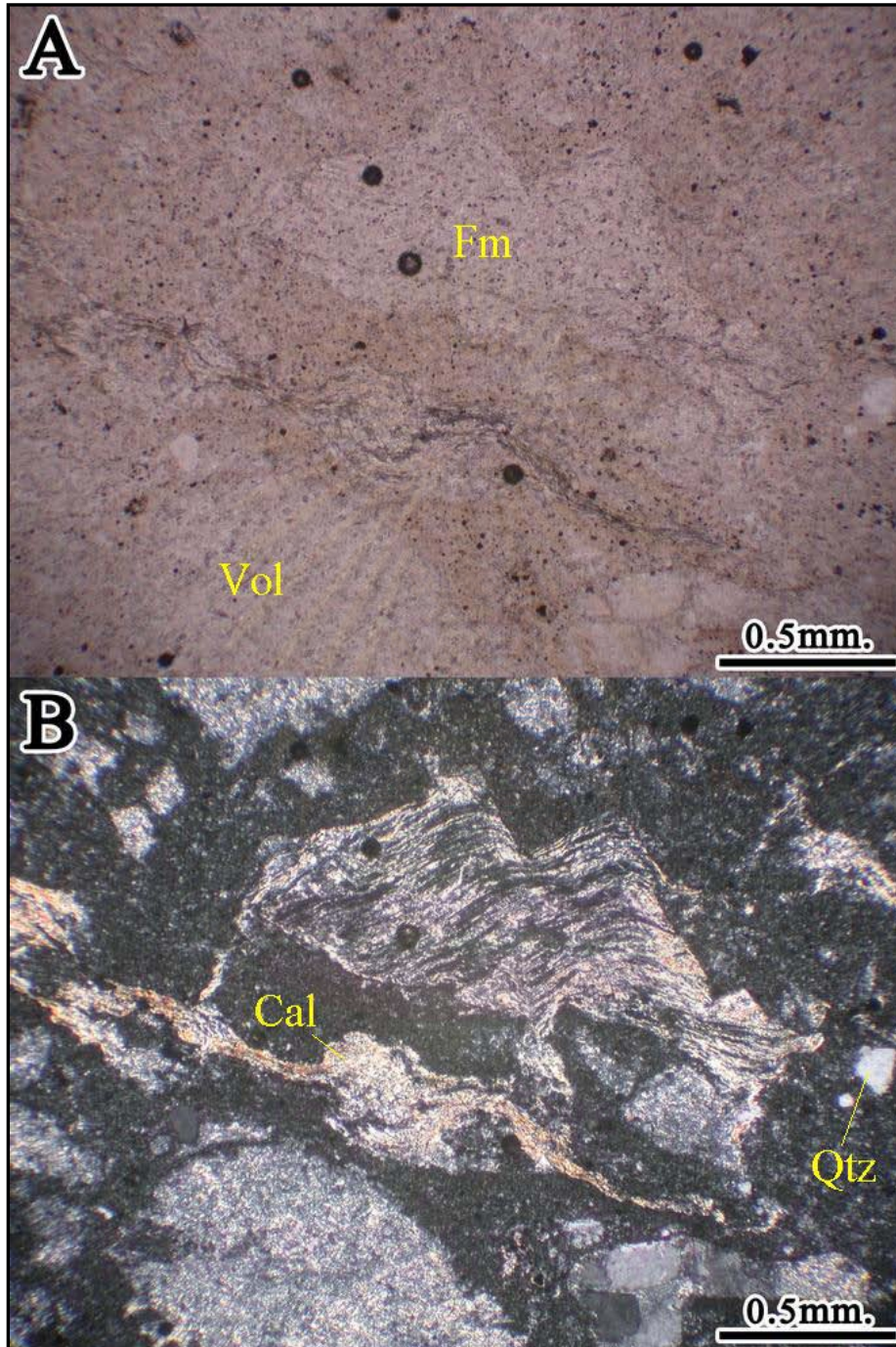
Figure 3. 20 Photomicrograph of fiamme breccias (unit 1) showing compressed and altered fiamme clast (Fm), volcanic clasts (Vol) and quartz fragments (Qtz) sit in fine-grained groundmass. Carbonate filled in fracture (Cal). (A) plane-polarized light, (B) crossed polars.

Alteration in Unit 2: epiclastic or volcaniclastic sediments with polymictic rhyolitic breccias unit are the main host rocks of the ore zone. The rocks proximal to the ore zone are subjected to two stages of alteration. Generally, silicification of Stage I is the earliest stage of alteration as the ground preparation stage and is characterized by gray chacedony flooding in the forms of pervasive alteration. The halo of stage I silicification is approximately 5–20 m from the vein zone. The stage III alteration is characterized by the occurrence of pink adularia, a low-temperature form of K-feldspar accompanying by silification. Adularia alteration halo can be identified by yellow staining test and occurs approximately 5–8 m from the vein zone (Figure 3.21).
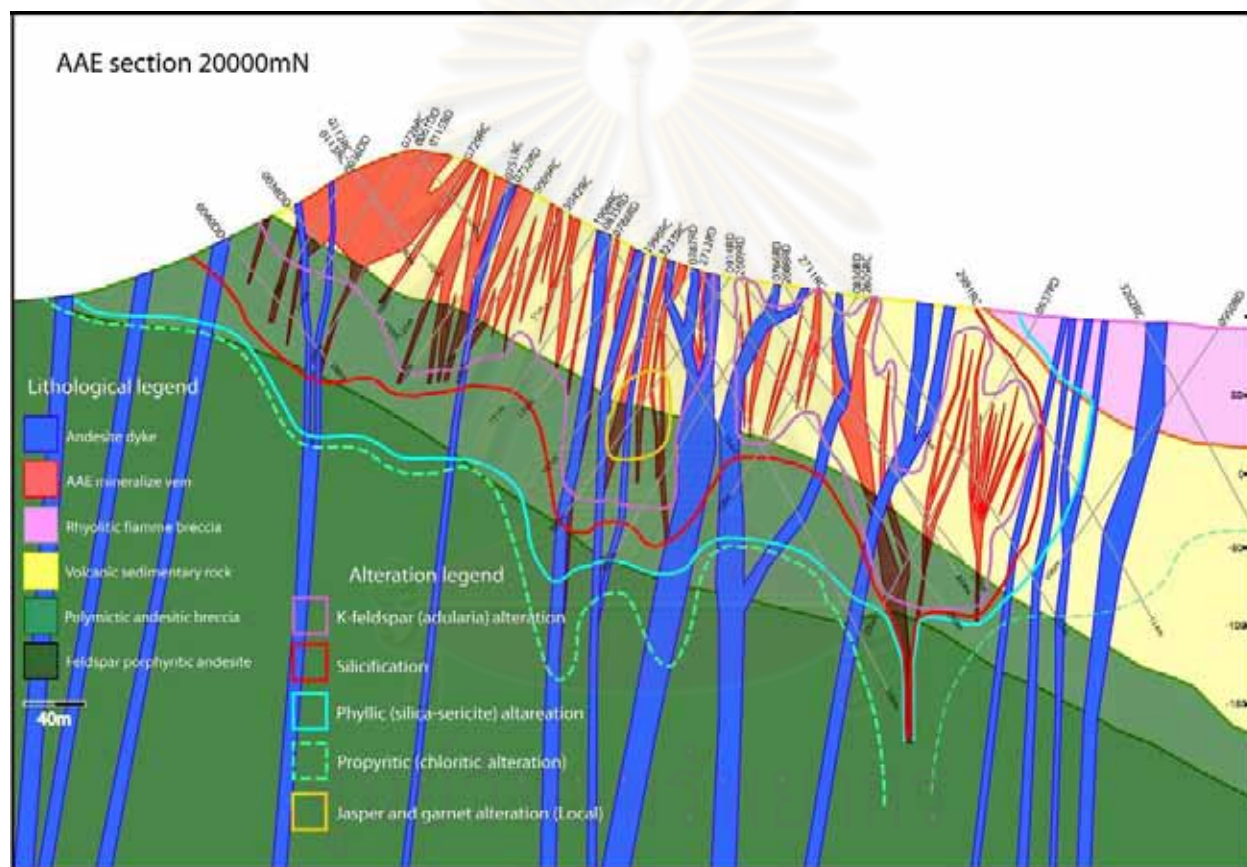
Figure 3. 21 Picture illustrating alteration halo on section 20000 mN.

Rocks Proximal to the Ore Zone

Alteration of Epiclastic Rocks

In hand specimens, epiclastic rocks show typical lamination of alternating light gray and very light gray layers, in which each individual thickness is up to 1.5 cm (Figure 3.22).
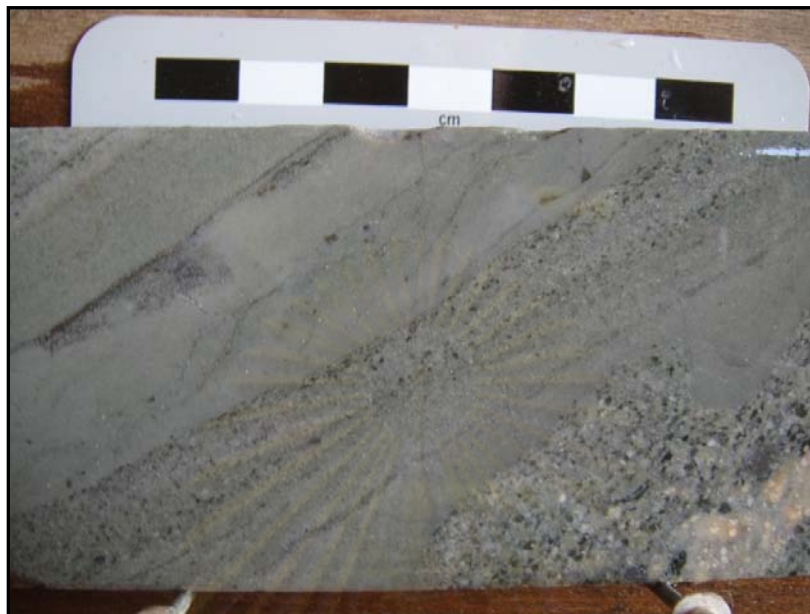
Figure 3. 22 Photograph of silicified laminated siltstone (Unit 2) displaying gradded lamination.

However, under microscope the light gray and very light gray layers are composed of the same minerals which constitute mostly of K-feldspar and quartz. The difference is that the light gray layers have grain sizes less than 0.005 mm across (Figure 3.23), whereas the very light gray layers have grain sizes in a range of 0.005 – 0.010 mm across (Figure 3.23). The medium dark gray to dark gray layers contains aggregates of quartz, K-feldspar and pyrite? (Figure 3.23). Micro-fractures in the rock are sealed by quartz, pyrite? (Figure 3.23) and calcite.
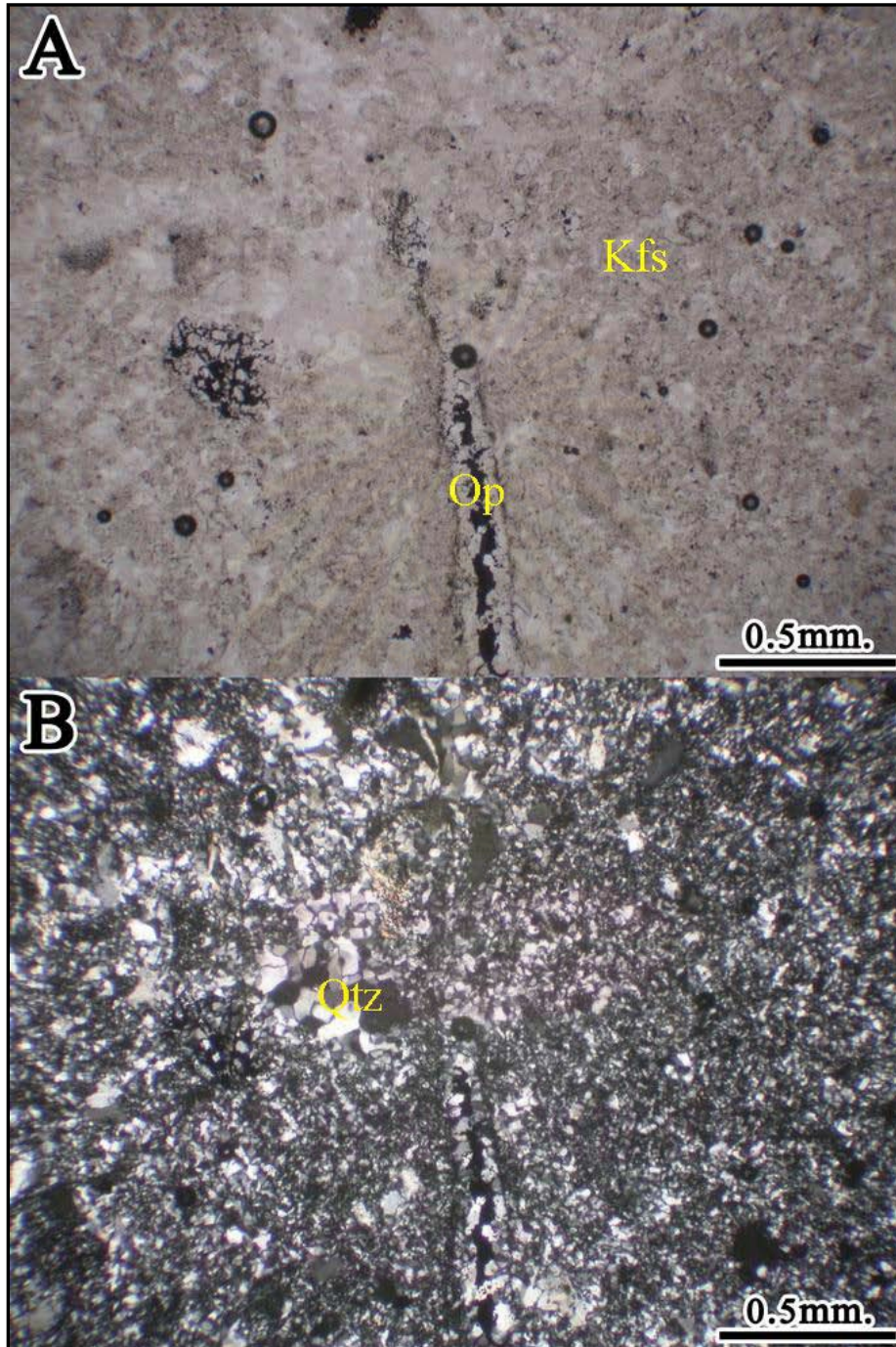
Figure 3. 23 Photomicrograph of silicified laminated siltstone (Unit 2) showing fine-grained quartz and K-feldspar (Kfs), drusy mosaic quartz (Qtz) and fracture sealed by quartz and opaque mineral (Op). (A) plane-polarized light, (B) crossed polars.

Moreover, in certain part of core slab, pink K-feldspar megacrysts (sizes up to 3 mm across) can replace very-fine-to-medium-grained, light-to-dark-gray epiclastic rocks which appear as spotted texture (Figure 3.24).
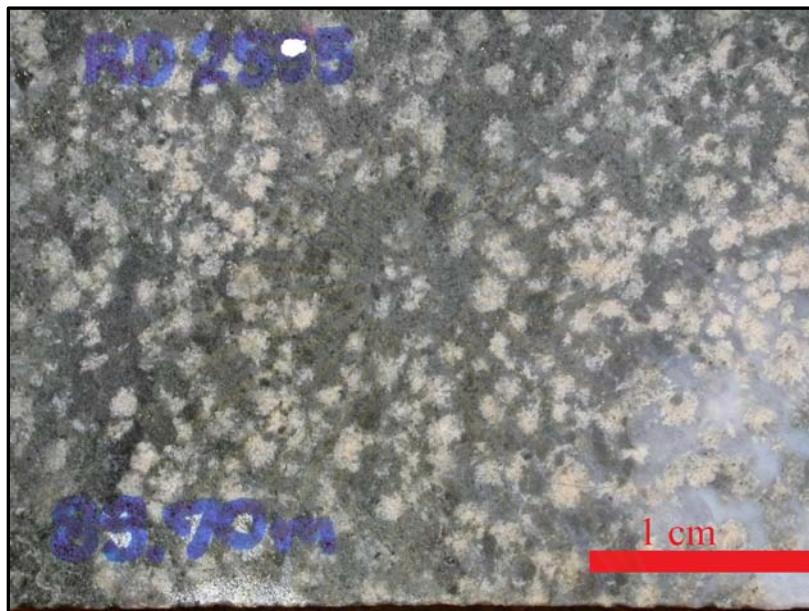
Figure 3. 24 Photograph of altered sedimentary rock (Unit 2) showing spotted replacement of pink adularia aggregate in light-to-dark-gray groundmass.

The microscopic observation reveals that almost all the spots as observed in hand specimen are K-feldspar aggregates commonly clouded with sericite/clay minerals (Figure 3.25), with grain sizes largely in a range of 0.1–0.15 mm across. These K-feldspar aggregates are embedded in the silicified matrix that are made up almost totally of variably sized quartz resulted from silicification (Figure 3.25), with minor chlorite patches, non-ferroan calcite and pyrite. Also abundantly present in the groundmass portion are cavities sealed by drusy mosaic quartz grains (Figure 3.25). Some drusy mosaic quartz has ferroan calcite at the cores. Larger quartz crystals formed as the silicification products (Figure 3.25) commonly display zonal patterns. This is also true for some quartz crystals as cavity-infilling. Some quartz grains, both as replacement products and as cavity-infillings, have ghost texture (recrystallization from moss texture) (Figure 3.25). The portions with medium light gray matrix have much less K-feldspar aggregates relative to the portions with medium dark gray matrix. Many non-ferroan calcite veinlets (Figure 3.25) are also present.

Originally, this rock was probably composed mainly of quartz (moss texture) and then it was recrystallized forming ghost texture, following by replacement of K-feldspar aggregates (showing spotted texture) partly overprinted by sericite/clay alteration that was related to quartz veinlets, finally, non-ferroan calcite veinlets crosscut earlier minerals.
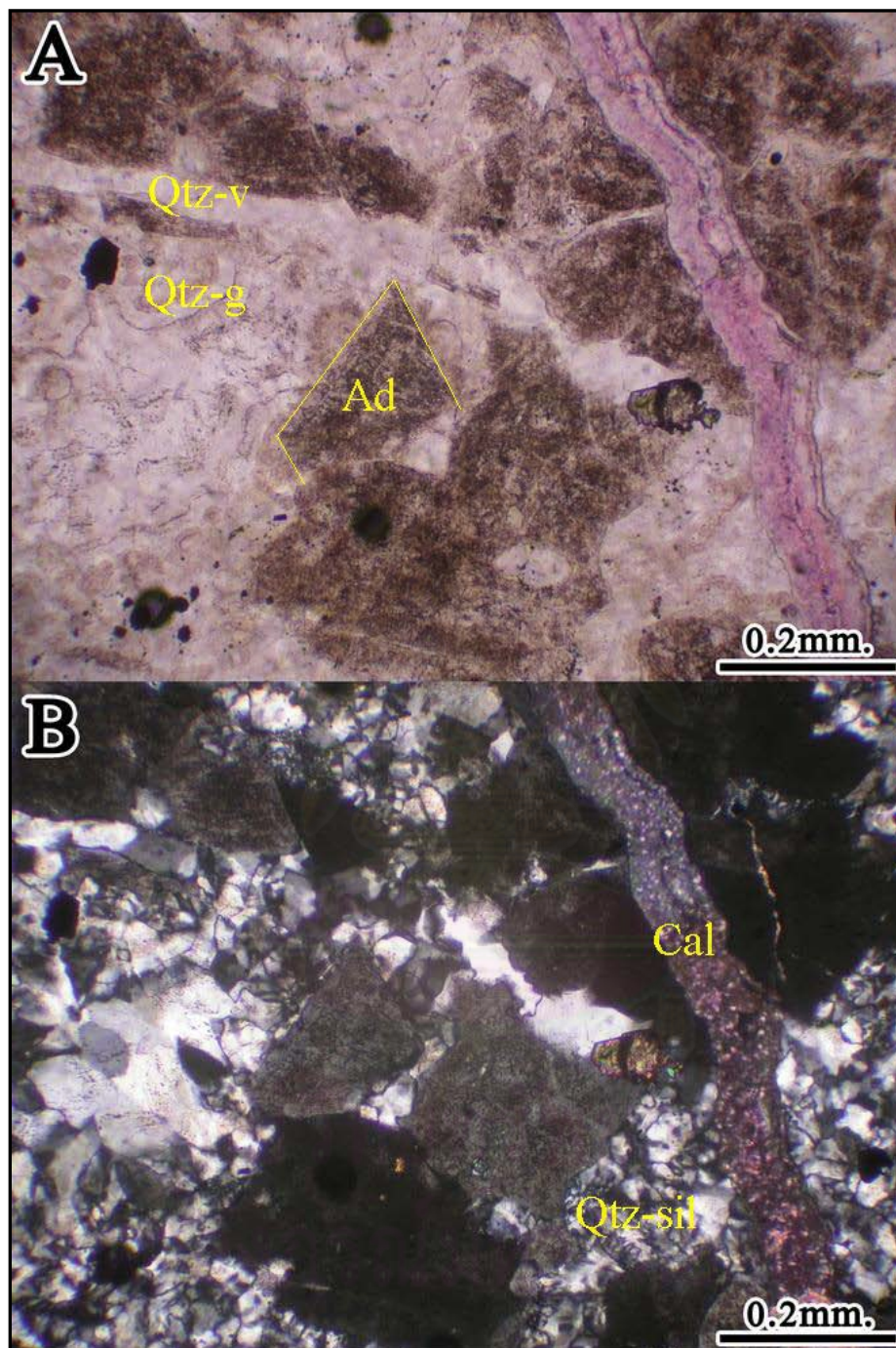
Figure 3. 25 Photomicrograph of spotted sedimentary rock (Unit 2) showing cloudy rhombic adularia aggregate (Ad) replacing chalcedonic quartz resulting from early silicified groundmass (Qtz-sil) with partly show ghost texture (Qtz-g). Fractures are filled by quartz (Qtz-v) and later crosscut by non-ferroan calcite veinlets (Cal). (A) plane-polarized light, (B) crossed polars.

<u>Alteration of Polymictic Rhyolitic Breccias</u>

On the core slabs, the rocks still show original fragmental texture of lapilli with the sizes up to 10 mm in finer-grained fragments and coarse ash. These fragments are white, pinkish gray and dark greenish gray (Figure 3.28).

Figure 3. 26 Photograph of polymictic rhyolitic braccia (Unit 2) showing relict polymictic lipilli and finer grained clasts in light gray matrix.

In thin sections the lapilli and finer-grained clasts comprise mainly volcanic rock fragments and minor fragments of feldspars and quartz (Figure 3.27). Volcanic rock fragments show subangular to rounded outlines and are aphyric to slightly phyric. The groundmass in volcanic fragments is glassy and/or very fine-grained feldspars (Figure 3.27) and/or quartz resulting from silicification (Figure 3.28). Feldspar fragments include both K-feldspar and plagioclase. They are subangular to subrounded and partly altered into and sericite and other clay minerals (Figure 3.27). Quartz fragments are subangular to subrounded (Figure 3.27), and may show rounded edges (Figure 3.27) and embayment. Rarely rim of feldspar have also been developed at the edges of these quartz fragments (Figure 3.28). Adularia crystals appear as euhedral to subhedral rhombic crystals, which may also occur as inclusions in feldspar rim (Figure 3.29). The groundmass is mainly replaced by feldspar and quartz crystalline mosaic resulting from potassic alteration.

After the formation of polymictic rhyolitic breccia, the rock was subjected to extensive silicification, after that it was partly replaced by quartz and feldspar as overgrowth with adularia inclusions and later some feldspar crystals were replaced by sericite. Finally, carbonate minerals overprinted.
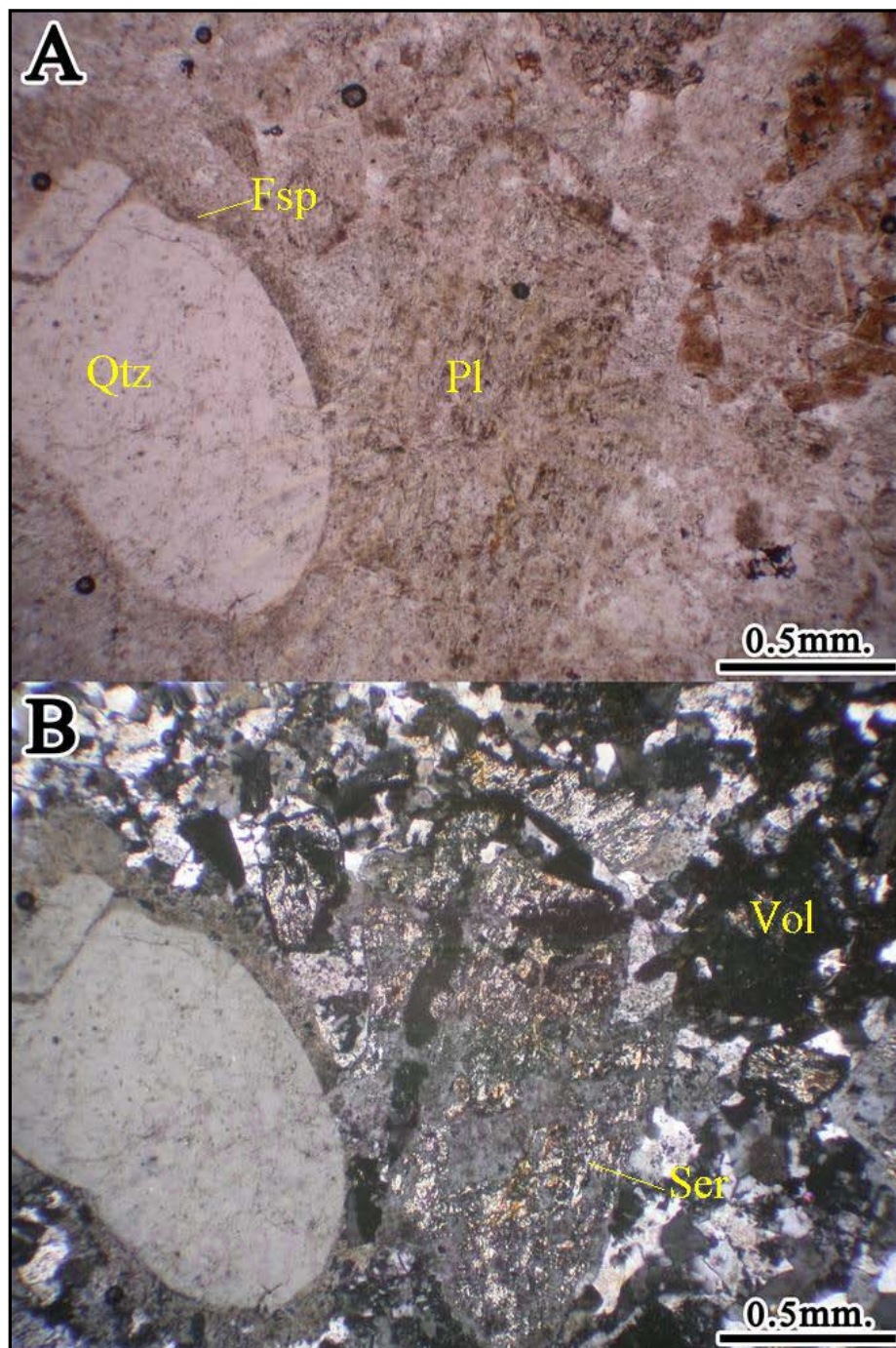
Figure 3. 27 Photomicrograph of polymictic rhyolitic breccias (Unit 2) showing rounded quartz grain (Qtz) with rim of feldspar (Fsp), large plagioclase feldspar (Pl) grains partly altered into sericite (Ser) and volcanic fragment (Vol). (A) plane-polarized light, (B) crossed polars.
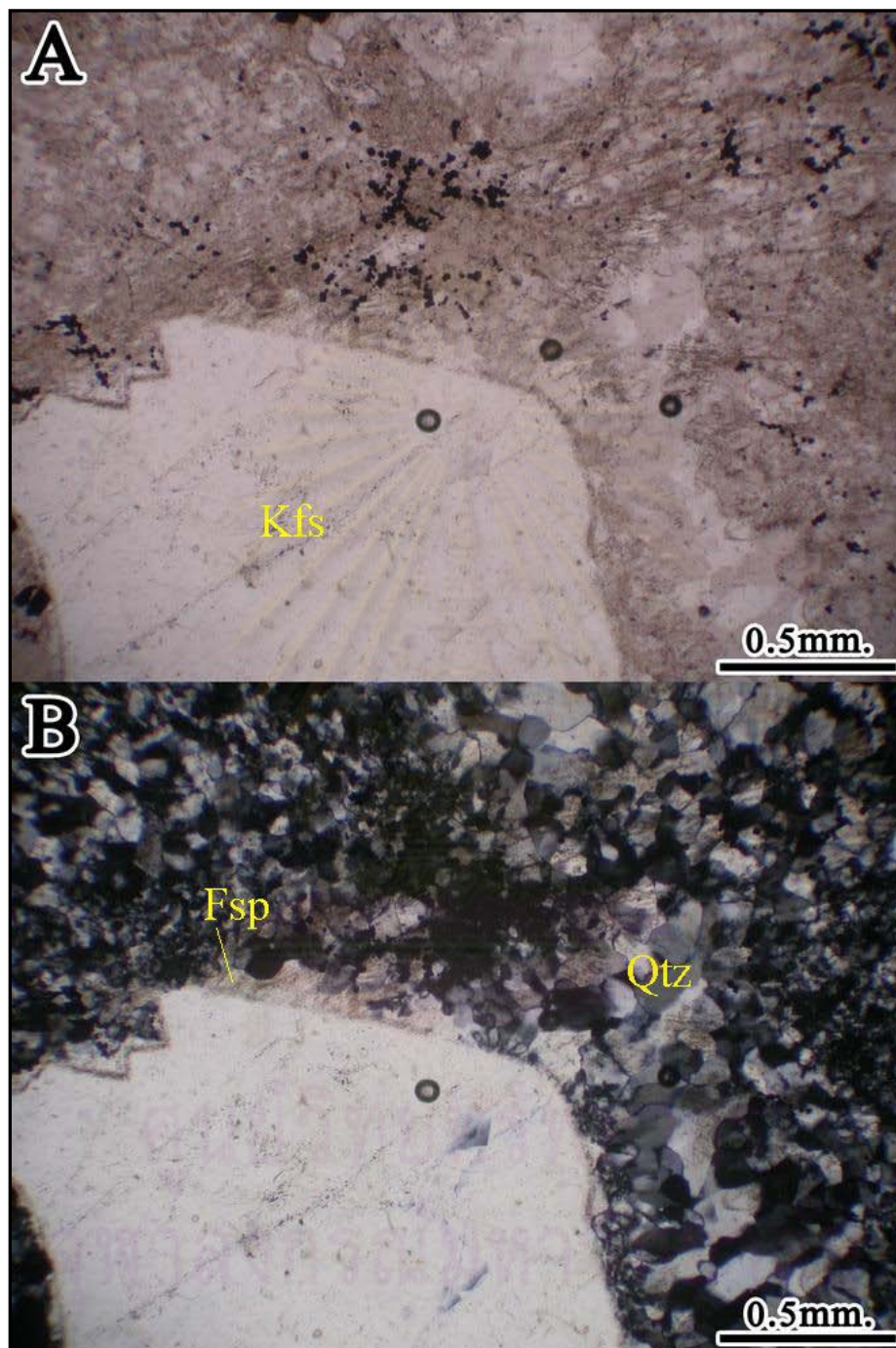
Figure 3. 28 Photomicrograph of polymictic rhyolitic breccias showing a large K-feldspar grain (Kfs) with feldspar overgrowth (Fsp) in feldspar and quartz mosaic crystalline groundmass resulting from potassic alteration (Qtz). (A) plane-polarized light, (B) crossed polars.
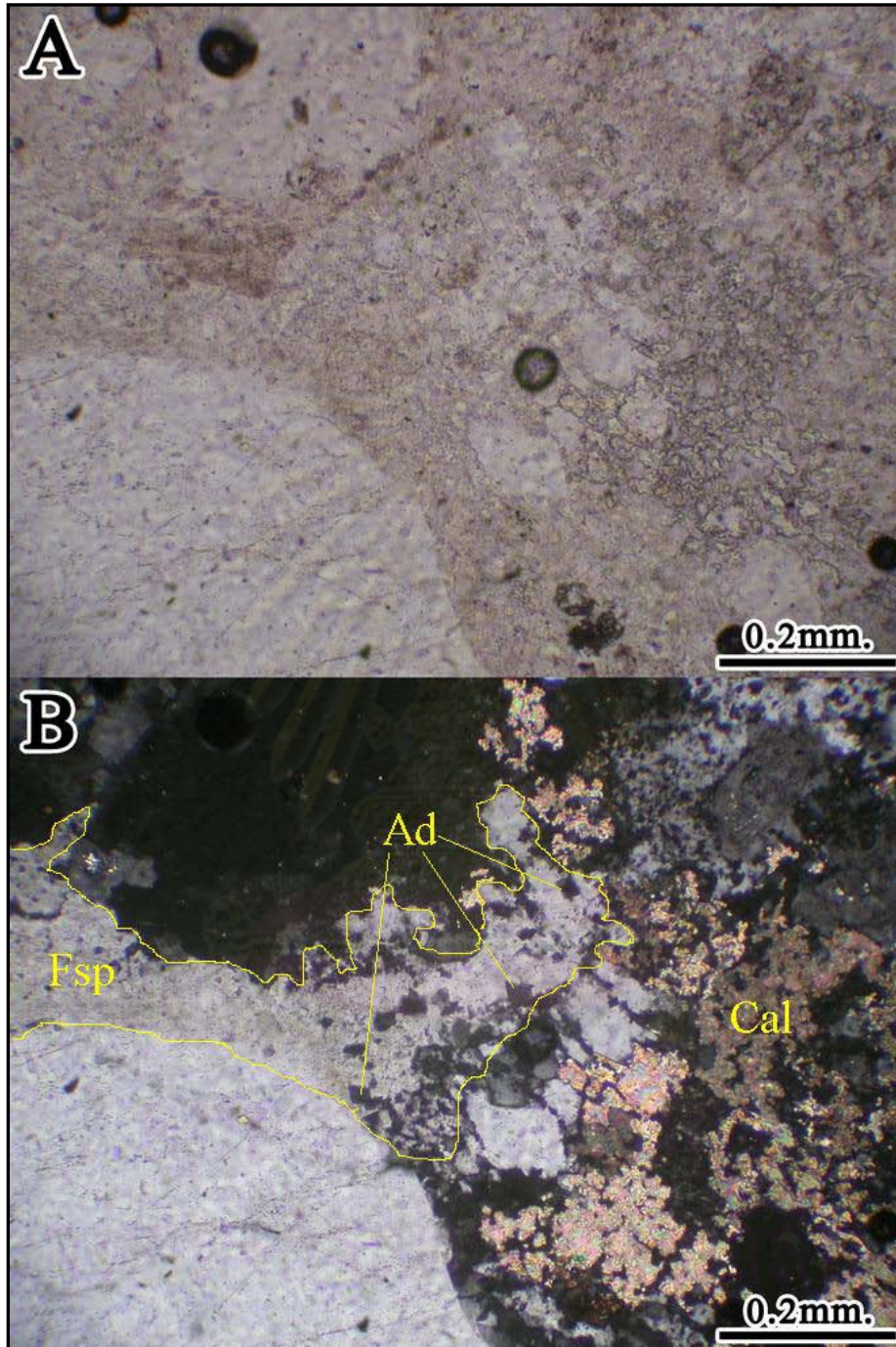
Figure 3. 29 Photomicrograph of polymictic rhyolitic breccias (Unit 2) showing small adularia rhombs (Ad) disseminated in overgrowth feldspar (Fsp) with overprinting carbonates (Cal). (A) plane-polarized light, (B) crossed polars.

In addition, sometime intensive K-feldspar alteration is also occurred. The core sample is generally very fine-grained and dense, and shows a medium bluish gray color, with irregular-shaped white patches (Figure 3.30).
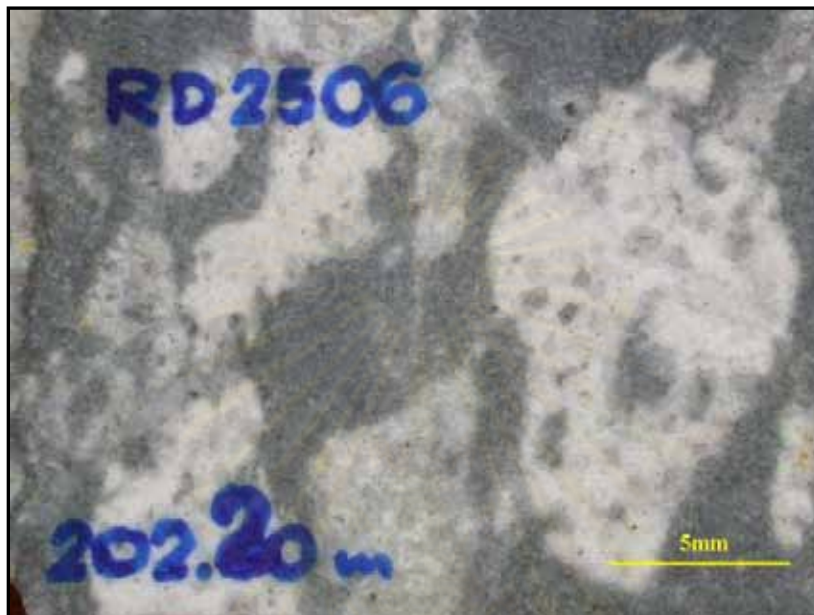
Figure 3. 30 Photograph of polymictic rhyolitic breccias (Unit 2) showing white patches of mainly altered feldspar fragments in medium bluish gray matrix comprising of mainly quartz and adularia.

Microscopically white patches are made up largely of recrystallized quartz, subordinate adularia and feldspar fragments and trace pyrite. Recrystallized quartz has sizes largely in a range of 0.3 – 0.5 mm across and contains adularia inclusions (Figure 3.31). Part of adularia was replaced by sericite/clay minerals. Feldspar fragments include both K-feldspar and plagioclase (partly replaced by sericite/clay minerals; Figure 3.31). Pyrite mainly shows subhedral to euhedral outlines. The white patches look like relict of original fragmental texture. The medium bluish gray portion has mainly very fine-grained secondary quartz and opaque minerals. It looks like matrix and groundmass of original wall rock. This sample has tiny vein quartz and pyrite, and non-ferroan calcite patches as overprinted minerals (Figure 3.31).

The rock has been recrystallized and then partly subjected to potassic alteration which is characterized by adularia and quartz replacement. The other replacement minerals include clay minerals, sericite, pyrite, opaque minerals and non-ferroan calcite as the overprint of early potassic alteration.
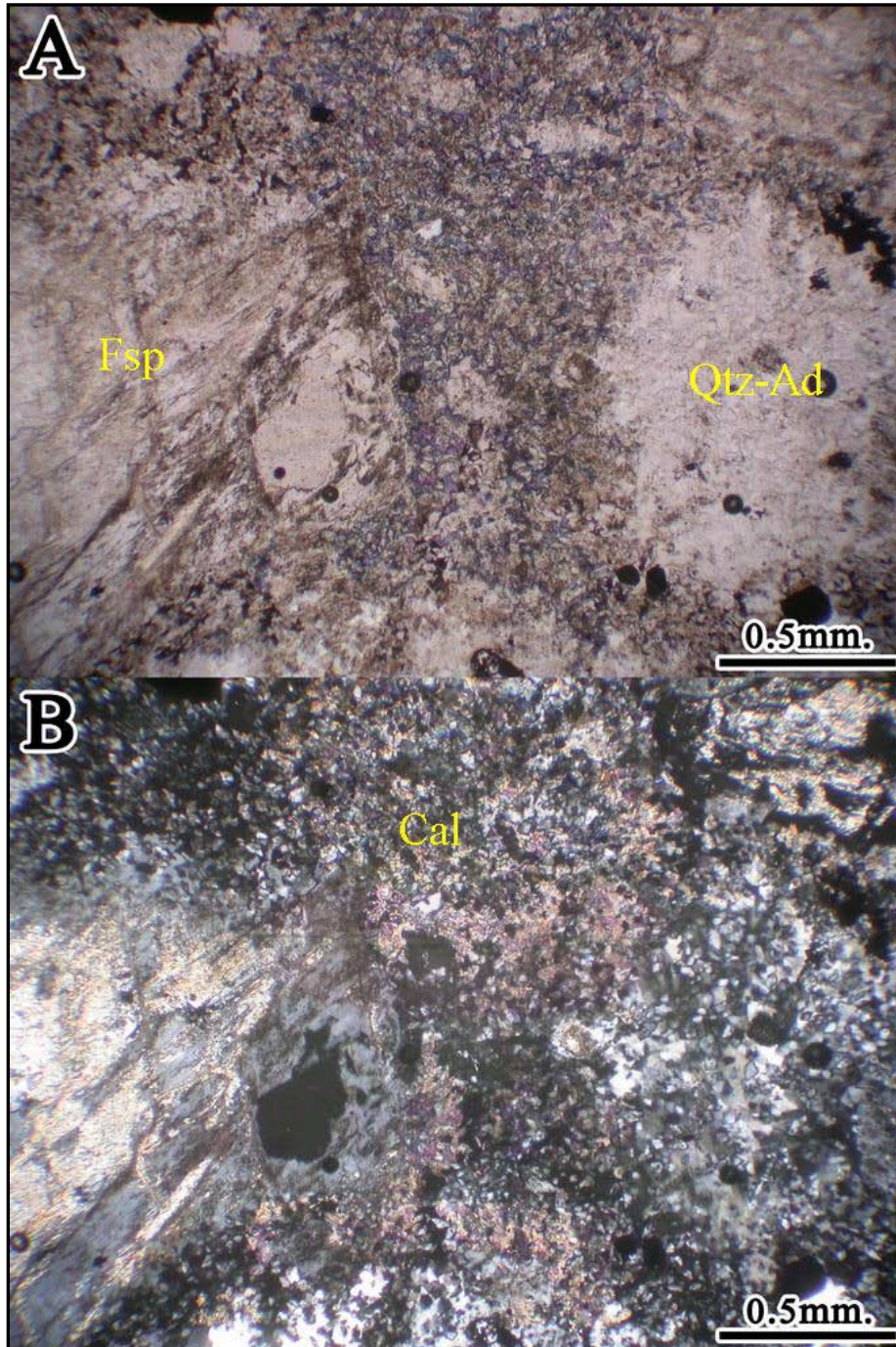
Figure 3. 31 Photomicrograph of polymictic phyolitic breccias (Unit 2) showing plagioclase? feldspar (mostly replaced by sericite/ clay minerals) (Fsp), in recrystallized quartz and adularia groundmass (Qtz-Ad) resulting from potassic alteration with overprinting late non-ferroan calcite (Cal). (A) plane-polarized light, (B) crossed polars.

Rocks Distal to the Ore Zone

Sericite and quartz alteration is found at approximately 5–20 m distal from the vein zone (Figure 3.21). Sericite and quartz are the key minerals of this alteration type which is found to replace host rock and some early altered minerals. Thin-sections show that sericite selectively replaces adularia, plagioclase phenocrysts and plagioclase groundmass, thus it is post-dated K-feldspar alteration. Tiny chlorite in feldspar relicts with subordinate carbonate minerals and pyrite crystals formed after quartz and/or carbonate veinlets are predominantly distal to the mineralized zone.

A hand specimen of polymictic rhyolitic breccia consists largely of angular to rounded lapilli with very fine-grained matrix (Figure 3.32). The rock is slightly porous and contains occasional pyrite crystals. It does not react with cold diluted hydrochloric acid and is non-magnetic. Veinlets of white to light gray minerals have been occasionally observed.
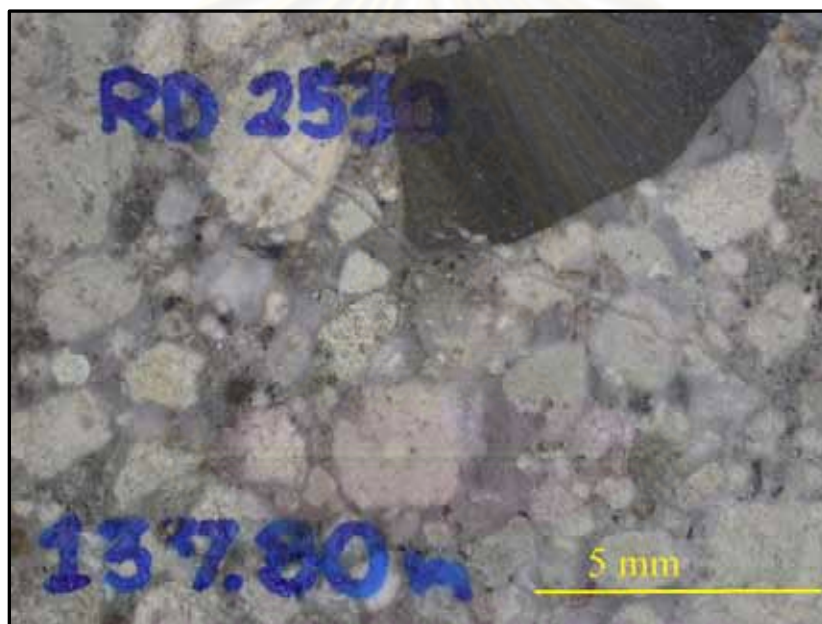
Figure 3. 32 Photograph of polymictic rhyolitic breccia slab (Unit 2) showing polymict rholitic clast in light gray cement and veinlets of light gray minerals.

Under microscope, the altered rock is made up of rock fragments and crystal fragments embedded in the finer-grained matrix. The rock fragments include silicified sedimentary rocks and carbonate rocks. The silicified sedimentary rocks may contain patches of clay mineral, pyrite and/or non-ferroan calcite patches in different proportions. The carbonate fragments show subangular outlines and consist largely of non-ferroan and ferroan calcite, with occasional pyrite. Crystal fragments are monocrystalline quartz and feldspars (Figure 3.33). Quartz grains are anhedral, with subangular to subrounded outlines. They commonly display rounded edges and /or embayed features (Figure 3.33).
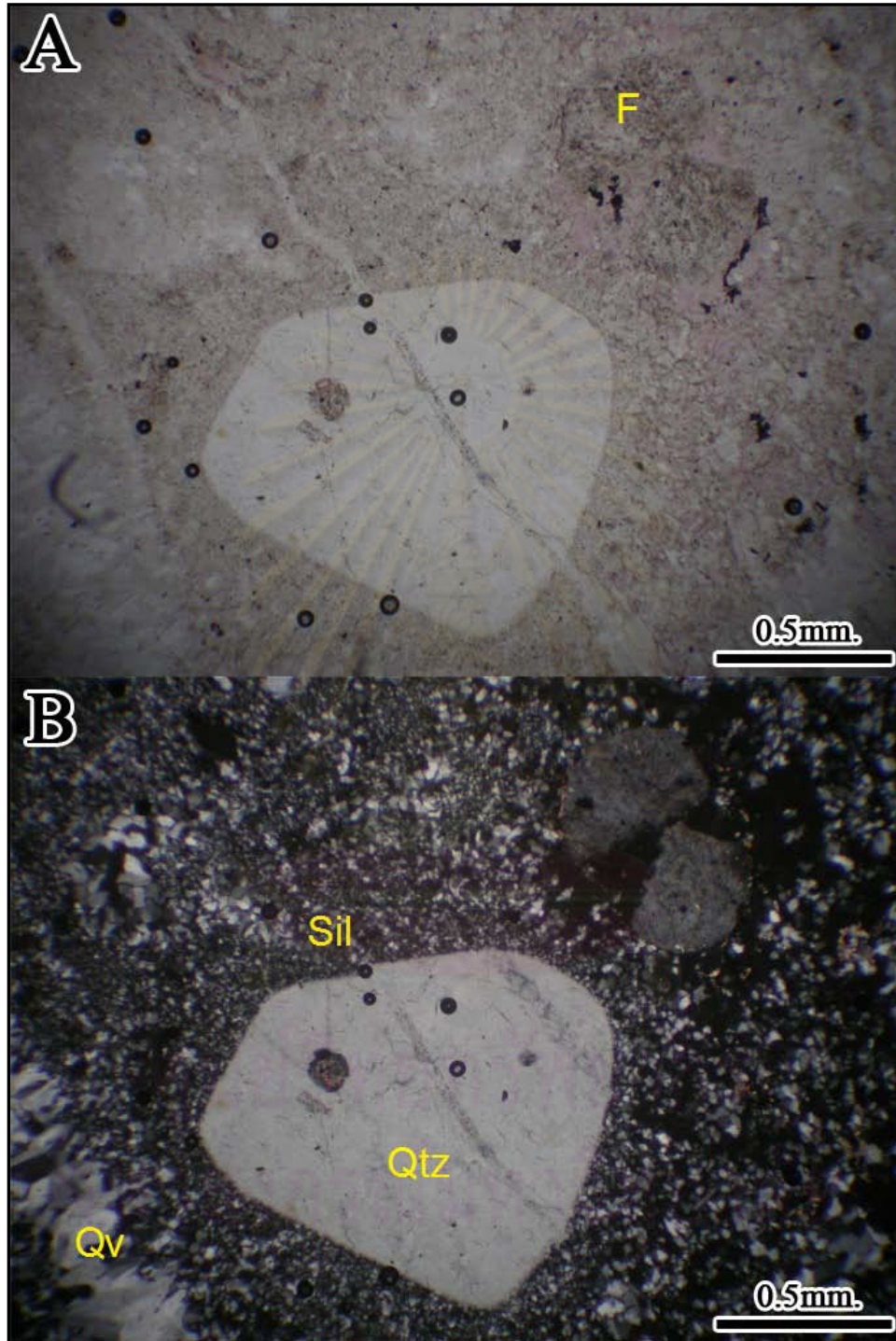
Figure 3. 33 Photomicrograph of rhyolitic tuff (Unit 2) with rounded quartz fragment (Qtz) quartz matrix result from silicification (Sil), and sericite clouded in K-feldspar which overprinted by non-ferroan calcite (F) . All of that crosscut by quartz veinlets (Qv). (A) plane-polarized light, (B) crossed polars.

Feldspar fragments (both K-feldspar and plagioclase) have anhedral to subhedral outlines; many show rounded edges. They are commonly monocrystalline and altered with clay mineral/sericite (Figure 3.33), pyrite and/or non-ferroan calcite as replacement products.

The finer-grained matrix is constituted almost totally of quartz resulted from silicification (Figure 3.33), with pyrite and non-ferroan calcite. Cavities sealed by drusy mosaic quartz have also been observed in the matrix portion. Many tiny veinlets of quartz (Figure 3.33), ferroan calcite and pyrite have been observed.

Moreover, some samples show brecciated fabric, consisting of light brownish gray to dark gray, angular fragments (sizes up to 3 mm across) in the white matrix (Figure 3.34).
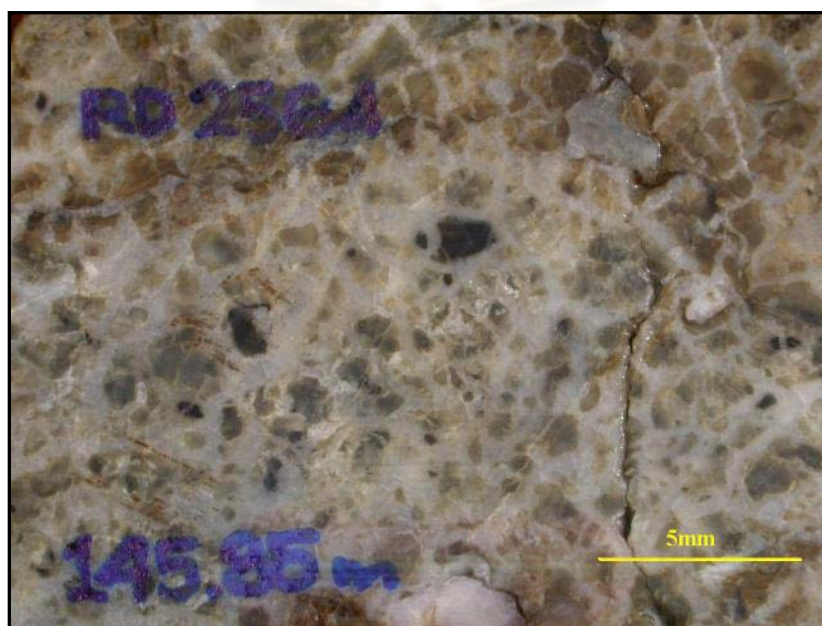
Figure 3. 34 Photograph of sericitized rock slab showing brecciated fabric in white cement.

Under microscope the rock is constituted by almost completely sericitized rock fragments (Figure 3.35), which are cemented almost totally by quartz with rare non-ferroan calcite. Irregular patches of pyrite are very rare in the rock. Many late fractures infilled by quartz and later non-ferroan calcite (Figure 3.35).
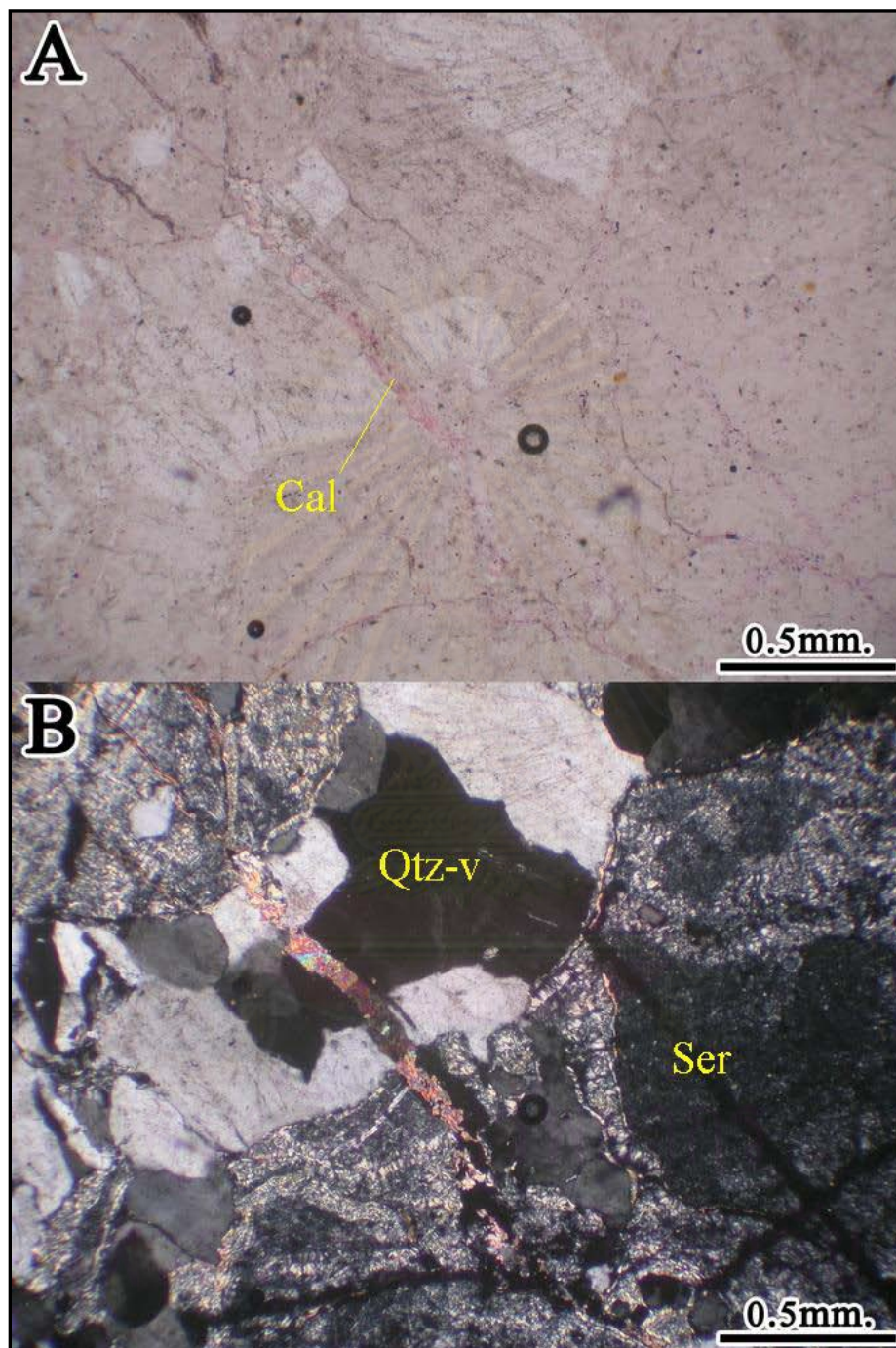
Figure 3. 35 Photomicrograph of sericitized rock (unit 2) showing sericitized clasts (Ser) cross cut by quartz vein (Qtz-v) and then cut by non-ferroan calcite veinlet (cal) again. (A) plane-polarized light, (B) crossed polars.

Local alteration

Locally in Unit 2 there are also jasper and garnet alterations. These alterations were probably related to quartz–carbonate (stage IV) veining. Jasper in hand specimen is generally very fine-grained and moderate red with gray and white spots or patches. The jasper also contains disseminated pyrite and rarely white veinlets (Figure 3.36). The white patches and veinlets react well with cold diluted hydrochloric acid.
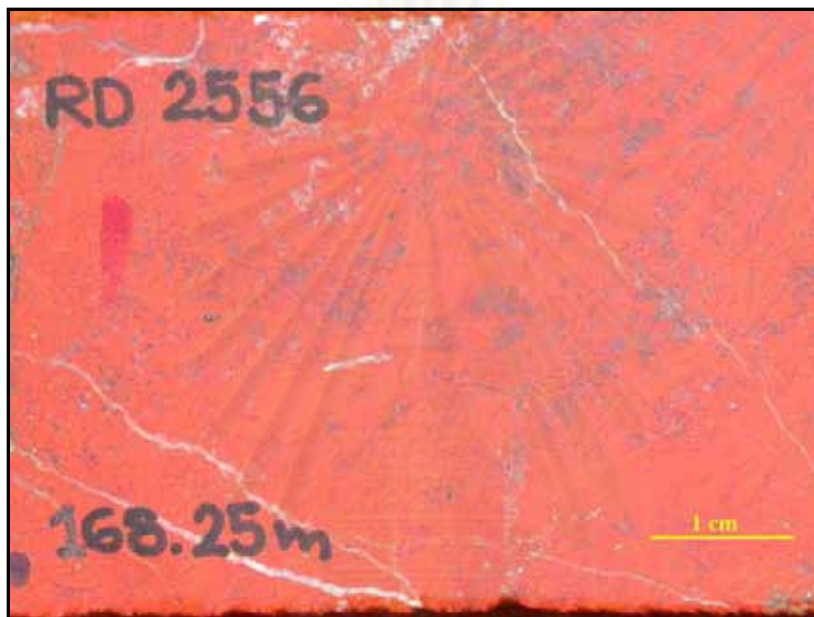
Figure 3. 36 Photograph of altered sedimentary rock (Unit 2) showing red jasper with grayish spots of carbonates and white quartz and calcite veinlets.

Microscopically jasper made up largely of chaotic patches of granular crypto-to-microcrystalline quartz and red hematite (Figure 3.37). Colorless to greenish carbonates occur as subordinate patches. Opaque mineral (pyrite?) has been observed in minor amount (Figure 3.37). Many small vugs sealed by drusy mosaic quartz crystals are also present. The rock was crosscut by calcite and quartz veinlets (Figure 3.37).
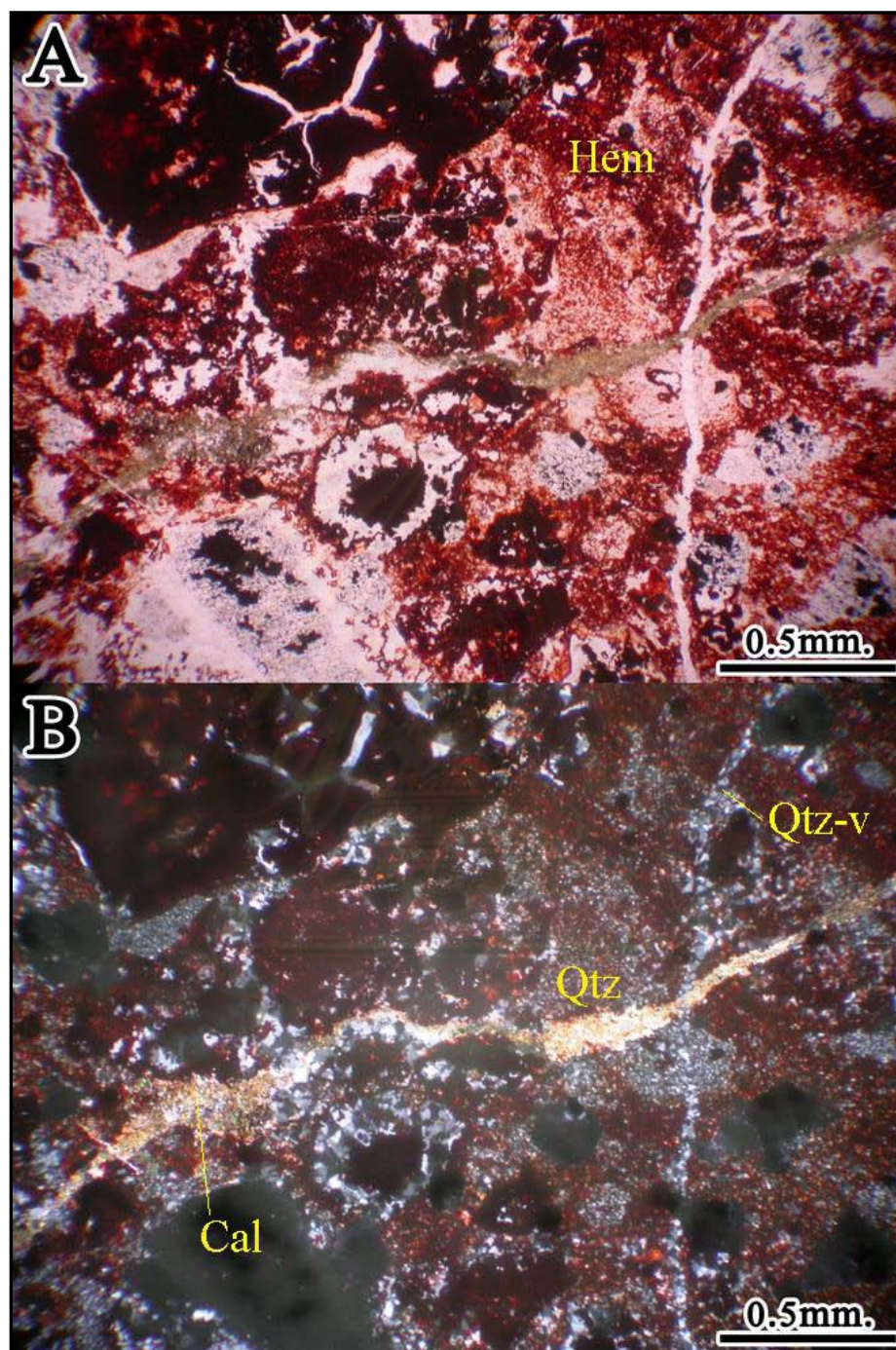
Figure 3. 37 Photomicrograph of jasper alteration comprising hematite (Hem) and quartz (Qtz) crosscut by quartz veinlet (Qtz-v) and then by late calcite veinlet (Cal). (A) plane-polarized light, (B) crossed polars.

Hand specimen of garnet alteration is generally dusty yellowish brown, with chaotic white and dusty yellowish brown patches (Figure 3.38). Small-scattered jasper patches have also been locally observed in the rock (Figure 3.38). Fractures sealed by white minerals, sulphide minerals and/or grayish yellow minerals are ubiquitous (Figure 3.38). Their walls show fine layering made up of very thin, lighter- and darker-colored layers which look like lamination texture of silicified sedimentary rock (Unit 2). The rock locally slightly reacts with diluted hydrochloric acid and is magnetic.
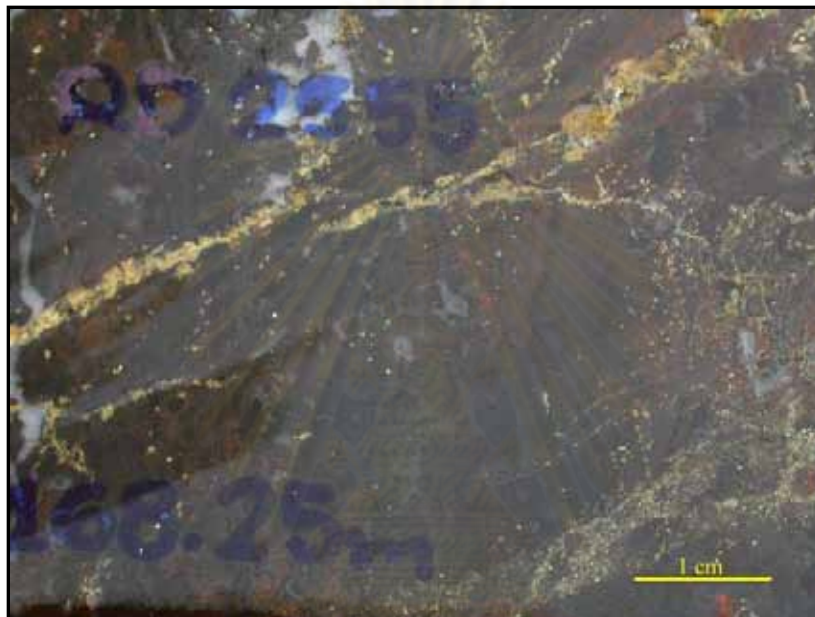
Figure 3. 38 Photograph of silicified siltstone (Unit 2) with grayish yellow sulphide layers and red jasper layers.

The rock is composed of chaotic patches of quartz (Figure 3.39), chlorite, ferroan calcite/ankerite (Figure 3.40), hydrogrossular(?) garnet (Figure 3.39) and hematite (Figure 3.39 and 3.40), opaque minerals (pyrite?) veinlets (Figure 3.40). Quartz occurs either as replacement products or as fracture-infillings (Figure 3.40). The fromer forms as aggregates of tiny equant, clear quartz grains, or as aggregates of radiating clouded crystals (chalcedony) (Figure 3.40). The latter is clear, and shows drusy mosaic features (Figure 3.39). Iron sulfide occurs as alteration mineral and vein. Chlorite and hematite are commonly associated with each other. Part of hydrogrossular(?) garnet and hematite form as zoned border of quartz veins (Figure 3.39). Hydrogrossular(?) garnet is commonly associated with ferroan calcite/ankerite.
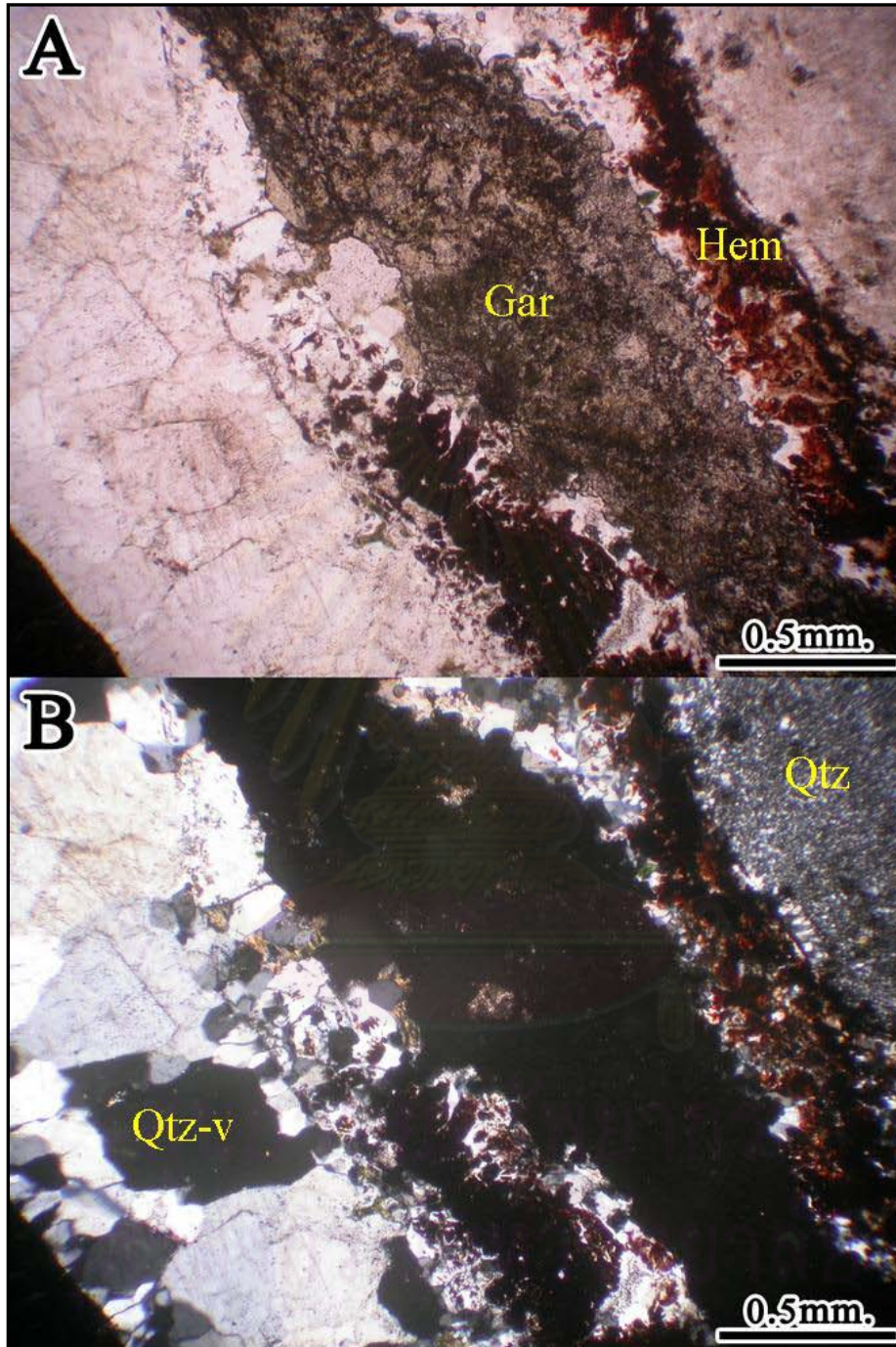
Figure 3. 39 Photomicrograph showing garnet (Gar) and hematite (Hem) halo around quartz vein (Qtz-v) with host rock replaced by quartz (Qtz). (A) plane-polarized light, (B) crossed polars.
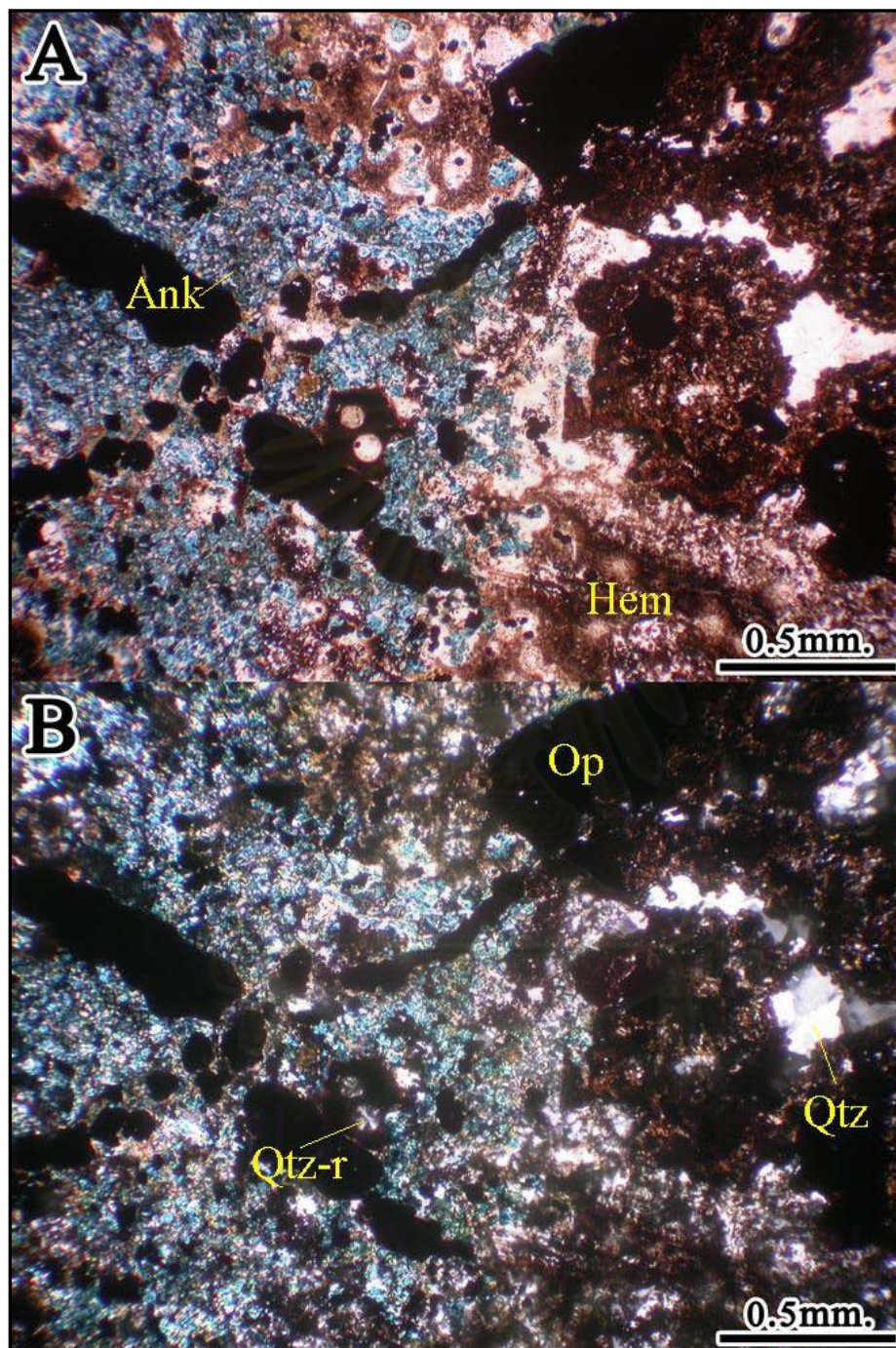
Figure 3. 40 Photomicrograph displaying ferroan calcite/ankerite (Ank), hematite (Hem) overprinted by opaque mineral(Op) veinlets, drusy mosaic quartz (Qtz) and radiated quartz (Qtz-r). (A) plane-polarized light, (B) crossed polars.

Alteration in Unit 3: the andesitic rocks unit is the lowest unit found in the A-Prospect. This unit has less data due to fewer drill holes with insufficient depth throughout this unit. Silicification, however, is found close to the vein zone (Figure 3.41). Next away from vein zone, the host rock show less alteration (Figure 3.42).
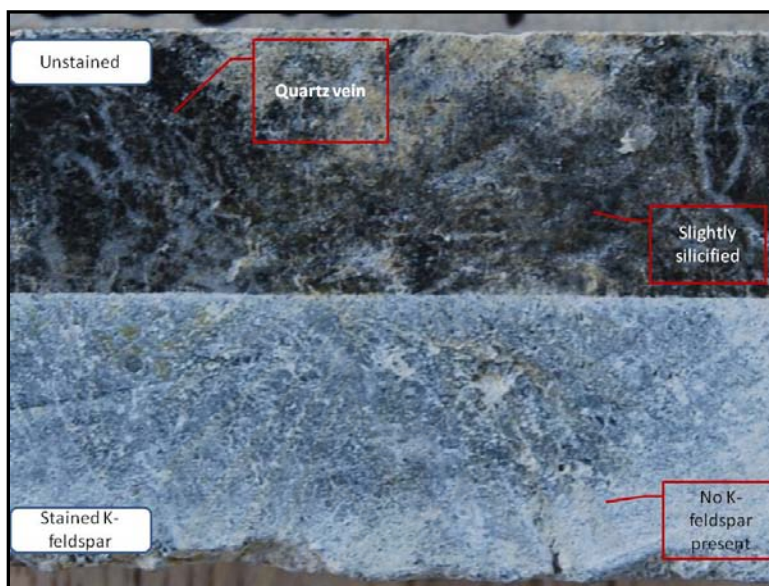
Figure 3. 41 Photograph of andesitic rock slab (Unit 3) showing quartz vein and slight silicification without K-feldspar (stained slab).

Figure 3. 42 Photograph of andesitic rock (unit 3) showing slight alteration and few crosscutting quartz–carbonate vein without K-feldspar (stained slab).

Type of Alteration of the A Prospect
Based on the above detailed description of alteration minerals, texture and distribution in relation to the vein system, they can be classified in term of alteration types as follows:

Silica alteration or Silification
The earliest alteration stage consists of pervasive silica flooding of host rocks. The pervasive alteration zones are associated with gray silica (Stage I). Early silicification was the ground preparation condition to make the host rocks harder and more brittle, which made them ready for open space in next stage.
Moss texture quartz closely occurs with adularia spots in Stage III veining. That texture was found in upper part of silica alteration zone and sedimentary rocks unit. However, moss texture has recrystallized and became ghost texture.

K-feldspar-Quartz or Potassic Alteration
K-feldspar alteration assemblages are wide spread and closely associated with pervasive silica alteration on Stage III mineralization. This alteration zone is characterized by low temperature K-feldspar and adularia.
K-feldspar alteration is generally occurred as replacement of feldspar in sedimentary rocks unit and overgrowth around feldspar in rhyolitic unit. Adularia is disseminated as euhedral to subhedral rhombic crystals. K-feldspar and adularia are locally replaced by sericite or illite.
K-feldspar and adularia, which are difficult to identify in hand specimens, can be.clearly distinguished their occurrences by staining (routinely undertaken at Issara mining laboratory). The K-feldspar alteration assemblages are related to Stage III veins, approximately 5–8 m from the vein zone.

Sericite-Quartz or Phyllic Alteration
Sericite–quartz alteration assemblages or phyllic alteration in general term, are associated with veining of Stage III and IV as alteration products of feldspars. Sericite is fine-grained white mica and typically white to pale yellow. Sericite occurs as cloudy in secondary K-feldspar and replacing plagioclase phenocrysts and plagioclase groundmass in host rocks next away from proximal ore zone.

Carbonate-Chlorite or Propylitic Alteration
Carbonate includes major calcite and trace ankerite. Calcite partly replaces feldspar and quartz in host rocks. Ankerite has been confirmed by staining. Ankerite/ ferron calcite is alteration product associated with garnet and close to jasper alteration.
Chlorite is found as completely alteration of fiamme clasts in Unit 1 and selective alteration in groundmass and clasts in polymictic rhyolitic breccias (Unit 2) and andesitic unit (Unit 3).
Propylitic alteration assemblage is associated with mineralization of mainly Stage III and minor in Stage IV and Stage V, However, it occurs distal from vein zone.

<u>Jasper alteration</u>

Jasper alteration assemblage consists mainly of hematite, quartz and pyrite with trace garnet, ankerite and chlorite. This assemblage is local alteration found only in two holes (2555RD and 2556RD). The zone is made up largely of chaotic patches of quartz and hematite. Quartz occurs either as replacement products or as fracture-infillings and shows drusy mosaic texture. Pyrite also occurs as replacement and fracture filling. Hydrogrossular(?) garnet is commonly associated with ferroan calcite or ankerite.

3.4 Timing Sequence of Ore, Gangue and Alteration Minerals

The paragenesis of alteration minerals in the A Prospect are summarized in Table 3.2. The result of study suggested that the silicification was related with Stage I mineralization, which was the ground preparation condition to make the rocks harder and more brittle. That made host rock ready for open space in next stages. The gold-bearing Stage III mineralization was related to the K-feldspar alteration proximal to the ore zone, while sericite and quartz alteration was found next away from the ore zone in the Stage IV. Chlorite or porpylitic alteration was found distal to the ore zone in Stages III-V. The late carbonate is assumed to occur in the Stage V.

Table 3. 2 Diagram summarizes mineralization and alteration paragenesis of the A Prospect. The ore and gangue are presented in vein while alteration is shown in host rocks.

Minerals	Stages	Pre-mineralized		Mineralized stage	Post - mineralized		
		Stage I	Stage II	Stage III	Stage IV	Stage V	Stage VI
Ore	Euhedral pyrite	Major	Minor		Minor		
	Anhedral pyrite			Major			
	Sphalerite			Major			
	Chalcopyrite			Minor			
	Electrum			Trace			
Gangue	Grey chacedony	Major					
	Quartz		Major	Major	Major		
	Chacedonic			Major			
	Non-ferrocalcite		Trace			Major	
	Dolomite			Major	Major		
	Ferrocalcite/ ankerite			Minor			
	Chlorite		Trace				
	Hematite			Trace			
	Zeolite						Major
Alteration	Quartz	Major		Major	Major		
	K-feldspar (adularia)			Major			
	Sericite/Clay minerals			Minor	Major		
	Calcite				Minor	Minor	
	Chlorite			Minor	Minor	Minor	
	Hematite				Trace		
	Ankerite/ ferrocalcite				Trace		
	Hydrogrossular(?) garnet				Trace		

▬▬▬▬		Major
────		Minor
- - - - -		Trace

CHAPTER IV
GEOLOGY, MINERALIZATION AND ALTERATION AT
THE H WEST PROSPECT

4.1 Lithology and stratigraphy

The H West Prospect consists of three units (Figure 4.1); Unit 1: uppermost fiamme breccia, Unit 3: andesite with polymictic and monomictic andesitic breccia, and Unit 4: andesite porphyry. The Unit 2, volcanic clastic unit is absent in this area. Hence the rock types of H West Prospect are composed dominantly of andesitic rocks. Andesitic and basaltic–andesitic dykes cut earlier units and veins. All rock units are overlain by laterite and alluvium. Detail of each unit (summarized from Salam, 2006; Lunwongsa et al., 2008; and this study) is described in descending order below.

Unit 1 is fiamme braccia. The thickness of this sequence is varied due to surface of the underlying andesite unit. This unit is greenish grey, massive and poorly sorted. The breccias consist mainly of pumice clasts (almost replaced by chlorite, Figure 4.2), minor euhedral to subhedral quartz and feldspar, and trace monomictic to polymictic andesitic breccias (found closer to the lower contact with andesite unit). Mostly the fiamme unit is matrix-supported although locally it is clast-supported. Average size is 0.5–1 cm across. Clast shapes vary from angular to subrounded.

Unit 3 at the H West Prospect is mainly andesite and monomictic andesitic breccias with minor polymictic andesitic breccias. The andesite is called pyroxene-plagioclase-phyric andesite, which is coherent lava. Salam (2006) called this rock, micro-porphyritic andesite, due to the occurrence of small phenocrysts of pyroxene and feldspar (Figure 4.3). The rock is dark greenish grey and massive. The textures of this rock vary from aphanitic to porphyritic. Euhedral to subhedral phenocrysts of plagioclase, clinopyroxene and few amphiboles occur within groundmass. The plagioclase phenocrysts are tabular to blocky shapes and are partly replaced by sericite. Clinopyroxene is mostly replaced by chlorite. The groundmass consists of plagioclase, clinopyroxene and crptocrystalline materials.

The monomictic andesitic breccias typically are poorly sorted, jigsaw-fit texture and coarse angular clast-supported. Breccia clasts are plagioclase-pyroxene phyric andesite sit in same composition groundmass (Figure 4.4), which was called "auto breccias" by Cumming (2004).

The polymictic andesitic breccias occur as lenses 20–40m thick and 150m long. This part contains fine-to-pebble-sized clasts of various type of mainly andesite such as fine grained equigranular, plagioclase pyroxene phyric andesite and porphyritic texture, with minor feldspar laths, chloritic clasts and hematitic clast (Figure 4.4). The polymictic andesitic breccias show fining upward graded bedding.

Between Unit 3 and Unit 4 there is also a rhyolitic pyroclastic flow. This flow occurs as lens 3–10m thick, partially intercalates with calcareous siltstone (Figure 4.5) and shows flow layering. This sub-unit is correlated well between the J, K and A Prospects.
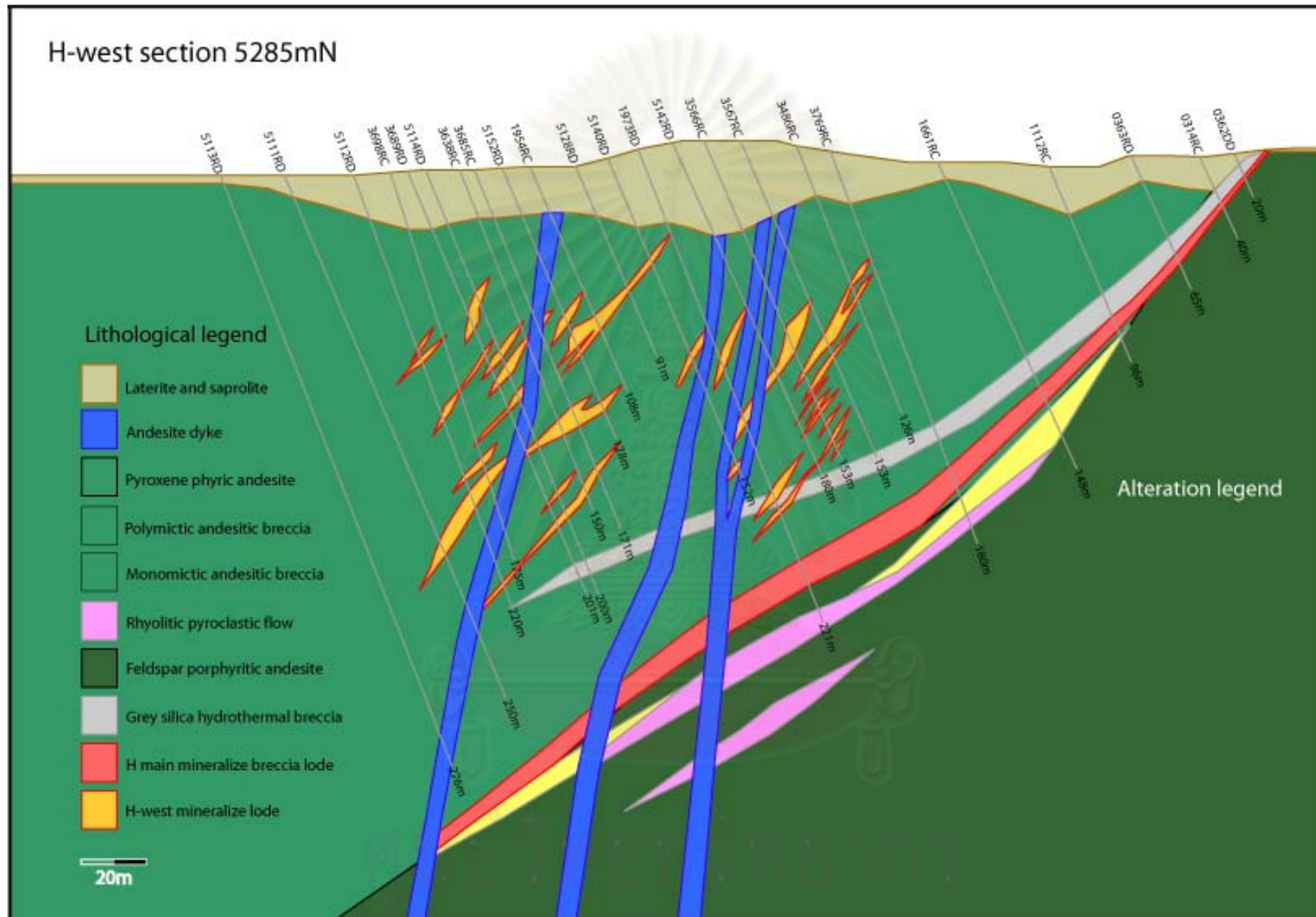
Figure 4. 1 Picture displays East–West cross-section 5285mN with the H West Prospect showing lithologic facies.
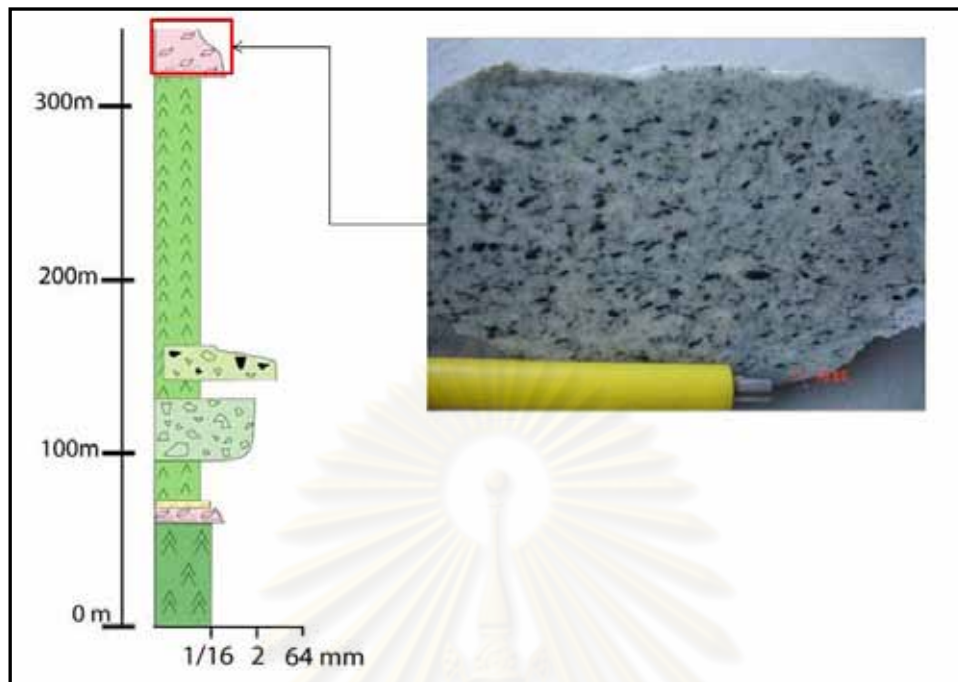
Figure 4. 2 Stratigraphic column showing the upper Unit 1 of lithic-rich fiamme breccia with photo of hand specimen.
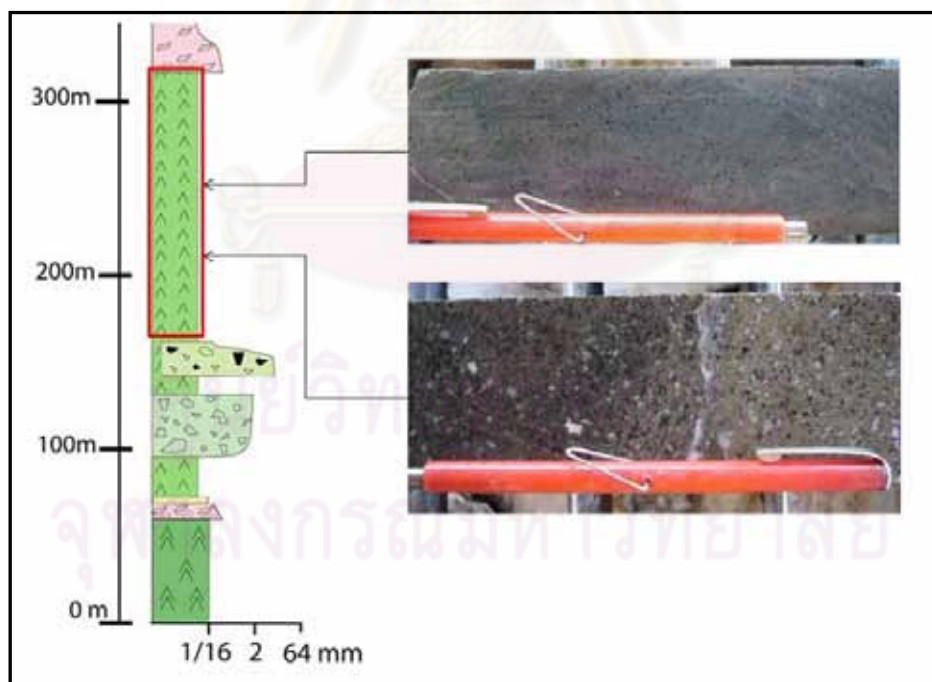
Figure 4. 3 Stratigraphic column showing the Unit 3 of pyroxene-feldspar phyric andesite with slab samples.
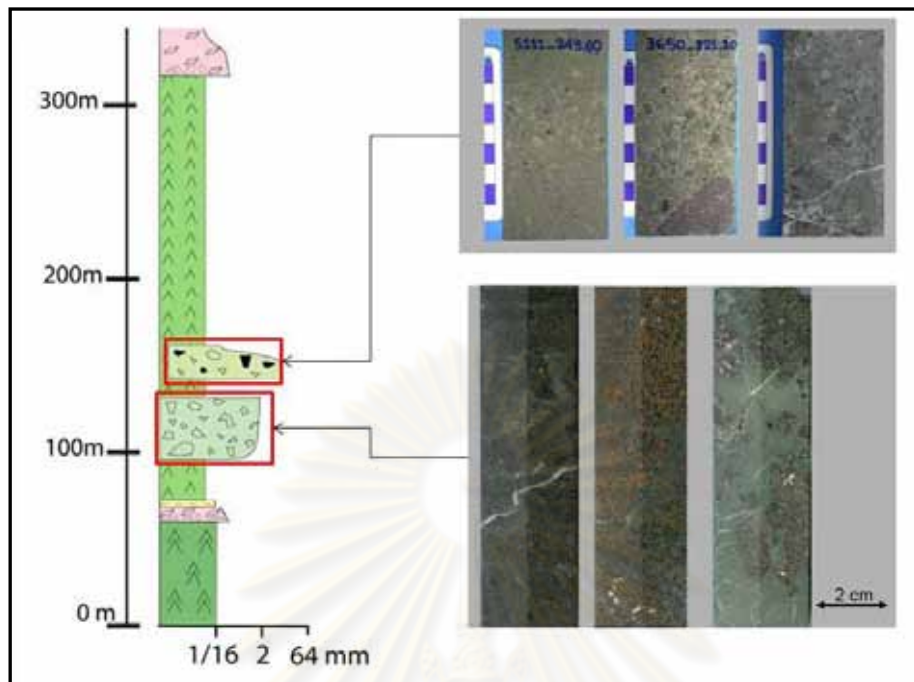
Figure 4. 4 Stratigraphic column showing the Unit 3 of monomictic andesitic breccias (lower) and lens of polymictic andesitic breccias (upper) with photos of slab samples.
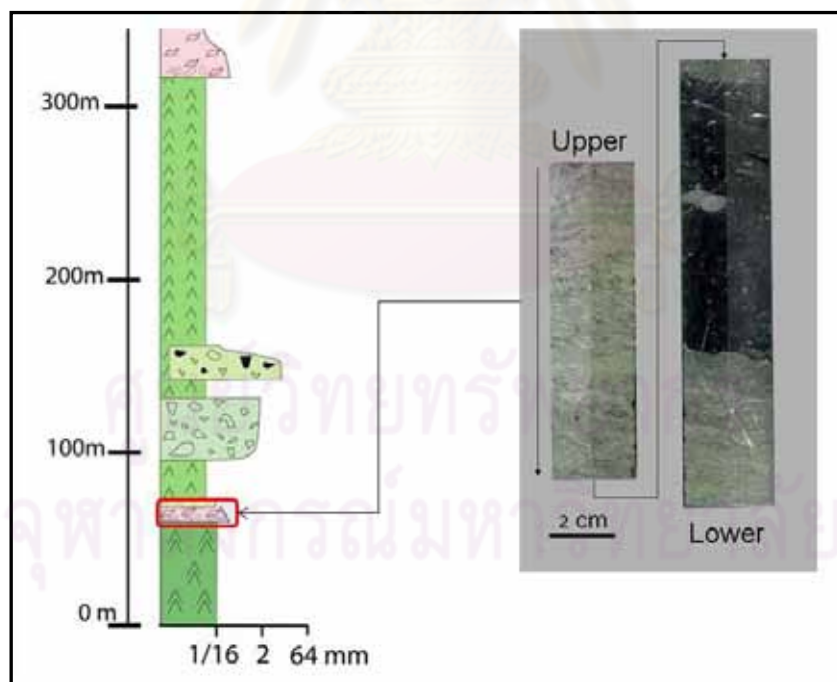
Figure 4. 5 Stratigraphic column showing the rhyolitic pyroclastic flow intercalate with calcareous siltstone with photo of slab samples.

Unit 4, the lowest unit, is andesite porphyry. The recent information is unable to show thickness or the lower most boundary of the unit. The andesite porphyry, or the so-called "andesite basement" in local usage, is a dark green rock with orange to brown spots. The lath-shaped phenocrysts are mainly K-feldspar with minor plagioclase and few pyroxenes (Figure 4.6). Groundmass is fine-grained and composed of major feldspar, subordinate chlorite and carbonate, and occasionally pyrite. This rock has average size 1 to 5 mm and non-magnetic. The contact between Unit 3 and 4 in the upper part (i.e., $210^{o}/50^{o}$) is steeper than that in the lower part (i.e., $210^{o}/30^{o}$) as shown in Figure 4.1.
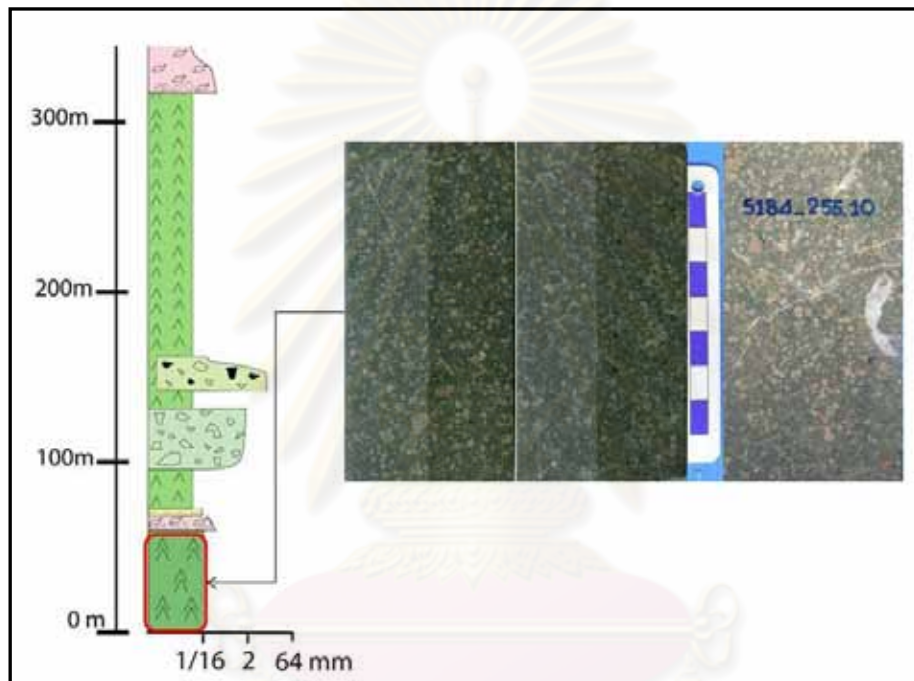
Figure 4. 6 Stratigraphic column showing the Unit 4 of porphyritic andesite with photo of slab samples.

4.2 Mineralization

The H West Prospect veins dip 30°-50° NW and strike NE-SW (040). The vein styles at the H West Prospect are also similar to those encountered in other low-sulphidation epithermal deposits described by Hedenquist (2000).

The nature of mineralization and vein stages in the H West Prospect are similar to those in the A Prospect and Their nature including vein morphology, texture, mineralogy and paragenesis of ore and gangue minerals are described in detail as follows.

Stage I: Grey Chalcedony

Grey chalcedonic breccia unit is made up to 10m thick, generally dipping west, as shown in cross section (Figure 4.1). It is grey to dark grey and greenish grey, general form as matrix-filling breccias (Figure 4.7), occasionally as veins (Figure 4.8). It is composed mainly microcrystalline quartz (Salam, 2006) and trace euhedral pyrite cementing breccia clasts that are mainly pyroxene phyric andesite. The clasts are angular and slightly-to-strongly-silicified. White quartz rims are also common (Figure 4.7). Moreover, between Unit 3 and Unit 4 there is also a rhyolitic pyroclastic flow. This flow occurs as lens 3–0m thick. Grey chacedony has also replaced and infiltrated rhyolitic flow unit with chlorite rims (Figure 4.9) that make this unit strongly silicified.
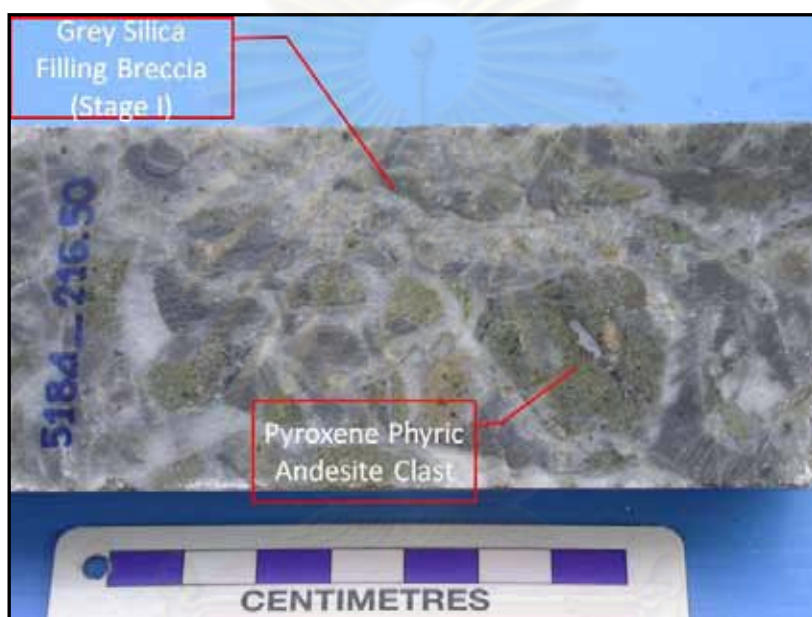
Figure 4.7 Photograph of Stage I core slab showing grey chalcedony filling breccias with angular clasts of pyroxene phyric andesite. White quartz rims also common.
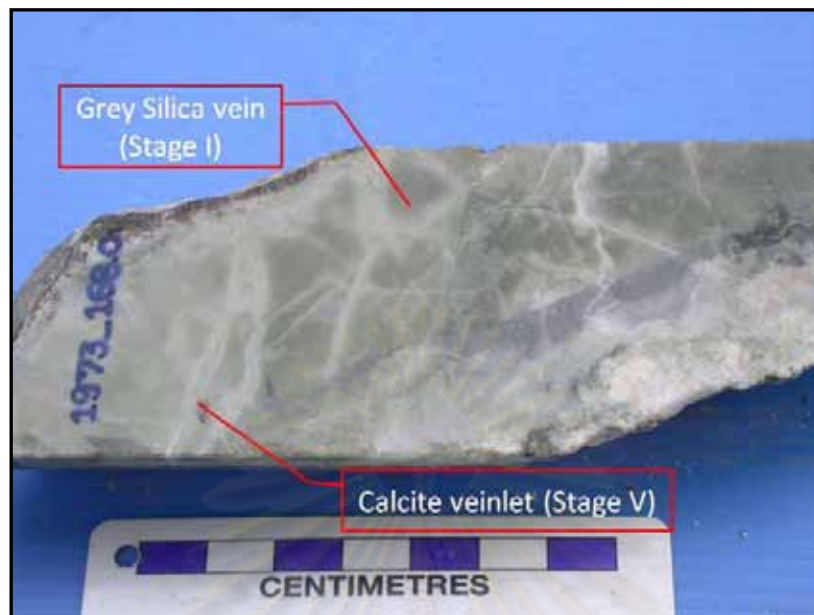
Figure 4.8 Photograph of Stage I core slab showing greenish grey chalcedony veins crosscut by calcite veins (Stage V).
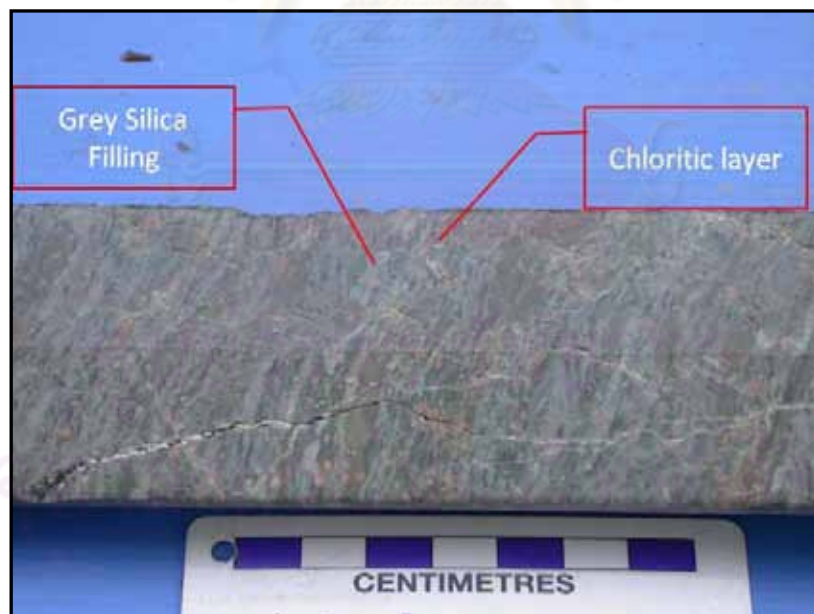
Figure 4.9 Photograph of rhyolitic flow unit slab showing grey chalcedony infiltrated with chlorite rims.

Stage II: Quartz–Euhedral Pyrite Vein

The Stage II mineralization in the H West Prospect was found only as breccias in other vein stages without continuity of veining (Figure 4.10). Quartz of this stage is fine-grained, milky and typically disseminated with fine-grained euhedral pyrite or occasionally contains sulphide layers. Pyrite of this stage can be separated from the Stage III pyrite by its euhedral shape in contrast to the anhedral form of Stage III pyrite.

Figure 4.10 Photograph of core sample showing quartz-euhedral pyrite (Stage II) clasts embedded in sulphide-rich veins (Stage III).

Stage III: Major Gold Mineralization

This is the main gold bearing stage. There are three vein mineralization styles that are recognized in this stage, namely, crustiform–colloform banding in the upper weathered zone, massive veining in the middle zone and breccia filling in the lower zone. No crosscut relationships or brecciation evidences to suggest that they are overprinting each other. However, they occur depending on depth and host rock types. Details of each style are described below:

a) Crustiform and colloform banding style in the upper weathered zone: quartz–carbonate alternating with sulphide and chalcedony bands are typical mineralization style in this zone (Figure 4.11), that is also similar to the Stage III of the A Prospect. Moreover, Stage II quartz-euhedral pyrite clasts were also found in sulphide-rich veins of this stage (Figure 4.10). Occaionally, carbonate minerals might have been completely leached out and appear as vuggy texture in this weathered zone (Figure 4.12). This may be due to weathering as it closer to the recent surface. The white to greenish grey chalcedony in Stage III occurs commonly in the upper zone, but decreases in

its amount with depth. The sulphide bands comprise pyrite, sphalerite, chalcopyrite and electrum. Pyrite, the most abundant sulphide mineral, is fine-to-medium-grained, anhedral to subhedral, and occurs in close association with sphalerite, chalcopyrite, electrum (Figure 4.13) and galena. It is noted that pyrite in the H West area displays optically duller in color than that of the A Prospect, thus suggesting that the composition of pyrite in the H West Prospect may be different from pyrite of the A Prospect. The EPMA analyses of pyrite grains give the composition of $Fe_1 S_{1.69}$ (Table 4.1). Sphalerite is considered as another major sulphide following pyrite. It occurs as honey-colored, fine-to-medium-grained, anhedral to subhedral. Electrum commonly occurs as inclusions in pyrite where sphalerite and chalcopyrite are sometimes found as inclusions as well (Figure 4.13). The EPMA analyses give sphalerite composition of $(Zn_{0.97}Fe_{0.03}) S_{0.68}$ with $Au_{0.05}$ (Table 4.2), chalcopyrite composition is $Fe_1 (Cu_{0.93}Zn_{0.01}Ni_{0.01}) S_{1.24}$ (Table 4.3), and galena composition is $Pb_1S_{0.67}$ (Table 4.4). This zone contains maximum 4.8 g/t Au.

Table 4. 1 The EPMA analyses of pyrite composition in Stage III of the H West Prospect, calculated in terms of atomic proportions.

No.	Sb	As	Ti	Mn	Au	Cd	S	Zn	Fe	Ag	Pb	V	Cu	Ni	Mo
21	0.00	0.00	0.00	0.00	0.00	0.00	1.48	0.00	0.84	0.00	0.00	0.00	0.00	0.00	0.00
23	0.00	0.00	0.00	0.00	0.00	0.00	1.41	0.00	0.86	0.00	0.00	0.00	0.00	0.00	0.00
24	0.00	0.00	0.00	0.00	0.00	0.00	1.43	0.00	0.86	0.00	0.00	0.00	0.00	0.00	0.00
25	0.00	0.00	0.00	0.00	0.00	0.00	1.41	0.00	0.83	0.00	0.00	0.00	0.00	0.00	0.00
26	0.00	0.00	0.00	0.00	0.00	0.00	1.41	0.00	0.85	0.00	0.00	0.00	0.00	0.00	0.00
27	0.00	0.00	0.00	0.00	0.00	0.00	1.43	0.00	0.85	0.00	0.00	0.00	0.00	0.00	0.00
28	0.00	0.00	0.00	0.00	0.00	0.00	1.46	0.00	0.84	0.00	0.00	0.00	0.00	0.00	0.00
30	0.00	0.00	0.00	0.00	0.00	0.00	1.41	0.00	0.84	0.00	0.00	0.00	0.00	0.00	0.00

ศูนย์วิทยทรัพยากร

จุฬาลงกรณ์มหาวิทยาลัย

Figure 4.11 Photograph of Stage III core sample showing alternating quartz–carbonate with sulphide bands and chalcedonic bands.

Figure 4.12 Photograph of Stage III core sample showing carbonate leached out from quartz – carbonate – chalcedony vein.
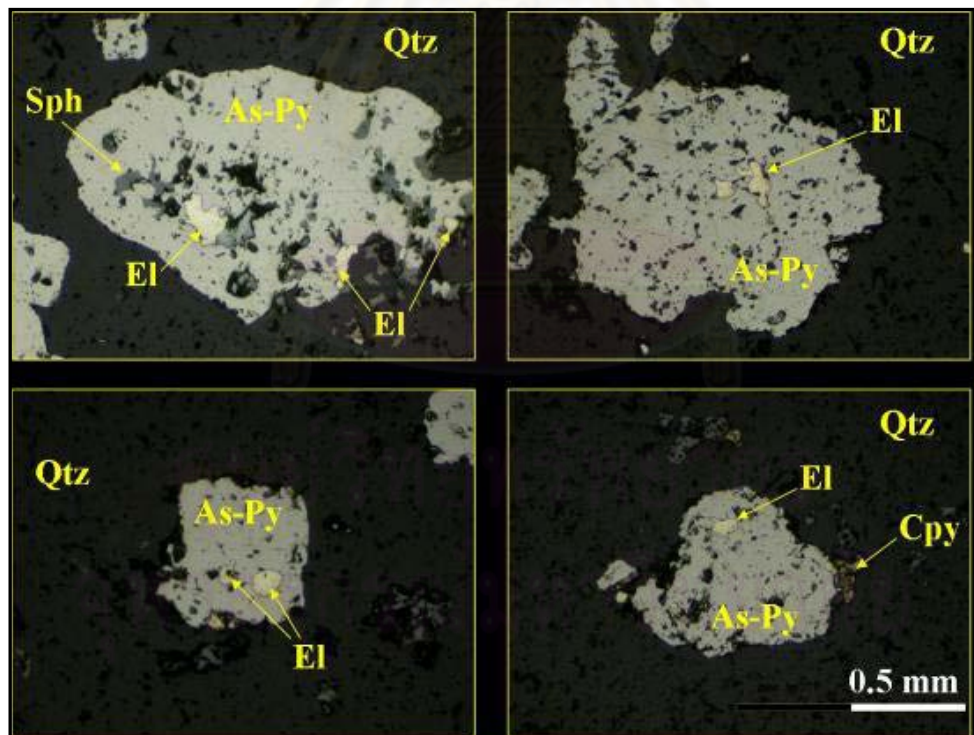
Figure 4. 13 Photomicrograph of Stage III mineralisation showing mineral assemblages. Qtz = quartz, As-Py = Dull pyrite (Asenian pyrite?), El = electrum, Cpy = Chacopyrite and Sph = Sphalerite (Reflected light).

Table 4. 2 The EPMA analyses of chalcopyrite composition in Stage III of the H West Prospect, calculated in terms of atomic proportions.

No.	Sb	As	Ti	Mn	Au	Cd	S	Zn	Fe	Ag	Pb	V	Cu	Ni	Mo
64	0.00	0.00	0.00	0.00	0.00	0.00	0.70	0.00	0.56	0.00	0.00	0.00	0.52	0.01	0.00
65	0.00	0.00	0.00	0.00	0.00	0.00	0.71	0.01	0.56	0.00	0.00	0.00	0.52	0.01	0.00
66	0.00	0.00	0.00	0.00	0.00	0.00	0.70	0.00	0.55	0.00	0.00	0.00	0.52	0.01	0.00
67	0.00	0.00	0.00	0.00	0.00	0.00	0.68	0.01	0.56	0.00	0.00	0.00	0.52	0.01	0.00
68	0.00	0.00	0.00	0.00	0.00	0.00	0.69	0.02	0.55	0.00	0.00	0.00	0.52	0.01	0.00
69	0.00	0.00	0.00	0.00	0.00	0.00	0.68	0.00	0.57	0.00	0.00	0.00	0.52	0.01	0.00
70	0.00	0.00	0.00	0.00	0.00	0.00	0.68	0.00	0.56	0.00	0.00	0.00	0.52	0.01	0.00
71	0.00	0.00	0.00	0.00	0.00	0.00	0.69	0.00	0.56	0.00	0.00	0.00	0.52	0.01	0.00
72	0.00	0.00	0.00	0.00	0.00	0.00	0.70	0.00	0.56	0.00	0.00	0.00	0.52	0.01	0.00

Table 4. 3 The EPMA analyses of sphalerite composition in Stage III of the H West Prospect, calculated in terms of atomic proportions.

No	Sb	As	Ti	Mn	Au	Cd	S	Zn	Fe	Ag	Pb	V	Cu	Ni	Mo
52	0.00	0.00	0.00	0.00	0.05	0.00	0.66	0.96	0.02	0.00	0.00	0.00	0.00	0.01	0.00
53	0.00	0.00	0.00	0.00	0.05	0.00	0.65	0.95	0.02	0.00	0.00	0.00	0.00	0.01	0.00
54	0.00	0.00	0.00	0.00	0.05	0.00	0.63	0.94	0.02	0.00	0.00	0.00	0.00	0.01	0.00
55	0.00	0.00	0.00	0.00	0.05	0.00	0.64	0.89	0.04	0.00	0.00	0.00	0.04	0.01	0.00
56	0.00	0.00	0.00	0.00	0.05	0.00	0.64	0.87	0.05	0.00	0.00	0.00	0.04	0.01	0.00
57	0.00	0.00	0.00	0.00	0.05	0.00	0.65	0.90	0.06	0.00	0.00	0.00	0.03	0.01	0.00
58	0.00	0.00	0.00	0.00	0.05	0.00	0.65	0.96	0.01	0.00	0.00	0.00	0.00	0.01	0.00
59	0.00	0.00	0.00	0.00	0.05	0.00	0.65	0.95	0.01	0.00	0.00	0.00	0.00	0.01	0.00
60	0.00	0.00	0.00	0.00	0.05	0.00	0.67	0.96	0.01	0.00	0.00	0.00	0.00	0.01	0.00
61	0.00	0.00	0.00	0.00	0.05	0.00	0.66	0.88	0.05	0.00	0.00	0.00	0.05	0.01	0.00
62	0.00	0.00	0.00	0.00	0.05	0.00	0.67	0.90	0.05	0.00	0.00	0.00	0.05	0.01	0.00
63	0.00	0.00	0.00	0.00	0.04	0.00	0.67	0.88	0.05	0.00	0.00	0.00	0.05	0.01	0.00
76	0.00	0.00	0.00	0.00	0.05	0.00	0.63	0.93	0.03	0.00	0.00	0.00	0.02	0.01	0.00

Table 4. 4 The EPMA analyses of galena composition in Stage III of the H West Prospect, calculated in terms of atomic proportions.

No.	Sb	As	Ti	Mn	Au	Cd	S	Zn	Fe	Ag	Pb	V	Cu	Ni	Mo
73	0.00	0.00	0.00	0.00	0.00	0.00	0.24	0.03	0.00	0.00	0.35	0.00	0.00	0.00	0.00
74	0.00	0.00	0.00	0.00	0.00	0.00	0.25	0.02	0.00	0.00	0.36	0.00	0.01	0.00	0.00
75	0.00	0.00	0.00	0.00	0.00	0.00	0.23	0.05	0.00	0.00	0.35	0.00	0.00	0.00	0.00

b) Massive quartz–carbonate veining style in the middle zone; the major gold production is derived from this zone. It is quite widely distributed, similar with Stage III of the A Prospect. It comprises major white quartz closely associated with subordinate white to pale creamy carbonates that infill open fractures (Figure 4.14). EPMA analyses of carbonate grains reveal that they are calcite having the average chemical formula as $(Ca_{0.95} Mn_{0.04}) CO_3$ (Table 4.5). Polymetallic sulphides occur mainly as dissemination (Figure 4.14) and minor as bands or layers in quartz which normally provides high grade ore (Figure 4.15). Adularia (confirmed by staining technique) is found in minor amount as pink rhombic crystals and closely associated with quartz and carbonates (Figure 4.14). Chlorite is green to black, coarse-grained and occurs as layers (Figure 4.14). Moreover, massive quartz–carbonate-sulphide mineralization cementing hydrothermal breccias of silicified andesite and filling stockwork veining was also found in minor amount in this zone (Figure 4.16). This zone contains up to 34.8 g/t Au.
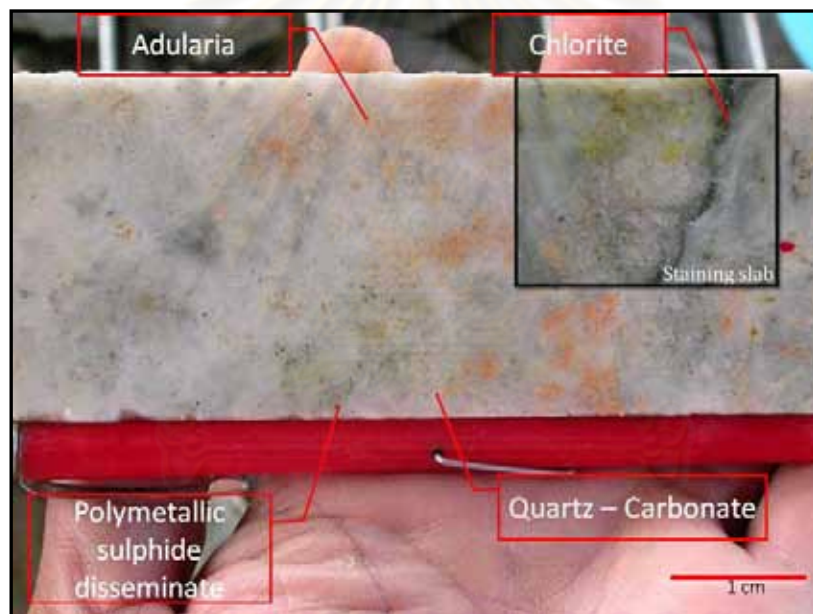
Figure 4.14 Photograph of Stage III core slab showing quartz–carbonate massive vein with minor pink adularia, disseminated polymetallic sulphides and chlorite band.
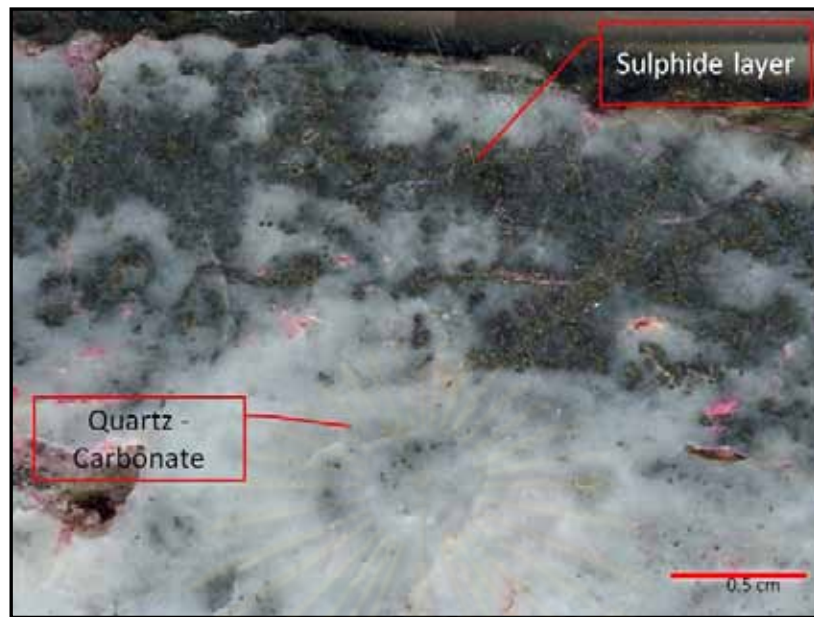
Figure 4.15 Photograph of Stage III core slab showing quartz–carbonate vein with sulphides as layers and dissemination in milky quartz.

Table 4. 5 The result from EPMA of calcite vein composition in stage III of the H West Prospect.

Element	Cal-V1	Cal-V2	Cal-V3	Avg	An-prop	Cation	Std-wall
SiO2	0.01	0.00	0.00	0.00	0.00	0.00	50.32
TiO2	0.01	0.00	0.03	0.01	0.00	0.00	0.03
Al2O3	0.00	0.00	0.01	0.00	0.00	0.00	0.00
FeO	0.00	0.00	0.19	0.06	0.00	0.00	0.05
MnO	3.11	3.06	3.32	3.17	0.04	0.04	0.36
MgO	0.06	0.04	0.12	0.07	0.00	0.00	0.03
CaO	61.08	61.87	58.03	60.33	1.08	0.95	47.51
Na2O	0.00	0.00	0.03	0.01	0.00	0.00	0.00
K2O	0.09	0.10	0.59	0.26	0.00	0.00	0.02
NiO	0.00	0.00	0.00	0.00	0.00	0.00	0.00
P2O5	0.00	0.00	0.00	0.00	0.00	0.00	0.00
As2O3	0.00	0.00	0.00	0.00	0.00	0.00	0.01
ZnO	0.01	0.01	0.08	0.03	0.00	0.00	0.00
BaO	0.00	0.00	0.00	0.00	0.00	0.00	0.00
CoO	0.02	0.00	0.01	0.01	0.00	0.00	0.00
SO3	0.02	0.03	0.01	0.02	0.00	0.00	0.03
ZrO2	0.01	0.00	0.00	0.00	0.00	0.00	0.00
Total	64.41	65.12	62.42	63.99	1.13	1.00	98.36
				Oxygen factor	0.89		

Figure 4.16 Photograph of core slab showing Stage III quartz–carbonate–sulphide minerals cementing silicified andesite clasts, and later crosscut by calcite veinlets (Stage V).

c) Breccia filling style in the lower zone; it is the continuation from the H Prospect mineralization. Cross-section shows west-dipping zones (Figure 4.1). It is characterized by quartz–carbonates-sulphide cementing hydrothermally-brecciated clasts of silicified andesite. Milky quartz intimately intergrown with white carbonate and sulphide and chlorite patches or dissemination (Figure 4.17) are the main mineralization cementing materials. Moreover, hydrothermally-brecciated andesite clasts cemented by quartz–carbonate–chalcedony-disseminated- sulphide were also found in this zone (Figure 4.18). Quartz shows colloform banding texture. Moreover, pyrite was also found in close association with sphalerite and chalcopyrite as dissemination in host rock (Figure 4.19) that may relate to the Stage III mineralization. Chlorite is typically medium green. This zone carried only 1 g/t Au on the average.
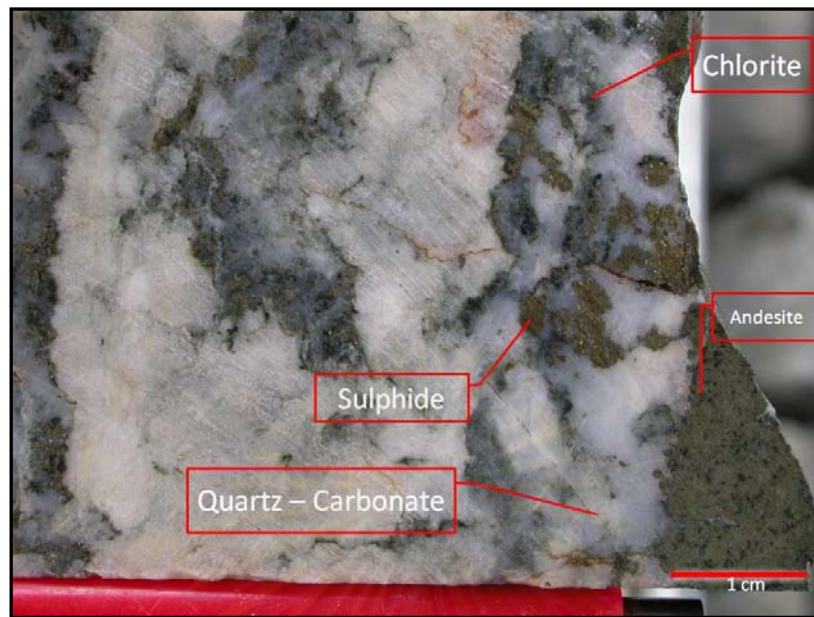
Figure 4. 17 Photograph of Stage III core slab showing quartz–carbonate with sulphide and chlorite patches and andesite clasts.
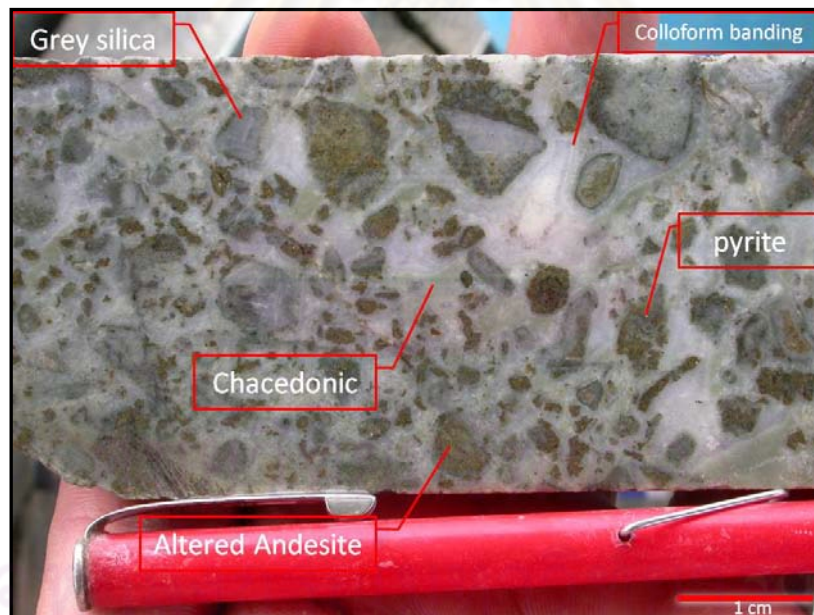
Figure 4.18 Photograph of Stage III core slab showing hydrothermally-brecciated clasts of grey silica (Stage I chalcedony) and silicified andesite, cemented by colloform banded quartz, carbonate, chalcedony with disseminated pyrite.
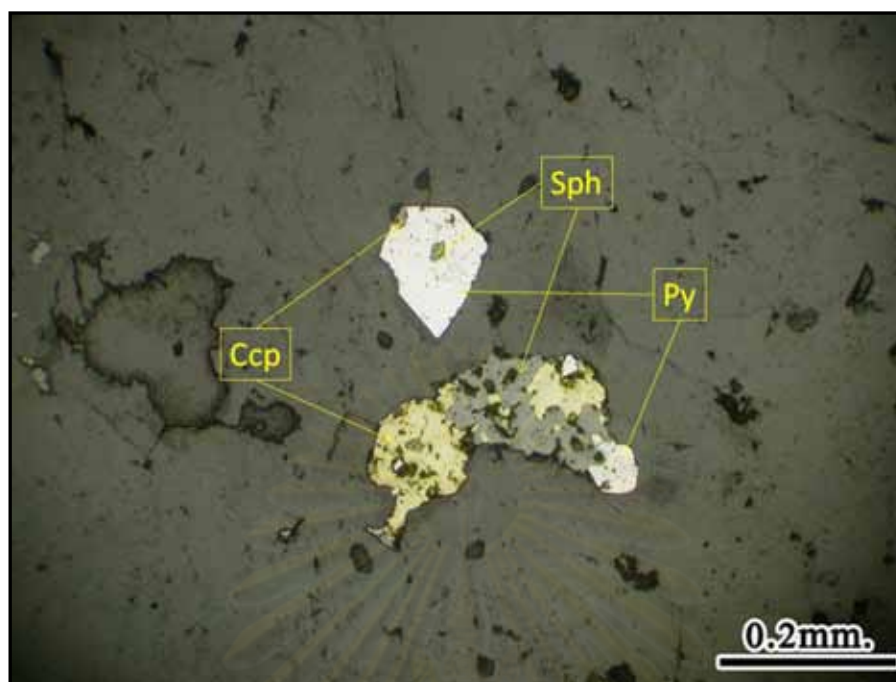
Figure 4. 19 Photomicrograph of pyrite (Py), chalcopyrite (Ccp) and sphalerite (Sph) disseminated in host rock as the products of hydrothermal alteration (reflected light).

Stage IV: quartz–carbonate–prehnite veinlets

This stage typically forms as veinlets of 1-8mm wide, crosscut early stages (Figure 4.20) and also exists as small patches, discontinuous trails and stockworks in wall rocks. The stage IV veins are composed of transparent comb quartz (Figure 4.21) with minor carbonates and adularia salvage (Figure 4.21). Euhedral pyrite also found in Stage IV veins and as replacement in the wall rock (Figure 4.22). Prehnite occurs in trace amount in stage IV veinlets and can be recognized only under the microscope (Figure 4.23). The EPMA analysis gives prehnite composition of $Ca_{2.03}$ ($Al_{2.24}$ $Fe_{0.34}$ $Mn_{0.05}$) $Si_{3.10}$ O_{10} $(OH)_2$ (Table 4.6).

Table 4. 6 The EPMA analysis of prehnite composition in stage IV of the H West Prospect.

Element	Prh1	Prh2	Prh3	Prh4	Prh5	Prh6	Prh7	Prh8	Prh9	Prh10	Prh11	Avg	STD-wall	Element	Mol-prop	Cation
Al2O3	26.94	24.92	23.31	24.68	26.02	22.77	22.84	22.71	24.98	23.88	23.27	24.21	0.00	Al	0.71	2.24
SiO2	38.30	37.94	37.92	38.08	38.21	42.32	42.85	43.04	38.02	38.07	37.58	39.30	50.77	Si	1.31	3.10
Cr2O3	0.03	0.00	0.02	0.00	0.02	0.03	0.00	0.00	0.01	0.02	0.00	0.01	0.00	Cr	0.00	0.00
ZrO2	0.01	0.00	0.03	0.03	0.03	0.00	0.00	0.00	0.00	0.01	0.00	0.01	0.00	Zr	0.00	0.00
NiO	0.00	0.00	0.06	0.00	0.05	0.02	0.00	0.03	0.00	0.02	0.00	0.02	0.00	Ni	0.00	0.00
MgO	0.01	0.03	0.03	0.04	0.03	0.00	0.01	0.00	0.03	0.03	0.03	0.02	0.04	Mg	0.00	0.00
Na2O	0.00	0.01	0.02	0.01	0.00	0.00	0.01	0.00	0.02	0.00	0.02	0.01	0.02	Na	0.00	0.00
ZnO	0.00	0.00	0.01	0.00	0.00	0.03	0.00	0.01	0.00	0.04	0.00	0.01	0.11	Zn	0.00	0.00
TiO2	0.04	0.03	0.00	0.00	0.05	0.05	0.05	0.04	0.00	0.00	0.00	0.02	0.07	Ti	0.00	0.00
MnO	0.94	0.97	1.12	1.05	0.97	0.42	0.44	0.42	0.93	0.62	0.94	0.80	0.42	Mn	0.01	0.05
SO3	0.00	0.00	0.02	0.00	0.01	0.00	0.00	0.02	0.00	0.00	0.01	0.01	0.01	S	0.00	0.00
As2O5	0.00	0.00	0.00	0.00	0.00	0.02	0.04	0.00	0.00	0.01	0.02	0.01	0.00	As	0.00	0.00
FeO	4.98	6.34	7.64	6.83	5.37	1.17	1.53	1.59	6.38	7.28	7.97	5.19	0.05	Fe	0.07	0.34
K2O	0.04	0.01	0.01	0.02	0.03	0.00	0.01	0.01	0.02	0.00	0.00	0.01	0.00	K	0.00	0.00
CaO	23.40	23.60	23.35	23.70	23.39	25.43	25.53	25.66	23.46	23.74	23.39	24.06	48.45	Ca	0.43	2.03
PbO	0.00	0.00	0.00	0.15	0.12	0.27	0.26	0.00	0.22	0.00	0.16	0.11	0.04	Pb	0.00	0.00
CuO	0.01	0.03	0.00	0.00	0.00	0.00	0.03	0.00	0.00	0.01	0.01	0.01	0.00	Cu	0.00	0.00
Total	94.69	93.88	93.56	94.58	94.29	92.53	93.59	93.53	94.07	93.73	93.40	93.80	99.98		2.54	7.78
			Prehnite		Ca2Al(Al2Si3O10)(OH)2									Oxygen factor		4.73
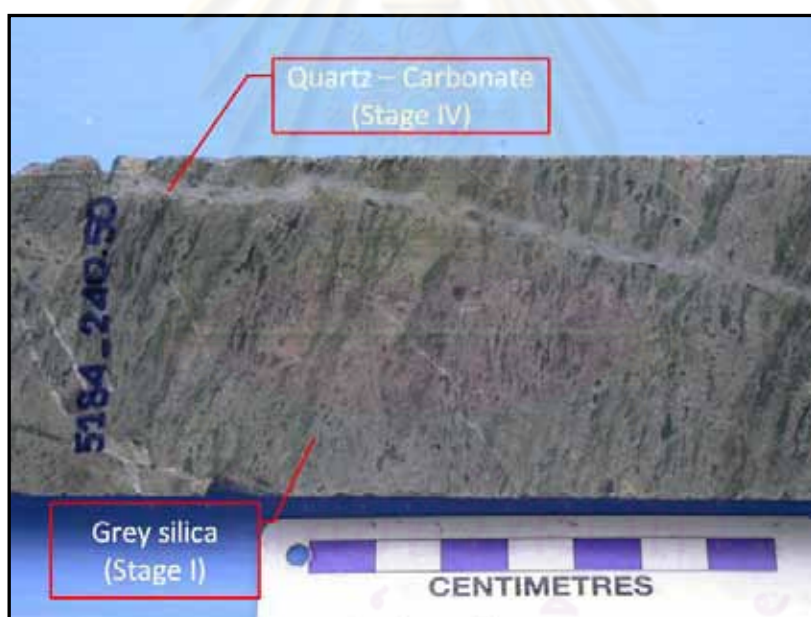
Figure 4.20 Photograph of silicified rhyolitic flow core slab showing grey chacedony (Stage I) replacing the host rock and later cut by quartz–carbonate veinlets (Stage IV).
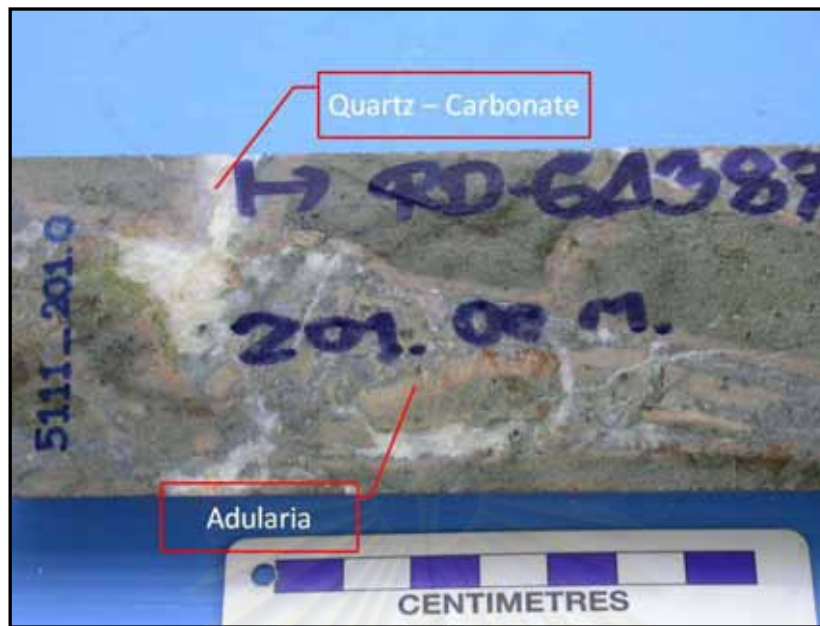
Figure 4.21 Photograph of Unit 3 andesite core slab showing quartz–carbonate veins (Stage IV) rimming by pink adularia bands.
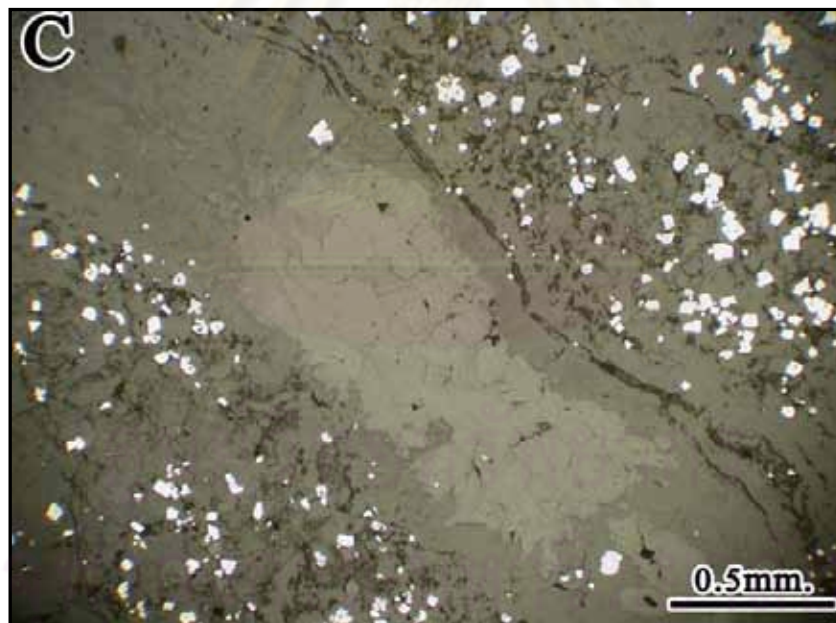
Figure 4. 22 Photomicrograph of quartz–prehnite–carbonate veinlets (Stage IV) with euhedral pyrite disseminated in vein and wall rock (reflected light).
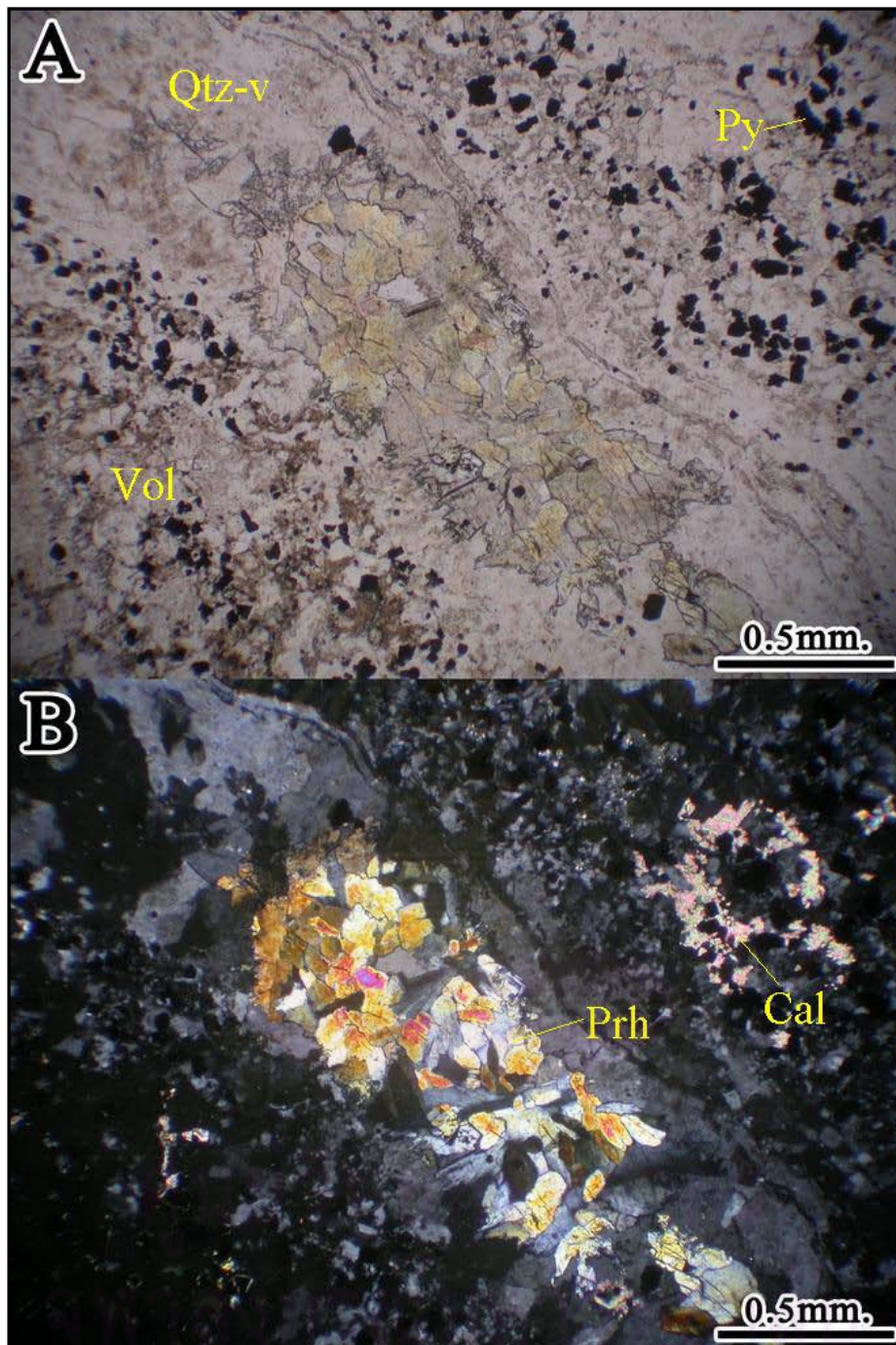
Figure 4. 23 Photomicrograph of andesite (Unit 3) (Vol) showing quartz (Qtz-v)-prehnite (Prh) veinlet crosscutting, and carbonate (Cal) and pyrite (Py) replacing wall rock. (A) plane-polarized light, (B) crossed polars.

Stage V: Non-ferroan calcite veinlets

The non-ferroan calcite veinlets form the later vein stage and crosscut all other vein stages and all rock units (Figure 4.24). Non-ferroan calcite veins are usually 1-5mm wide and also exist as small patches, discontinuous trails and stockworks in wall rock. This stage is similar to the Stage IV of the A Prospect.
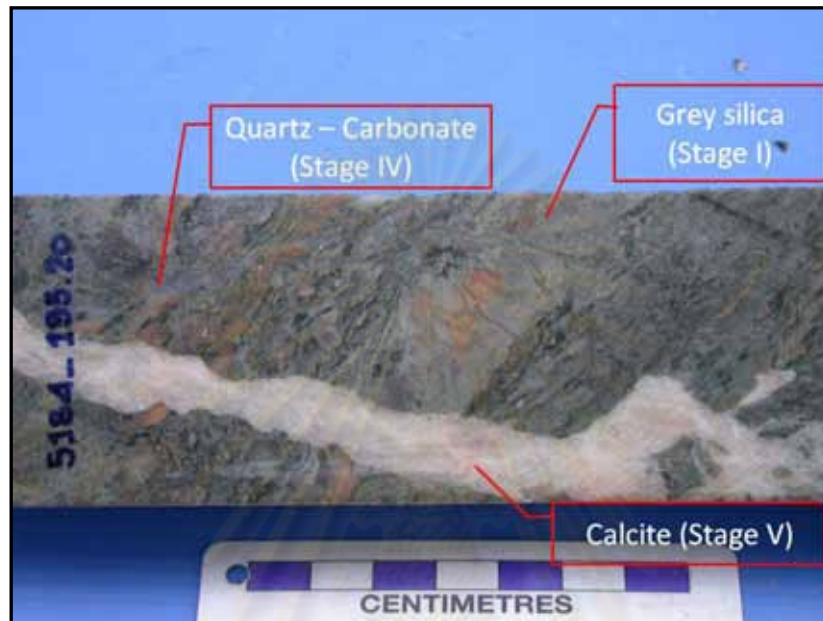
Figure 4.24 Photograph of silicified rhyolitic flow unit showing grey chacedony (Stage I) cut by quartz–carbonate veinlets (Stage IV), and later crosscut by non-ferroan calcite veinlet (stage V).

Stage VI: Laumontite

Laumontite marks the latest stage of the H West Prospect. Laumontite (comfirmed by XRD analysis) filled in fractures of late stage dykes and andesite (Unit 3).

4.3 Wall Rock Alterations

This section describes mineral alteration petrography and paragenesis of host rocks in the H West Prospect based on diamond drill core logging (especially selected section; 5285mN), thin sections, carbonate staining and K-feldspar staining techniques. These alterations are described following each rock units:

Alteration in Unit 1: the Fiamme breccia in the upper most part of the H West Prospect, likes the A Prospect characteristic, show less mineralization and alteration except dark green chlorite replaced fiamme clasts (Figure 4.25).
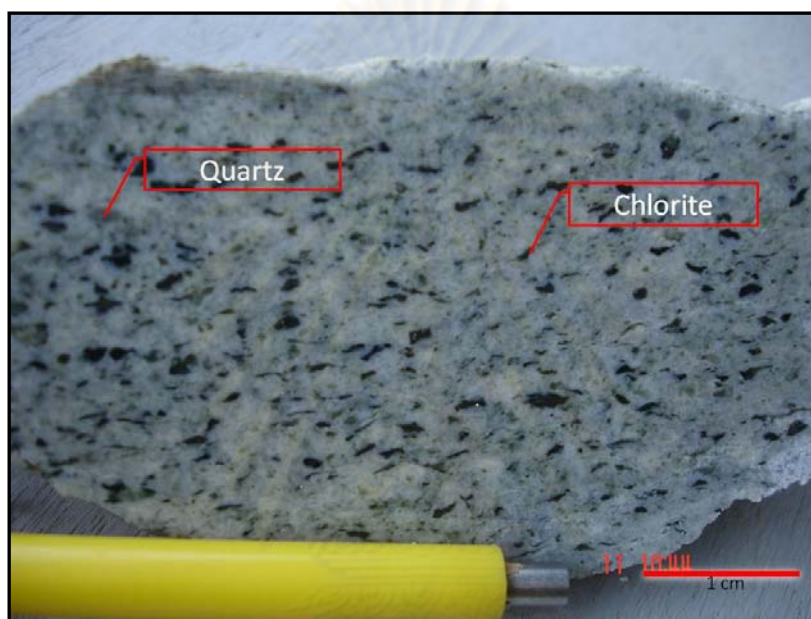
Figure 4. 25 Photograph of fiamme (Unit 1) hand specimen showing chlorite-replaced-fiamme clasts and quartz eyes.

Alteration in Unit 3: the andesitic rocks are the dominant wall rocks that host the mineralization in the H West Prospect. They comprise andesite, monomictic andesitic breccia and polymictic andesitic breccia. The host rocks proximal to the vein zone in this unit show two types of alteration, namely silicification and/or K-feldspar ± quartz (or potassic) alteration (Figure 4.26). The halos of these types of alterations in the H West Prospect are rather narrow as compared with those found in the A Prospect and normally about 1-2 mm scale or may be upto 20 cm wide around veins system only.   Under microscope the rocks contains aggregates of quartz (resulting from silicification), K-feldspar and euhedral pyrite (Figure 4.27). Those are most likely to have formed by deposition in tiny cracks. The rocks have occasional fractures that are sealed by late quartz and calcite. Silicification may associate with Stage I, whereas K-feldspar ± quartz (potassic) alteration may associate with Stage III and IV vein systems.
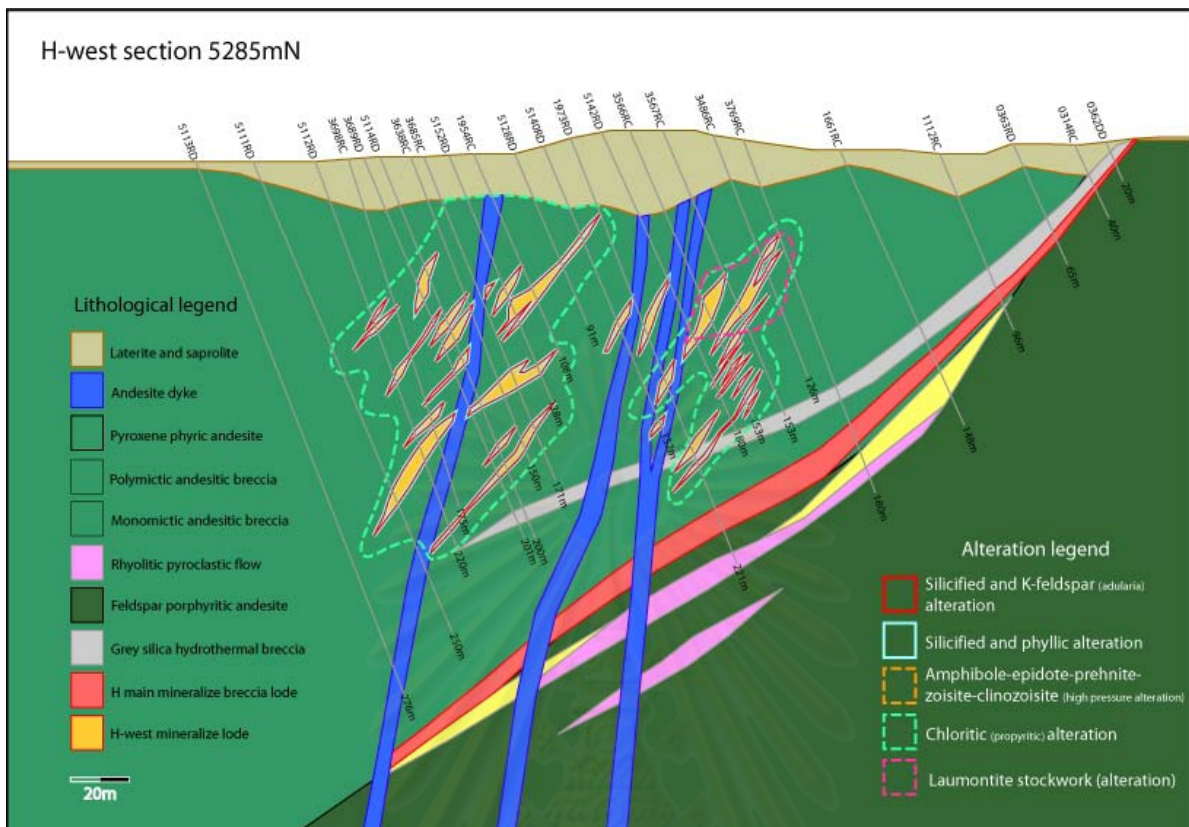
Figure 4. 26 Picture display cross section of 5285mN with alteration assemblages and widespread in host rock.

In fact, K–feldspar (potassic) alteration is discovered as a narrow zone around Stage IV vein system. In hand specimens, the Stage IV quartz–carbonate vein is rimmed by pink adularia band (about 5 mm wide; Figure 4.21) or occurs as phenocryst-like in porphyritic andesite host rock. XRD analysis confirmed that the pink mineral is adularia (Figure 4.28). Microscopically the pink adularia is sub-rhombic and rimming comb quartz-carbonate vein associated with subhedral pyrite aggregates (Figure 4.29). However, the result from EPMA analysis show composition as $(K_{0.84}Na_{0.02}Ba_{0.05})$ $(Al_{1.61}Si_{0.54})$ Si_4O_{10} $(OH)_2 - xH_2O$ (Table 4.7) that suggested adularia was overprinted by illite (clay minerals).

Moreover, thin section shows subhedral plagioclase phenocrysts in felty texture groundmass and subhedral to euhedral pyrite (Figure 4.30). That phenocrystic plagioclase feldspar might have overgrown on by sub-rhombic adularia. Growth direction is point to quartz vein. Cavities and veins are sealed by drusy mosaic quartz and carbonate (Figure 4.30). This feature might have been associated with Stage III vein system.

Next away from the veins zone, sericite (phyllic) selectively replaces plagioclase and K-feldspar in both phenocrysts and groundmass. This alteration type is found in narrow zone outlining silicification zone or by overprinting K-feldspar and adularia alteration zone.

Chlorite (propyritic) alteration is found distal from the vein zone as widespread halo. Chlorite selectively replaces feldspar both in groundmass and phenocrysts. Carbonate is later than chlorite (Figure 4.31).
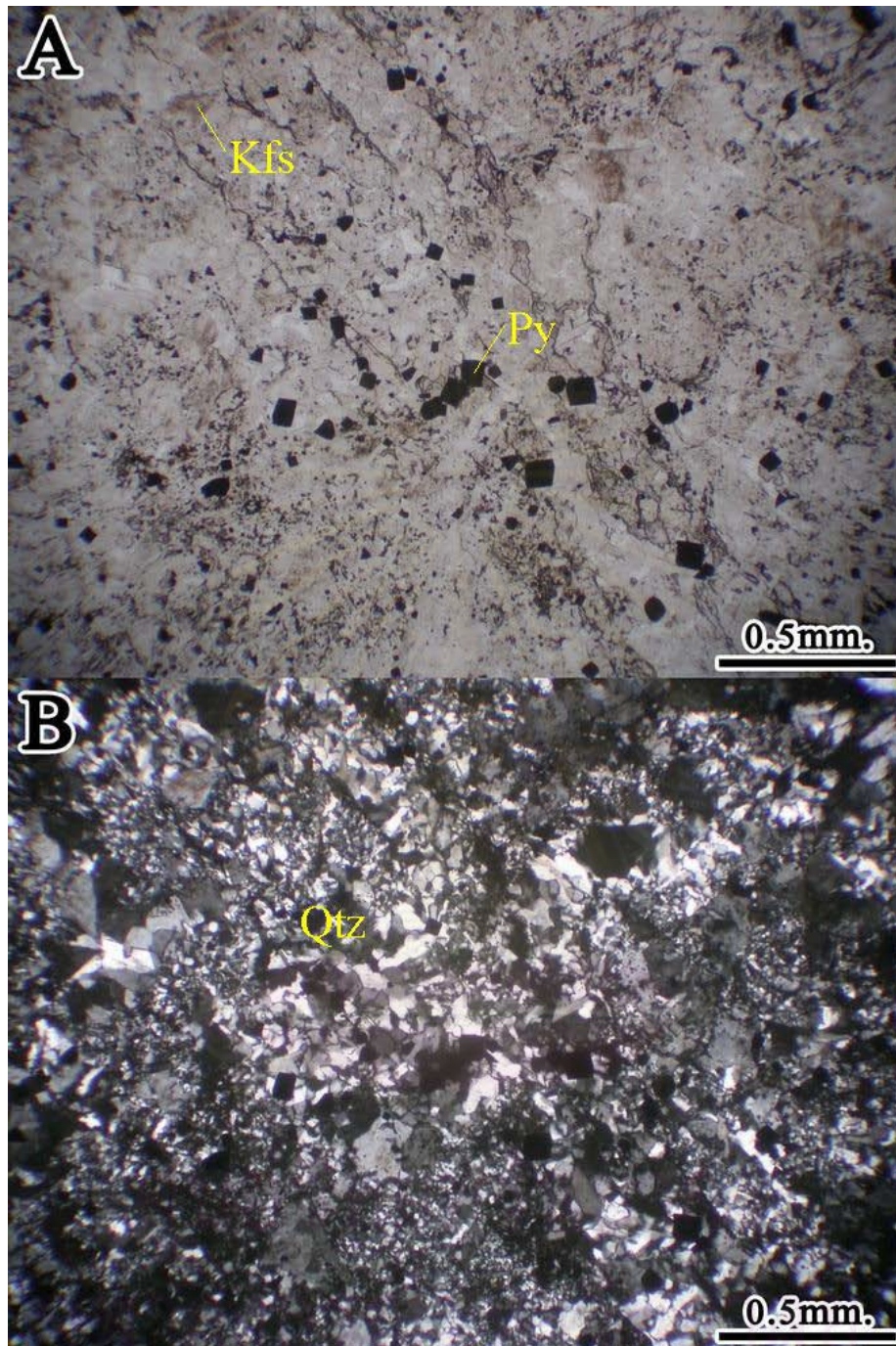
Figure 4.27 Photomicrograph of silicified andesite (Unit 3) showing fine-grained quartz and K-feldspar (Kfs), drusy mosaic quartz (Qtz) and euhedral pyrite (Py) replacing the host rock. (A) plane-polarized light, (B) crossed polars.
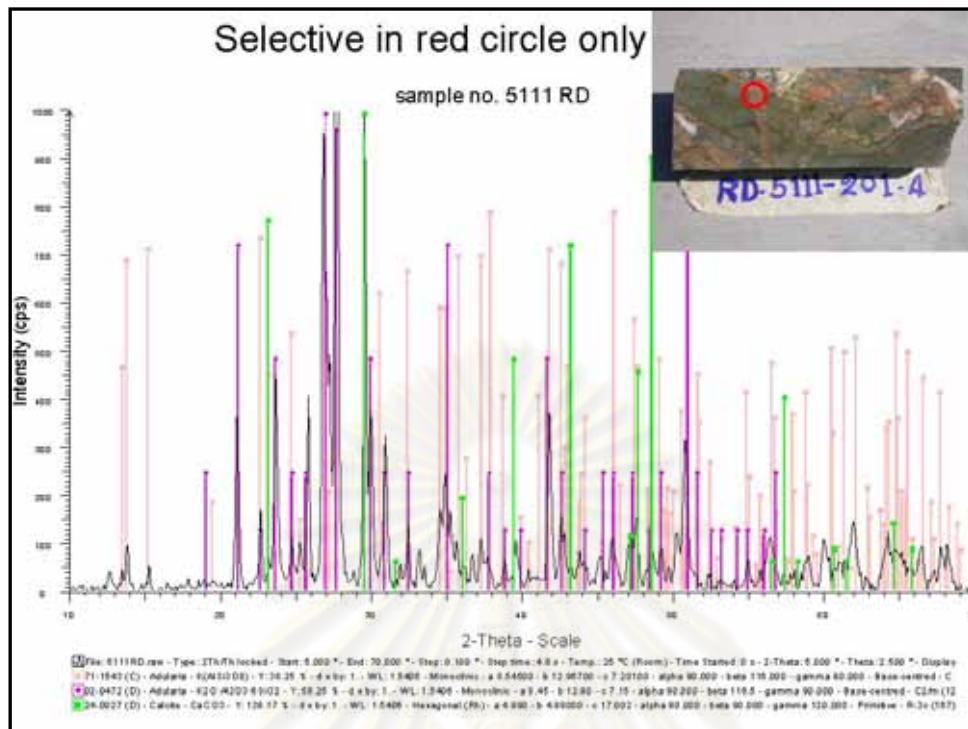
Figure 4.28 The XRD pattern of minerals in red circle (right–upper picture) indicating adularia.

Table 4. 7 The EPMA result of Stage IV adularia alteration composition.

Comment	Ad1	Ad2	Ad3	Ad4	Ad5	Average	An Prop	Element	Cation
SiO2	63.14	57.61	63.06	62.79	64.10	62.14	0.00	**Si**	4.54
TiO2	0.02	0.06	0.04	0.02	0.00	0.03	2.07	**Ti**	0.00
Al2O3	18.36	22.93	16.86	18.10	17.25	18.70	0.00	**Al**	1.61
FeO	0.29	0.27	0.09	0.20	0.18	0.21	0.00	**Fe**	0.01
MnO	0.02	0.06	0.00	0.00	0.01	0.02	0.55	**Mn**	0.00
MgO	0.12	0.18	0.00	0.01	0.00	0.06	0.00	**Mg**	0.01
CaO	0.07	0.10	0.04	0.00	0.01	0.04	0.00	**Ca**	0.00
Na2O	0.12	0.19	0.14	0.14	0.19	0.16	0.10	**Na**	0.02
K2O	9.36	6.99	8.18	11.15	9.38	9.01	0.00	**K**	0.84
BaO	1.30	4.35	0.99	0.78	0.62	1.61	0.01	**Ba**	0.05
Total	92.80	92.74	89.40	93.19	91.73	91.97	2.74	**Total**	7.08
						oxygen factor	4.39		
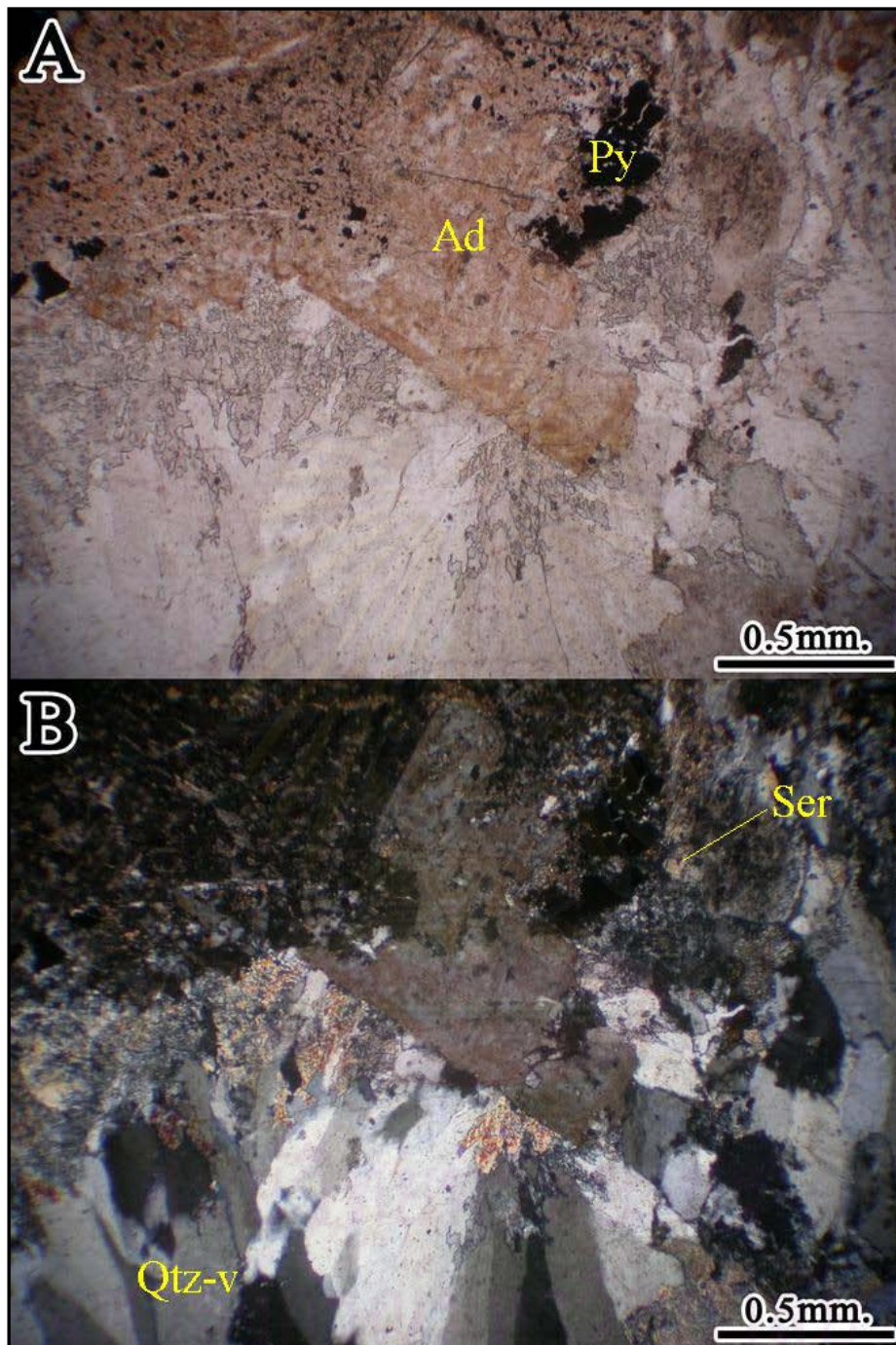
Figure 4.29 Photomicrograph of highly altered andesite (Unit 3) showing sub-rhombic adularia (Ad) as rim of comb quartz-carbonate vein (Qtz-v) with subhedral pyrite aggregate (Py) and feldspar replaced by sericite (Ser). (A) plane-polarized light, (B) crossed polars.
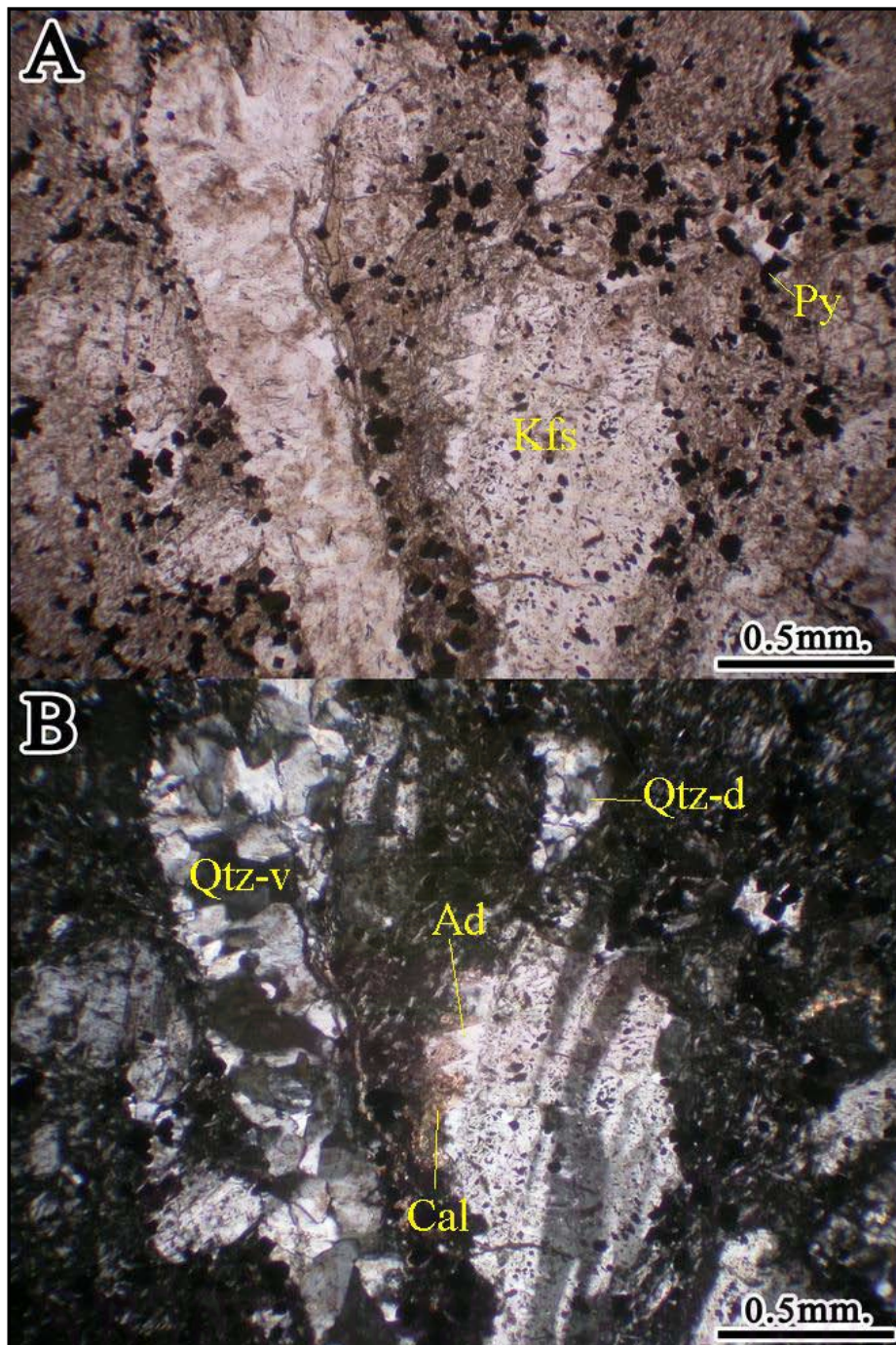
Figure 4.30 Photomicrograph of porphyritic andesite (Unit 3) showing sub-rhombic overgrowth adularia (Ad) as rim of K-feldspar-replaced plagioclase grains (Kfs) and disseminated euhedral pyrite (Py). Cavities are sealed by drusy mosaic quartz (Qtz-d) and carbonate (Cal). Late quartz vein (Qtz-v) crosscut this rock. (A) plane-polarized light, (B) crossed polars.
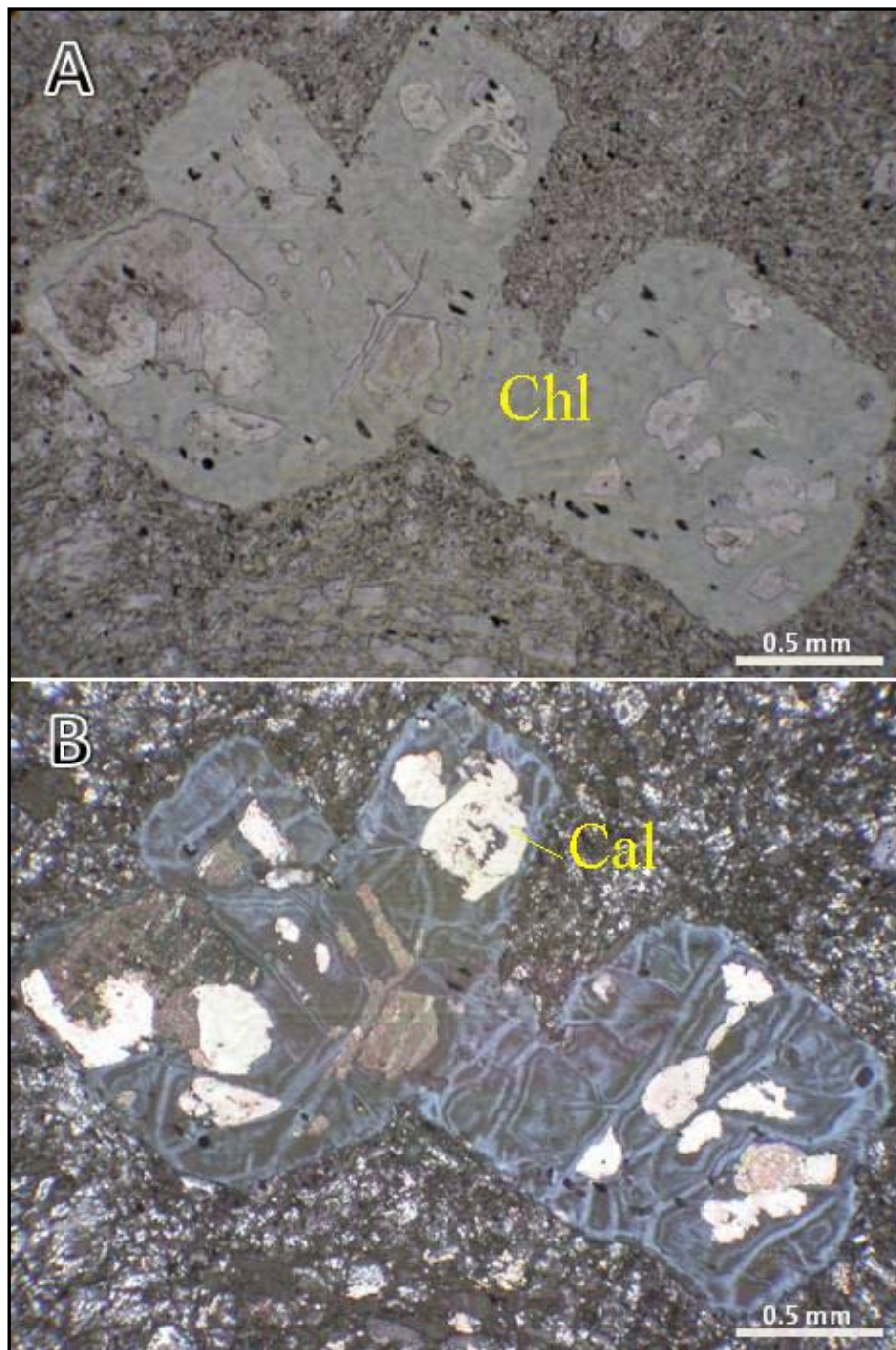
Figure 4.31 Photomicrograph of propylitic alteration of Unit 3 andesite host rock displaying chlorite (Chl) and carbonate (Cal) replace pyroxene(?) phenocryst. A = plane-polarized light, B = crossed polars.

Alteration in Unit 4: andesite porphyry unit, the lowest unit in Chatree Deposit and in the H West Prospect, shows propylitic alteration only. The alteration in this unit is characterized by major chlorite and minor sericite replacing primary K-feldspar, plagioclase and mafic mineral (pyroxene?) both in phenocrysts and groundmass. Later carbonate has overprinted on altered phenocrysts (Figure 4.32).
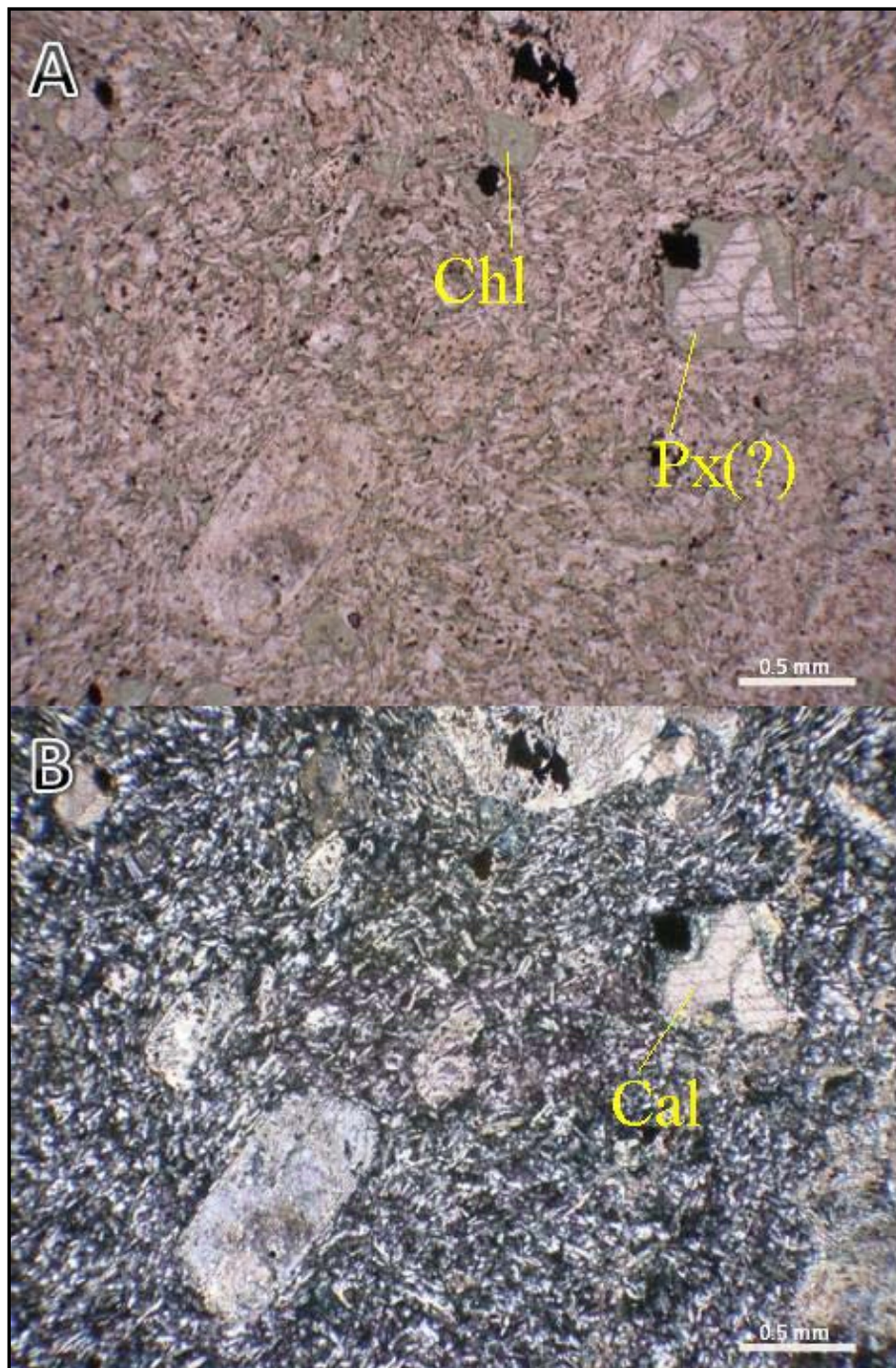
Figure 4.32 Photomicrograph of propyritic altered andesite porphyry of of Unit 4 displaying pyroxene relict (Px(?)) with chlorite (Chl) and carbonate (Cal) replacement. A = plane-polarized light, B = crossed polars.

Type of alteration

Based on the above detailed description of alteration minerals, texture and distribution in relation to the vein system, they can be classified in term of alteration types below.

Silica Alteration or Silification

The earliest alteration stage consists of pervasive silica flooding of rhyolitic unit between Unit 3 and Unit 4. The pervasive alteration zones are associated with grey chalcedony (Stage I). Silicification may be affected from stage III and stage IV vein systems. This alteration usually about 1–2 mm wide and may be up to a maximum of 20 cm wide.

K-feldspar (±Quartz) or Potassic alteration

K-feldspar or potassic alteration is characterized by low temperature K-feldspar and adularia. K-feldspar is generally replacement and overgrowth plagioclase in andesite of Unit 3. Adularia is euhedral to subhedral rhombic rim. The K-feldspar alteration may relate to stage III and IV vein systems, approximately 1–5 cm from the vein zone.

Sericite (±Quartz) or Phyllic Alteration

Sericite is the key mineral of phyllic alteration and usually fine-grained and typically white to pale yellow. Sericite occurs as cloudy in secondary K-feldspar and replacing plagioclase phenocrysts and plagioclase groundmass in host rocks next away from proximal ore zone and may associate with vein Stage III and IV.

Chlorite (± Carbonates) or Propyritic alteration

Chlorite is found as completely alteration of fiamme clasts in fiamme unit 1 and selective alteration in phenocrysts and groundmass in andesitic unit (Unit 3). This alteration assemblage associated with mainly vein Stage III and minor in Stage IV and V veins that are distal from vein systems. Carbonate minerals were found to replace feldspar, pyroxene and other groundmass minerals in host rocks which may associate with vein Stage III, IV and V.

4.4 Timing Sequence of Ore, Gangue and Alteration Minerals

The paragenesis of ore, gangue and alteration minerals in the H West Prospect are summarized in Table 4.8. Stage I was started with silicification. After that silicification still continued with K-feldspar alteration, phyllic alteration and propylitic alteration from Stage III and continued to Stage IV, especially K-feldspar alteration. The late carbonate is assumed to be in the Stage V or quartz–carbonate veins.

Table 4. 8 Diagram summarizes mineralization and alteration paragenesis of the H West Prospect. Ore and vein occur as vein mineralization while alteration is alteration mineral assemblage in host rock.

Minerals \ Stages	Pre-mineralized Stage I	Pre-mineralized Stage II	Mineralized stage Stage III	Post - mineralized Stage IV	Post - mineralized Stage V	Post - mineralized Stage VI
Ore Euhedral pyrite	▬▬▬	───	───			
Anhedral pyrite			▬▬▬			
Sphalerite			▬▬▬			
Chalcopyrite			───			
Electrum			--------			
Galena			--------			
Gangue Gray chacedony	▬▬▬		--------			
Quartz		▬▬▬	───	───		
Chacedony			▬▬▬			
Adularia			───			
Calcite		--------			▬▬▬	
Chlorite			--------			
Prehnite				--------		
Laumontite						▬▬▬
Alteration Quartz	▬▬▬		▬▬▬	───		
K-feldspar (adularia)			▬▬▬	───		
Sericite/Clay minerals			───	───		
Calcite				───		
Chlorite				───		

▬▬▬▬	Major
────────	Minor
--------	Trace

CHAPTER V

DISCUSSION AND CONCLUSION

5.1 Contrasing Vein Stage Mineralization of the A and H West Prospects

The Stage I mineralization of the A Prospect was found only in minor amount as brecciated clasts in other stages. In contrast the Stage I mineralization of the H West Prospect was recognized as hydrothermal breccia unit (up to 10m thick) surrounded by andesitic rocks. This breccia unit is characterized by silicified andesitic clasts that are cemented by gray chalcedony showing jigsaw to cockage breccia texture. It was probable that the the Stage I mineralization of both A and H West Prospects represented by pervasive silica flooding in the form of grey chalcedonic replacement of rhyolitic and andesitic host rocks as well as in the form of cementing material of silicified brecciated clasts (i.e., in the H West Prospect). This imply that the Stage I grey silica flooding occurred as early replacement and also continued as cementing material of hydrothermally brecciated clasts after hydro-fracturing event causing sudden failure of silicified host-rocks accompanying with rapid influx of ore-forming fluids evolved from crystallizing water-saturated magma.

The Stage II mineralization of A Prospect occurred as milky-quartz-euhedral-pyrite veins and veinlets, whereas the Stage II mineralization of the H West Prospect was found only as breccias in stage III vein system. Hence the Stage II veins were formed by open fissure filling, which might have been brecciated later by the Stage III fluid.

Stage III mineralization in the A Prospect is dominated by chalcedony on top of the hill and by milky quartz at deeper level in the forms of crustiform-colloform banded veins, massive veins and breccia-filling. The crustiform-colloform banded veins are alternating layers of chalcedony, quartz and/or carbonates, chlorite and sulphides, the so-called "Ginguru band" by Corbett (2002). Microcrystalline anhedral quartz tends to form close to vein or breccia clasts occasionally associated with fine-grained sulphides (pyrite, chalcopyrite and sphalerite) whereas coarser-grained subhedral to euhedral quartz tends to confine in inner veins with carbonate (calcite, dolomite and rhodochrosite), fine to course grained chlorite, sulphides and electrum. Furthermore, amethyst occurs as coarse-grained euhedral crystals in veins. Carbonate is also common gangue mineral and widely distributed. It usually forms as bands alternated with quartz and chlorite bands and closely associated with quartz and/or chlorite in massive veins. Opal or amorphous silica is not present in the A Prospect. This may imply that the silica sinter part of the system might have been completely eroded away.

In contrast, Stage III mineraliztion of the H West Prospect is dominated primarily milky quartz, subordinate chalcedony and carbonates, and minor sulphides, adularia, chlorite in the forms of as massive veins, colloform-crustiform banded veins and breccia filling similar to those of the A Prospect. The sulphide minerals occur as pyrite, chalcopyrite, and sphalerite while gold occur as electrum.

.

Stage IV mineralization of the A Prospect is characterized by veins and veinlets of transparent quartz with minor non-ferroan calcite, dolomite and rhodochrosite, while that of the H West Prospect has similar veining and mineralogy except with additional prehnite.

Stage V and VI mineralization are characterized similarly by non-ferroan calcite veinlets and fracture-filled zeolite, respectively, in both Prospects.

5.2 Comparison of Mineralization with other Prospects in the Chatree Gold Deposit

The vein characteristics of the A and H West Prospects can be compared with other prospects (Table 5.1). The different Prospects at the Chatree Gold deposit show slightly different interpreted number of vein stages. However, veins texture and mineralogy are similar. Crustiform-colloform and breccias are the main textures. In the same way, electrum is the most abundance and occurs as dissemination and inclusions mainly in pyrite and minor in other sulphide minerals.

Table 5. 1 Comparison of vein characteristics of the A and H West Prospects with other Prospects in the Chatree Gold Deposit.

Prospect	A	D	C	H	All chatree (combine)	A	H West
Referance	Dedenczuk (1998)	Dedenczuk (1998)	Greener (1999)	Kromkhun (2005)	Salam (2010)	This study	This study
Number of vein stage	4	6	3	4	6	6	6
Ore Stage	2	3	2b	2	3	3	3
Ore orientation	350/near vertical	350/near vertical	350/ 50-60	250/45	depend on prospect but 2 major directions; N-S and NE-SW	350/ 50-60w	040/40-50w
Ore vein texture	Crustiform-colloform band, cockade	Crustiform-colloform band	Crustiform band, comb	Crustiform band, comb, breccia, vuggy	Crustiform-colloform band, breccia, massive	Crustiform-colloform band, breccia, massive	Crustiform-colloform band, breccia, massive
Gange minerals	Quartz, calcite, dolomite, jasper, illite/smectite, adularia, epidote	Quartz, calcite, dolomite, jasper, illite/smectite, adularia, epidote	Quartz, calcite, chalcedony, prehnite, adularia	Quartz, calcite, chlorite, illite, illite-smectite, sericite, ankerite, dolomite, epidote, adularia, hematite, rhodochrosite, chalcedony,	Quartz, carbonate, chlorite, adularia	Quartz, chalcedony, calcite, dolomite, chlorite, adularia, hematite	Quartz, carbonate, chalcedony, chlorite, adularia
Ore minerals	pyrite, electrum, chalcopyrite,	pyrite, electrum, chalcopyrite	sphalerite, galena, chalcopyrite, tetrahedrite, electrum, native silver	pyrite, sphalerite, galena, chalcopyrite, electrum	Pyrite, sphalerite, chalcopyrite, galena, electrum	pyrite, sphalerite, chalcopyrite, electrum	Pyrite, sphalerite, chalcopyrite, galena, electrum
Electrum occurance	Disseminate and inclusion in sulphide minerals	Disseminate and inclusion in pyrite	Bleb with sulphide minerals	Disseminate, inclusion and adjacent with sulphide minerals	free grains and inclusionsin sulphide minerals	Disseminate and inclusion mainly in pyrite	Disseminate and inclusion mainly in pyrite

5.3 Contrasting Textual Styles and Mineral Assemblages of the A and H West Prospects

Hedenquist (2000) described some typical textures of many gangue minerals in mineralized veins vary with depth. So it is possible to use some gangue mineral textures to indicate the depth level of the A and H West Prospects with respect to a typical epithermal system. For example, chalcedonic–adularia–calcite–illite assemblage is typical of shallow depths (0–300 m.) while quartz–carbonate–rhodonite–sericite– adularia ± barite ± anhydrite ± hematite ± chlorite assemblage is common at deep level (300–800 m.).

Quartz is a common gangue mineral in epithermal low–sulphidation system. Quartz textures, assuming vertical zonation, can be used to give information on crystallization condition, paleo-isotherms and proximity to ore (Dong et al., 1995). At high level of the system it should be found as opal or amorphous silica indicating temperature about 150 C^o. At deeper level opal gives way to chalcedonic quartz indicating temperature between 100–190°C. Chalcedony gives way to crystalline quartz at deep level indicating temperature between 180–190°C (Hedenquist, 2000). The other quartz texture such as massive, moss, crustiform and crystalline were consistent with the part of crustiform-colloform zone (Morrison et al., 1990).

In the A Prospect, quartz occurs as crustiform–colloform bands but shows contrasting textural styles in upper and lower levels. In the upper zone it is dominant by chalcedonic to microcrystalline bands with fine-grained sulphide bands, whereas in the lower zone it is dominant by crystalline bands with associated adularia and disseminated sulphides and sulphide bands (Figure 5.1).

Quartz precipitates in wide temperature range and generally forms as a result of decreasing fluid temperature (Thomson and Thomson, 1996). Generally chalcedony is found in vein system in acid to neutral pH conditions with rapid cooling or boiling. It was formed mostly less than 190 C^o in shallow epithermal deposits (Lawless et al., 1999). Abundant fine-grained quartz in the lower level suggests temperature were over 180–190 C^o (Simmons and Christenson, 1994).

In the H West Prospect quartz occurs as coarse crystalline crustiform–colloform bands with adularia, coarse-grained sulphides and carbonates. Generally there is a decrease of sulphides and adularia, but an increase of crystalline carbonates and quartz with depth (Figure 5.1).

Based on the above observations, it is likely that the A Prospect was formed at a higher level than that of the H West Prospect.

In the same way, adularia is one of common gangue minerals in both the mineralized veins and as alteration product in host rock. Dong and Morrison (1995) suggested morphology and texture assuming proportional to temperature, pressure, crystallization and thermal history. The sub-rhombic crystals indicate slow crystallization, small rhombs are found in crustiform and colloform banding, tabular forms occur on rapid boiling, and pseudoacicular crystals is the psuedomorph of carbonate precursor. Abundance of adularia decreases with increasing depth. Adularia in ore zone is present in boiling, low salinity and near neutral fluid. Adularia may have formed due to gas loss, pH increases and cooling in good permeability zones (Simmons et al., 2000). Adularia in veins is a good indicator of boiling fluid (Dong et

al., 1995). Therefore Adularia was likely to precipitate from near neutral to alkaline fluid with pH > 5.2 in good permeability zone (Lawless et al., 1999).

The presence of sub-rhombic adularia disseminated in or bordering veins or as crystal aggregates in host rocks of both prospects suggests slow crystallization from boiling hydrothermal solution at more than 100 m below paleo-surface of epithermal system (Dong et al., 1995; Dong and Morrison, 1995). Upon initial of boiling, hydrothermal fluid becomes alkaline which allow for precipitation adularia, and CO_2 loss occurs allowing for precipitation calcite. Comb quartz with sub-rhombic adularia, are formed by slow crystallization of hydrothermal fluid in open space

Carbonate minerals are mainly found in veins and have variable compositions, suggesting a range of fluid temperature, pressure and chemical condition during their formation. Calcite is the major carbonate mineral and forms over a wide temperature range. Calcite occurring in open-spaces may form from boiling and exsolution of CO_2. Whiles calcite alteration in host rock has suggested that CO_2 – rich fluid in rock with low porosity and low permeable. Dolomite is deposited from near-neutral fluids. It commonly precipitates from fluid with temperature < 200 c^o and rarely > 250 C^o. Ankerite and dolomite may form by fluid mixing in cooler zones (Lawless et al., 1999).
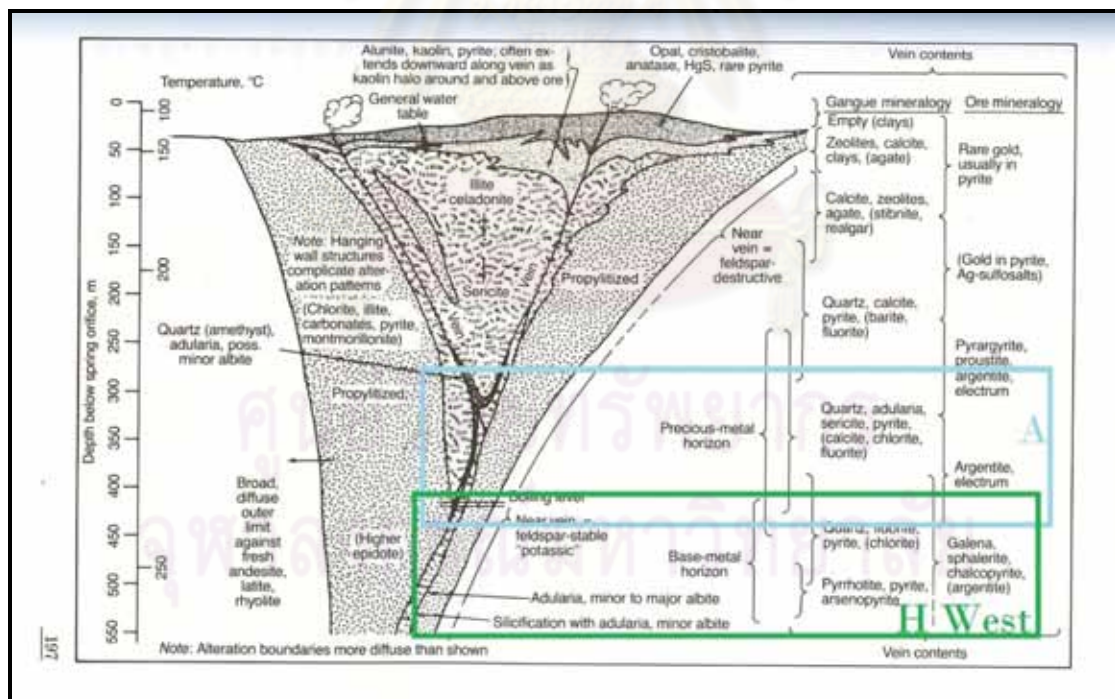
Figure 5. 1 Model of Epithermal system (modified from Buchanan, 1981 and Morrison et al., 1991) showing the position of the A Prospect (blue square) and the H West Prospect (green square) with respect to the textures of quartz and adularia.

5.4 Contrasting Mineral Alteration Halos of the A and H West Prospects

Proximal to the ore zone of the A Prospect, it is dominated by abundant K-feldspar alteration as well as silicification. The silification halo is approximately 5–20 m away from the vein zone while K-feldspar alteration halo is approximately 5–8 m away from the vein zone. The K-feldspar alteration is characterized by the occurrence of pink rhombic adularia inclusions in feldspar overgrowth as well as K-feldspar aggregates and ghost texture (recrystallization from moss texture) in the upper part of A Prospect. In contrast the alteration halo in the H West Prospect is millimeter to centimeter scale around veins only. Silicification is the main alteration forming halo around vein zone usually about 1–2 mm wide and may be up to a maximum of 20 cm wide. In addition, pink K–feldspar alteration is discovered as a narrow zone (about 5 mm) around stage IV quartz-carbonate veins. Phenocryst-like plagioclase in host rock was replaced by K-feldspar and rarely with syntaxial feldspar overgrowths, euhedral pyrite aggregate and adularia rhombs.

Distal to the ore zone at the A Prospect it is dominated by sericite and quartz or phyllic alteration at approximately 5–20 m from the vein zone. Sericite and quartz was found as selective replacement of host rock and some early altered minerals. In contrast phyllic alteration is found only as narrow zone outlining silicification zone by overprinting K-feldspar and adularia at the H West Prospect. Sericite is usually formed under slightly acid conditions with pH 4 – 6 and temperatures ~200–250 C^{o} (Thompson and Thompson, 1996).

Propyritic alteration is found distal from the vein zone as widespread halo in both Prospects. Chlorite selectively replaces feldspar both in groundmass and phenocrysts and carbonate post-dated chlorite. The presence of chlorite may indicate near neutral fluids of pH of 6–7 (Lawless et al., 1999), and suggest the lack of intense ion exchange. Propylitic alteration usually occurs at low temperature (200 – 300 C^{o}) in distal setting (Lawless et al., 1999) and forms from near-neutral pH fluids.

In conclusion, the A Prospect has more widespread alteration halo than that of the H West Prospect which may be the combined results of different host-rock types, dissimilar permeability (Figure 5.2), and the depth of the epithermal system.
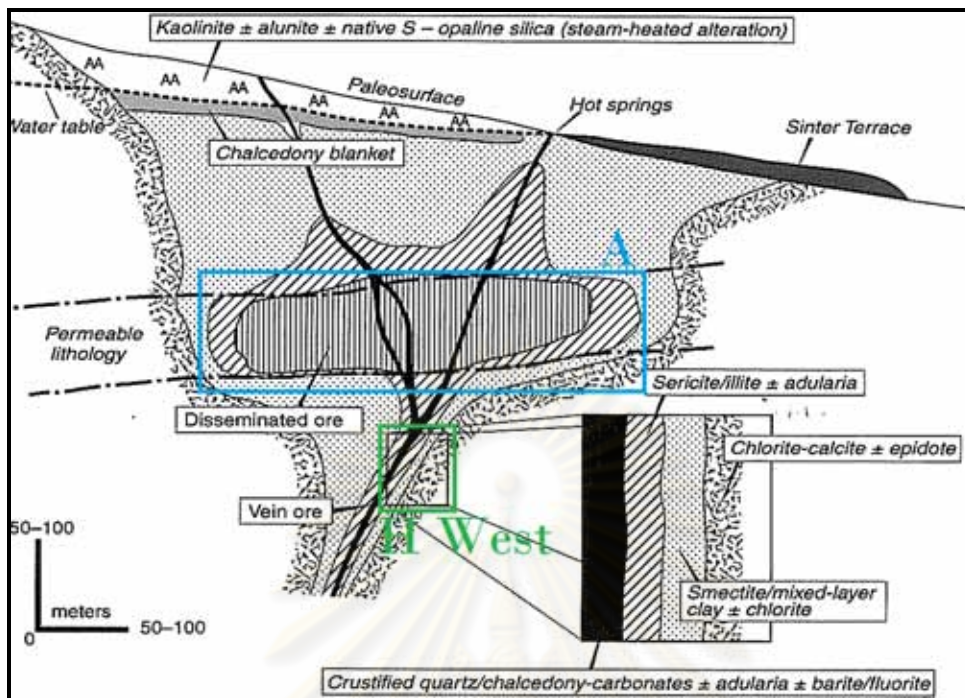
Figure 5. 2 Cartoon to illustrate generally patterns of alteration in low sulphidation system, showing the variable form with increasing depth, and the typical alteration zonation. Approximate of the A Prospect (blue square) the H West Prospect (green square) location on the model (modified from Hedenquist et al., 2000).

5.5 Minerals as the Indicator of depositional conditions

5.5.1 Temperature

The mineral assemblages suggested temperature in the A and the H West Prospects range between 100 to 300 C^o (Figure 5.3). This temperature range is consistent with those reported by Dedenczuk (1998) and Greener (1999) who suggested that the fluid temperature ranged between 100 to 300 C^o from fluid inclusion study in the A, C and D Prospects. Temperature of the H West Prospect from fluid inclusion is not studied in this work. The wide temperature range explains the range of different minerals found in the study areas. The highest temperature range is found from Stage IV with sericite at 250 C^o.
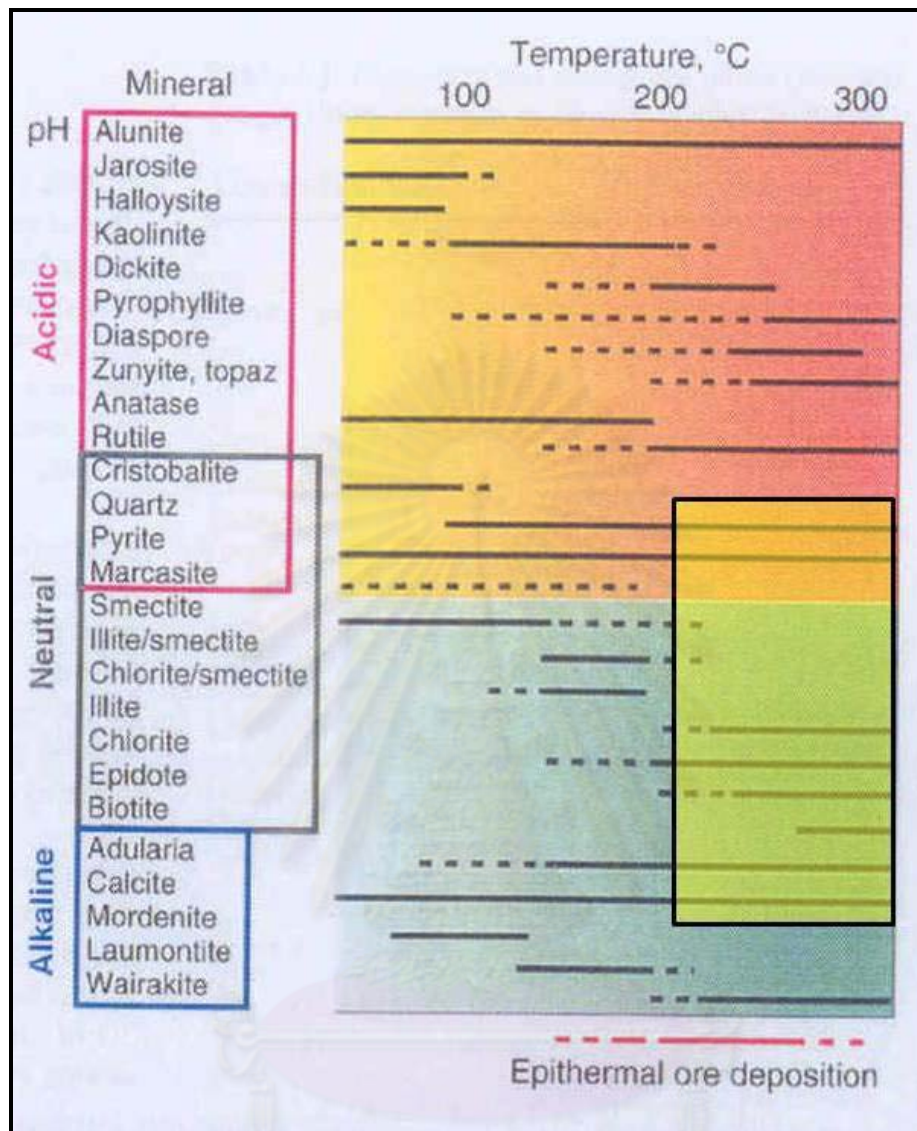
Figure 5. 3 Diagram of alteration mineral assemblages shown the study areas minerals alteration associated with pH and temperature (modified from Hedenquist et al, 1996).

5.5.2 pH and salinity

The presence of quartz, pyrite, sericite, illite, chlorite, adularia and epidote assemblage suggest that they were form from a near neutral pH fluid (Figures 5.3 and 5.4). Moreover, adularia might have been precipitated in the mineralized veins of the A Prospect according to the reaction

$$K^+ + Al(OH)_3 + 3H_4SiO_4 \leftrightarrow KAlSi_2O_8 + H^+ + 7H_2O \qquad (1)$$

$Al(OH)_3$ is the predominant aluminium species in near – neutral – pH and low – salinity waters (Lawless et al., 1999). Moreover, Dedenczuk (1998), Greener (1999) and Mizuta et al. (2009) suggested that the Chatree ore fluids have low salinity (< 4.5 wt% NaCl equivalent) based on fluid inclusion studies of the A, C and D Prospects.
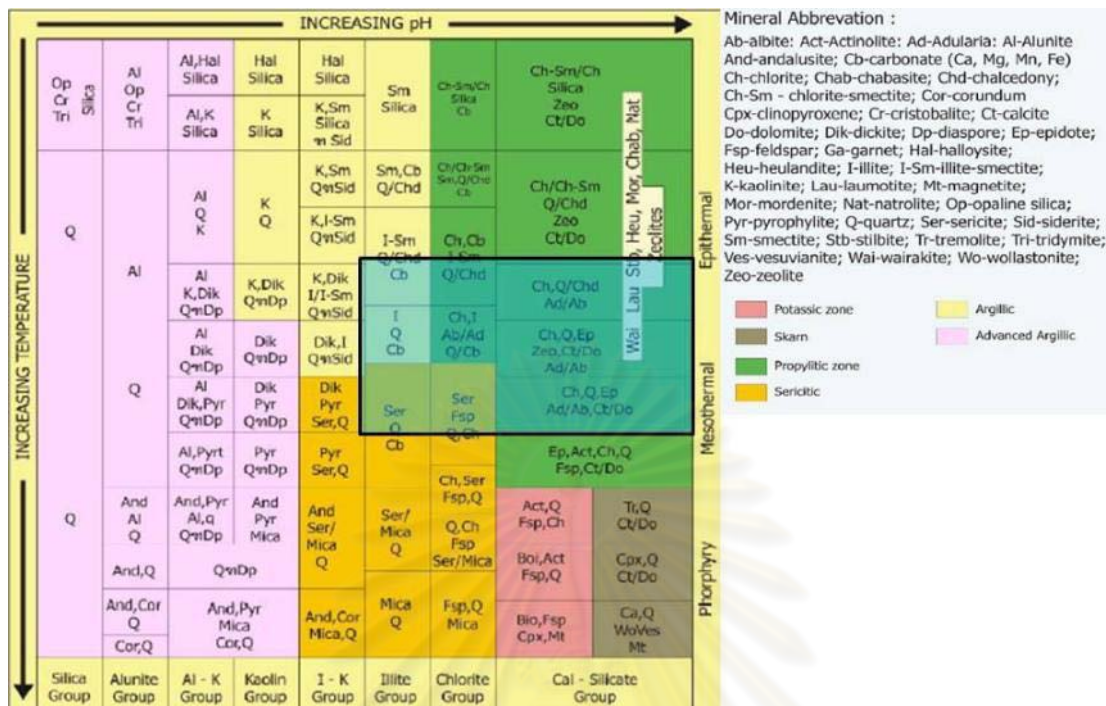
Figure 5. 4 Diagram of alteration mineral assemblages shown the study areas minerals alteration associated with pH, temperature and standard terminology of alteration (modified from Leach and Corbett, 1997).

5.5.3 Depositional process

The Chatree Gold Deposit has gold and silver as ore elements, they might have been transported as bisulphide complex or chloride complex. Gold of the A Prospect and the H West Prospect may be transported as $Au(HS)_2^-$ in dilute, reduced, near neutral pH waters (Cooke and Simmons, 2000) and precipitated from solution with an equation

$$2Au(HS)_2^- + H_2 + 2H^+ \leftrightarrow 2Au + 4H_2S \qquad (2)$$

Based on the above equation, gold can be deposited from a hydrothermal solution depending on the change in temperature, pH, salinity and chemical condition. Depositional mechanisms that caused gold precipitation may include boiling, cooling and water-rock interaction.

Boiling

Boiling of ore-forming fluids in the study area is suggested by the presence of adularia in the mineralized veins (Dong et al., 1995). Boiling results in reduction and loss of temperature, CO_2 and H_2S. After that equation (2) may be driven to the right, causing the increase of the pH and deposition of gold. The loss of CO_2 and H_2S due to boiling may lead to the association of bicarbonate and bisulphide species. The pH increase might have been partly offset by precipitation of sulphide (eg. pyrite) and carbonate minerals (e.g. calcite). Loss of CO_2 may also cause the

fluid to become more alkaline and result in the drop of gold from the solution. Gold precipitations may begin during the first increment of boiling (Lawless et al., 1999).

In addition, the wall rock alteration of the A Prospect resulted from the interaction with the major volcanic sedimentary rocks, which are more permeable than andesitic host rock of the H West Prospect. Gold may precipitate dominant in veins and minor in altered wall rocks. The permeability of wall rock has direct effect on pressure. The releasing pressure leads to boiling (Hedenquist et al., 2000). Adularia alteration zone occur in bottom layer of volcanic sedimentary unit. Low grade gold precipitated in wall rock and hydrothermal fluid altered host rocks as well (See alteration cross section in Chapter 3).

Cooling

Based on mineral assemblages in veins system, the dominant presence of quartz, carbonate, pyrite, sphalerite, chalcopyrite and electrum in the lower part of the H West Prospect suggest that the fluid could precipitate those minerals at temperatures between 250 and 190 C^o. In contrast the occurrence of quartz, chalcedony, carbonate, adularia and pyrite in middle part of the H West prospect and lower part of the A Prospect suggest that the assemblage was formed from a fluid having temperature between 250 and less than 190 C^o. Finally the presence of chalcedony, quartz, illite and pyrite near the surface in the A Prospect suggest that they could form from a fluids having temperatures less than 230 c^o. As such the simple cooling process is unlikely to be the predominant process to precipitate gold in the study areas. This is because it is very difficult to cool 250 C^o water without boiling or mixing in the upper few kms from surface (Cooks and McPhail, 2001). The carbon and oxygen isotope study are required to confirm this process.

Water-rock interaction

The major wall rock alteration of H West Prospect was the result of the interaction of hydrothermal fluid with the major andesitic host rock, whereas the major wall rock alteration of the A Prospect was the result of the interaction of the fluid with the major volcanic sedimentary rocks. Interaction of fluid with the host rock can be a potential site for the deposition of gold. However, because the gold-grade mineralization is present only in veins of the study areas, this suggests that the water-rock interaction is unlikely to be an important process for deposition of gold in the areas.

5.6 Conclusion

The difference between the A and the H West Prospects are

- Host rock: the A Prospect is mainly sedimentary rocks while the H West Prospect is major andesite. This suggests the difference of permeability. The A Prospect is dominant lithological control mineralization and alteration. The H West Prospect is mainly structure control mineralization and alteration. Moreover the alteration halo of the A Prospect is wider than the H West prospect. The A Prospect is meter scale while the H West Prospect is centimeter scale.

- Adularia form: The adularia alteration of the A Prospect shows fine-grained euhedral crystals or rhombic crystals. The adularia alteration of the H West Prospect shows medium-grained sub-rhombic crystals.
- Structure or mineralization trend: the A Prospect is NNW direction. The H West is North-East direction.
- The local alteration: the A Prospect contains hematite and garnet alterations while prehnite was discovered in the H West Prospect vein only.
- The A Prospect is shallower than the H West Prospect

The similarity of the A and the H West Prospects:
- Mineral assemblages: ore, gangue and alteration minerals are mostly same assemblages.
- The mineral assemblage and their features suggested the A and the H West Prospects are epithermal low- to intermediate sulphidation system. Temperature less than 300 C^o, low salinity and near neutral to alkaline fluid.

5.7 Recommendations

Many aspects still exist in the A and the H West Prospects for further investigation.

- The A Prospect should be drilled following bedding of the Unit 2, due to the lithological control.
- The H West Prospect needs more study on structural geology for more drilling targets.
- Assessment of the relationship between sphalerite and Au content.
- The PIMA or SWIR or ASD analyses require for better and quick mapping.
- Microprobe analysis of garnet is required to identify and understand its nature and association with jasper.

REFERENCES

Bailey, E.H and Stevens, R.E., 1960, <u>Selective staining of K-feldspar and plagioclase on rock slabs and thin sections,</u> The American Mineralogist, 45.

Buchanan, L.J., 1981. Precious metal deposits associated with volcanic environments in the southwest. In: W.R. Dickinson and W.D. Payne (Editors), <u>Relations of Tectonics to Ore Deposits in the Southern Cordillera</u>. Arizona Geological Society Digest, 14: 237-262.

Bunopas, S., 1991, <u>The late Triassic collision and stratigraphic belts of Shan Thai and Indochina microcontinents in Thailand</u>. Proceedings of papers presented at the 1st international symposium of IGCP Project 321, Gondwana; Dispersal and accretion of Asia, Kunming, China.

Bunopas, S., 1992, <u>Regional stratigraphic in Thailand: Potential for Future Development.</u> Piancharoen, C., editor –in – chief, Department of Mineral Resources, Bangkok, Thailand, 17 – 24 November, 1992, 2 : 2 – 24

Bunopas, S., and Vella, P., 1983, <u>Tectonic and geologic evolution of Thailand</u>. Proceedings to the workshop on the stratigraphic correlation of Thailand and Malaysia, Geological Society for Thailand, Bangkok Geological society, Malaysia, Kuala Lumpar : 307 – 322

Chausiri, P., Daorerk, V., Archibald, D., Hiscala, K. I., and Ampaiwan, T., 2002, <u>Geotectonic Evolution of Thailand: A new Synthesis</u>, Journal of the Geological Society of Thailand No. 1.

Cooke, D.R., and McPhail, D.C., 2001, <u>Epithermal Au-Ag-Te mineralization, Acupan, Baguio district, Philippines: Numerical simulations of mineral deposition</u>, Economic Geology, 96 : 109-132.

Cooke, D. R., and Simmons, S. F., 2000, <u>Characteristics and genesis of epithermal gold deposits</u>, Reviews in Economic Geology, Gold in 2000, 13 : 221-244.

Corbett G., 2002, <u>Epithermal Gold for Explorationits</u>, AIG Journal – Applied geoscientific practice and research in Australia, Australia : 26.

Corbett, G., 2005, <u>Comments for Continued Mineral Exploration in the Chatree Gold Mine Environs from a Visit in August 2005</u>, Company report (unpublished)

Corbett, G., 2006, <u>Comments on the controls to gold mineralization at Chatree</u>, Company report (unpublished)

Crossing, J., 2004, Geological Mapping of the Chatree Regional Thailand, Company report (unpublished)

Crossing, J., 2006, Additional Geological Mapping Of The Chatree Regional Thailand, Company report (unpublished)

Cumming, G. V., 2004, An assessment of the volcanic facies at the Chatree mine and other selected areas in the Loei – Petchabun Volcanic belt, B.Sc. (Hons) Thesis (unpublished), Centre for Ore Deposit Research, School of Earth Sciences, University of Tasmania, Hobart, Australia.

Cumming, G. V., Allen, S., McPhie, J., and Khin Zaw, 2006, Polymictic andesitic lithic breccias from central Thailand: evidence for the collapse of a volcanic edifice, In: Geochronology, Metallogenesis and deposit styles of the Loei foldbelt in Thailand and Laos PDR, ARC Linkage Project report, Centre for Ore deposit research, Company report (unpublished)

Cumming, G. V., Lunwongsa, W., Salam, A., James, R., Nuanla-ong S., and Munsamai, S., 2008, Geology and Mineralization of the Chatree Epithermal Au-Ag Deposit, Central Thailand, report prepared for Kingsgate Consolidated NL (unpublished)

Dedenczuk, D., 1998, Epithermal Gold mineralization Khao Sai, Central Thailand, , B.Sc. (Hons) Thesis (unpublished), Centre for Ore Deposit Research, School of Earth Sciences, University of Tasmania, Hobart, Australia.

Diemar, M.G., 1990. TGF1508 Summary, (unpublished) report to Thai Goldfields Limited.

Diemar, M. G., and Diemar, V. G., 1999, Geoloogy of the Chartee Epithermal Gold deposit, Thailand, Pacific Rim Conference 1999, Indonesia 10 -13 October, Proceedings : 227 - 231

De Little, J. V., 2005, Geological setting, nature of mineralization, and fluid characteristics of Wang Yai prospects, central Thailand, B.Sc. (Hons) Thesis (unpublished), Centre for Ore Deposit Research, School of Earth Sciences, University of Tasmania, Hobart, Australia.

Dong, G., and Morrison, G., 1995, Adularia in epithermal veins, Queenland: morphology, structureal state and origin, Mineral Deposita 30 : 11 -19.

Dong, G., Morrison, G., and Jaireth, S., 1995, Quartz texture in epithermal veins Queenland – Classification, Origin, and Implication, Economic Geology 90: 1841 – 1856.

Evamy, B. D. (1963) : <u>The application of a chemical staining technique to a study of dedolomitisation</u>. Sedimentology, 2, 164-170.

Gemmell, J. B., 2004, <u>Low- and intermediate-sulphidation epithermal deposit,</u> in 24 carat Au Workshop, CODES Special Publication 5, Centre for Ore Deposit Research, School of Earth Sciences, University of Tasmania, Hobart, Australia.

_____, <u>Gold</u> [Online], 2010, Avaliable from : http://en.wikipedia.org/wiki/Gold [2010, April 26].

Greener, S., 1999, <u>Wall rock alteration and Vein Mineralogy of a Low Sulfidation Epithermal deposit, Thailand</u>, B.Sc. (Hons) Thesis (unpublished), Centre for Ore Deposit Research, School of Earth Sciences, University of Tasmania, Hobart, Australia.

Hedenquist, J. W., 2000, <u>Exploration for epithermal gold deposits</u>, Reviews in economic geology, Gold in 2000, 13 : 245 – 277.

Hill, R., 2004a, <u>Interpretation of Regional Structural Setting from Ground Resistivity Data, Chatree Mine Area, Thailand</u>, Company report (unpublished).

Hill, R., 2004b, <u>Interpretation of the 2004 Aeromagnetic Data, Thailand</u>, Company report (unpublished).

Intasopa, S., 1993, <u>Petrology and Geochronology of the volcanic rocks of central Thailand volcanic belt</u>, Ph. D. thesis, University of New Brunswick : 242.

James, R., and Cumming, G. V., 2007, <u>Geology and Mineralization of the Chatree Epithermal Au-Ag deposit, Phetchabun Pronince, Central Thailand</u>, GEOTHAI'07 International Conference on Geology of Thailand: Toward Sustainable Development and Sufficient Economy, 378-390.

Jongyusuk, N., and Kositanont S., 1992, <u>Volcanic rocks and associated mineralization in Thailand</u>. In: Pianchaoen C. (Ed), Potential for future development; Bangkok : 522 – 537.

Kamvong, T., 2004, <u>Geochemistry and Genesis of Phu Lon Copper-Gold Skarn Deposit, Northeast Thailand,</u> B.Sc. (Hons) Thesis (unpublished), Centre for Ore Deposit Research, School of Earth Sciences, University of Tasmania, Hobart, Australia.

Kamvong, T., Charusiri, P., and Intasopa, B.S., 2006, <u>Petrochemical characteristic if igneous rocks from the Wand Pong area, Petchabun North Central Thailand: implication for tectonic seeting,</u> Journal of Geological Society of Thailand, 1, 9 -26.

Khin Zaw, Burret C. F., Berry R. F., Bruce E., and Pasqua D. F., 1999, <u>Geological, tectonic and metallogenic relations of mineral deposits in Mainland SE Asia, Geochronological studies, AMIRA Project P390A: Final Report: December 1999</u>, (unpublished), Centre for Ore Deposit Research, School of Earth Sciences, University of Tasmania, Hobart, Australia.

Khin Zaw, Meffre S., Salam, A., and Cumming, G. V., 2007, <u>Chatree epithermal Au-Ag deposit, Central ThailandCo-ordinates:16.2964N; 100.6525E</u>, ARC Linkage Project report (unpublished), Centre for Excellence in Ore Deposits, University of Tasmania, 7001, Hobart, Australia.

Krompkhun, K., 2005, <u>Geological setting, mineralogy, alteration, and nature of ore fluid of the H zone, the Chatree deposit, Thailand</u>. M.Sc. Thesis (unpublished), Centre for Ore Deposit Research, School of Earth Sciences, University of Tasmania, Hobart, Australia.

Lawless, J. V., White, P. J., Bogie, I., and Cartwright, A. J., 1999, <u>Finding Mineralisation is Easy; Why is it so Hard to Find A Mine?</u>, Kingstone Morisson, Short Course PacRim 99 Congress, Bali, 9 – 10 October 1999, Indonesia.

Leach, T.M. and Corbett, G.J.,1997, <u>SOUTHWEST PACIFIC RIM GOLD-COPPER SYSTEMS: Structure, Alteration, and Mineralization,</u> Short course manual, SME/SEG Meeting, Phoenix, USA, 318

Lunwongsa, W., Sangsiri, P., and Anonymous, 2008, <u>Update geology, mineralization and alteration of H West Prospect,</u> Company report (unpublished).

Marhotorn, K., Mizuta, T., Ishiyama, D., Takashima, I., Won-in, K., Nuanlaong, S. and Charusiri, P., 2008, <u>Petrochemistry of Igneous rocks in the Southern Parts of the Chatree Gold Mine, Pichit, Central Thailand,</u> extended abstract in International Symposium on Geoscience Resources and Environments of Asain Terranes (GREAT2008), 24 – 26 November, Bangkok, Thialand, 289 - 298.

Mizuta, T., Mori, Y., Fukushima, M., Ishiyama D., Yoshida H. and Charusiri P., 2009, <u>Geochemical characteristics of Chatree epithermal vein-type gold-silver deposit, Phetcyhabun Province, Central Thailand</u>, presentation prepared for Issara Mining limited (unpublished).

Morrison, G., Dong, G., and Subhash, J., 1990, <u>Textural zoning in epithermal quartz veins</u>, Gold research group, James Cook University, 36.

Panjasawatwong, Y. and Phaejuy, B., 2008, <u>Pre-Cretaceous volcanic rocks of Thailand</u>, Abstract in conference Tectonic of Northwestern Indochina, Chiang Mai 2008, Igneous Rocks and related Ore Deposits Research Unit, Chiang Mai University, Chiang Mai, Thailand, 28-34

____, <u>Reserves / Resources Statement </u>[Online], 2010, Avaliable from : http://www.kingsgate.com.au [2010, April 26].

Salam, A., 2006, <u>Geological report prepared for Akara Mining limited</u>, Company report (unpublished).

Salam, A., 2008, <u>progress study prepared for Akara Mining limited</u>, Company report (unpublished).

Salam, A., 2010, <u>Progress study of Mineralogy of Chatree Volcanic Complex</u>, Company report (unpublished).

Salam, A, Khin Zaw, Meffre, S, James, R, Stein, H, and Vasconcelos, P, 2007a, <u>Geological setting, mineralization and geochronology of Chatree epithermal gold-silver deposit, Phetchabun Province, central Thailand</u>, in Proceedings of Asia Oceania Geosciences Society (AOGS), 4th Annual meeting, 31 July-4 August 2007, Bangkok, 249.

Salam, A, Khin Zaw, Meffre, S, James, R, Stein, and H 2007b. <u>Geological setting, alteration, mineralisation and geochronology of Chatree epithermal gold-silver deposit, Phetchabun Province, central Thailand</u>, in Proceedings of Ores and Orogenesis Symposium, 24-30 September, 2007, Tucson, Arizona, USA, 181.

Salam, A, Khin Zaw, Meffre, S, McPhie, J, Cumming, G, Suphananthi, S, and James, R, 2008a. <u>Stratigraphy and geochemistry of Permian to Triassic Chatree volcanics, Phetchabun Province, central Thailand</u>, in Proceedings of Tectonic of Northwestern Indochina Conference, 6-8 February 2008, Chiang Mai, Thailand, 37-37.

Salam, A, Khin Zaw, Meffre, S, Vasconcelos, P, Stein, H, and Macintyre, P, 2008b. <u>Geological setting, mineralisation and geochronology of Chatree epithermal gold-silver deposit, Phetchabun Province, central Thailand</u>, in Proceedings of Australian Earth Sciences Convention, Perth, Western Australia, Australia, 20-24 July, 2008, 216.

Simmons, S. F., and Browne, R. L., 2000, <u>Hydrothermal minerals and precious metals in the Broadlands - Ohaaki geothermal system: implications for understanding low sulfidation epithermal environments</u>, Economic geology 95(5), : 971 – 999.

Simmons, S. F., and Christenson, B. W., 1994, Origins of calcite in a boiling geothermal system, American Journal of Science, 294 : 361-400.

Thomson, A. J. B., and Thomson, J. F. H., 1996, Atlas of alteration: A field guide and petrograpnic guide to hydrothermal alteration minerals, Newfoundland, Geological Association of Canada : 119.

Tomkinson, M., 2004, Vein and alteration paragenesis at the Chatree Gold Mine – Thailand, presentation prepared for Akara Mining limited (unpublished).

White, N.C., and Hedenquist, J.W., 1995, Epithermal gold deposits: styles, characteristics and exploration, Society of Economic Geologists Newsletter, 23 : 1-13.

BIOGRAPHY

Mr. Phuriwit Sangsiri was born in Chiang Mai, northern part of Thailand, on September 16, 1981. After finishing the high school from the Yupparaj Wittayalai School, Chiang Mai in 1999; he was chosen to study in Chiang Mai University, where he acquired the B.Sc. degree in Geology from the Department of Geology, Faculty of Science, Chiang Mai University in 2005. After graduation, he worked with Akara Mining Ltd. and Issara Mining Ltd. He continued his study in the M.Sc. program in geology at Graduate School, Chulalongkorn University, in 2007. The research work has been focused on mineralization and alteration.